REPORT SD-TR-85-39

(2)

Cassegrain Reflector Sidelobe Reduction Study

H. E. KING, S. LAZAR, G. G. BERRY,
H. B. DYSON, W. S. WALES, and W. C. WYSOCK
Electronics Research Laboratory

D. S. CHANG
Mathematics and Analysis Department
Laboratory Operations
The Aerospace Corporation
El Segundo, Calif. 90245

15 July 1985

Prepared for

SPACE DIVISION
AIR FORCE SYSTEMS COMMAND
Los Angeles Air Force Station
P.O. Box 92960, Worldway Postal Center
Los Angeles, CA 90009-2960

This report was submitted by The Aerospace Corporation, El Segundo, CA 90245, under Contract No. F04701-83-C-0084 with the Space Division, P.O. Box 92960, Worldway Postal Center, Los Angeles, CA 90009. It was reviewed and approved for The Aerospace Corporation by D. H. Phillips, Director, Electronics Research Laboratory.

Lt Harold J. Morgan, SD/CGX, was the Air Force project officer.

This report has been reviewed by the Public Affairs Office (PAS) and is releasable to the National Technical Information Service (NTIS). At NTIS, it will be available to the general public, including foreign nationals.

This technical report has been reviewed and is approved for publication. Publication of this report does not constitute Air Force approval of the report's findings or conclusions. It is published only for the exchange and stimulation of ideas.

Harold J. Morgan

HAROLD J. MORGAN, Lt, USAF
USAF Project Officer
SD/CGX

Joseph Hess

JOSEPH HESS, GM-15
Director, AFSTC West Coast Office
AFSTC/WCO OL-AB

UNCLASSIFIED

SECURITY CLASSIFICATION OF THIS PAGE *(When Data Entered)*

REPORT DOCUMENTATION PAGE		READ INSTRUCTIONS BEFORE COMPLETING FORM
1. REPORT NUMBER SD-TR-85-39	2. GOVT ACCESSION NO. AD-A158	3. RECIPIENT'S CATALOG NUMBER 625
4. TITLE *(and Subtitle)* CASSEGRAIN REFLECTOR SIDELOBE REDUCTION STUDY		5. TYPE OF REPORT & PERIOD COVERED
		6. PERFORMING ORG. REPORT NUMBER TR-0084A(5409-73)-1
7. AUTHOR(s) H. E. King, Steven Lazar, Gerald G. Berry, Howell B. Dyson, William S. Wales, William C. Wysock, and Dorothy S. Chang		8. CONTRACT OR GRANT NUMBER(s) F04701-83-C-0084
9. PERFORMING ORGANIZATION NAME AND ADDRESS The Aerospace Corporation El Segundo, Calif. 90245		10. PROGRAM ELEMENT, PROJECT, TASK AREA & WORK UNIT NUMBERS
11. CONTROLLING OFFICE NAME AND ADDRESS Space Division Los Angeles Air Force Station Los Angeles, Calif. 90009-2960		12. REPORT DATE 15 July 1985 13. NUMBER OF PAGES 116
14. MONITORING AGENCY NAME & ADDRESS *(if different from Controlling Office)*		15. SECURITY CLASS. *(of this report)* Unclassified 15a. DECLASSIFICATION/DOWNGRADING SCHEDULE

16. DISTRIBUTION STATEMENT *(of this Report)*

Approved for public release; distribution unlimited.

17. DISTRIBUTION STATEMENT *(of the abstract entered in Block 20, if different from Report)*

18. SUPPLEMENTARY NOTES

19. KEY WORDS *(Continue on reverse side if necessary and identify by block number)*

Cassegrain reflectors
Space frame radome
Horn-subreflector feed patterns
Tunnel reflector antennas

20. ABSTRACT *(Continue on reverse side if necessary and identify by block number)*

This report presents the results of a 4-month study to reduce the sidelobe levels of a 38 GHz, 2 ft diameter Cassegrain reflector. Both partial and full circumferential shrouds were added to the main reflector. Various shielding techniques to reduce the horn and subreflector radiation characteristics were evaluated. Measured primary patterns for the various horn-subreflector combinations were used to compute the secondary reflector patterns to evaluate the sidelobe improvement. The computed patterns were compared with measured results.

DD FORM 1473 (FACSIMILE)

UNCLASSIFIED

SECURITY CLASSIFICATION OF THIS PAGE *(When Data Entered)*

AEROSPACE FORM 4341-1 REV 5-74

19. KEY WORDS *(Continued)*

20. ABSTRACT *(Continued)*

Concurrent with the in-house study, an independent theoretical approach was undertaken by Professor R. C. Rudduck at Ohio State University to develop techniques to analyze sidelobe characteristics. The most effective sidelobe reduction technique found in this study consists of partial or full circumferential shrouds added to the main reflector edge, which reduces the backlobes but has negligible effect on the forward-region sidelobes. His analysis also includes the effects of a metal space frame radome on the sidelobe levels of a reflector antenna.

CONTENTS

CONTENTS (cont'd)

FIGURES

FIGURES (Cont'd)

FIGURES (cont'd)

FIGURES (cont'd)

I. INTRODUCTION

Sidelobe levels of paraboloidal reflector antennas result from 1) direct radiation from the feed system, 2) diffraction from aperture blockage, subreflector, spars and the main-reflector edge and 3) contributions from the aperture distribution, which become minimal with increasing angle from the main beam. In many applications, the resultant sidelobe levels are acceptable; for other applications, antennas with reduced sidelobe levels are required. This report summarizes a four-month effort to investigate the effectiveness of corrugations, shrouds, and absorber rings in sidelobe reduction. The experimental and analytical results for a 2-ft diameter reflector operating at 30 GHz are presented. This antenna selection was based on equipment availability.

The objective of this study was to acquire sidelobe reductions of 10 to 20 dB over as wide an angular region as possible, excluding the region $\pm 30°$ from the main beam. The addition of sidelobe control techniques is required to have a minimal impact on gain performance. The study approach used experimental tradeoffs of the feed system parameters in conjunction with computed reflector[1] patterns to identify the more promising techniques. These techniques installed in the 2-ft reflector were experimentally measured. The correspondence between measured and analytically projected results was very good.

Several physical constraints were imposed for this study. The feed horn size was limited to an aperture of 1.2 in., thus the spillover and the reflector-edge illumination could not be controlled, which are important contributors to the reflector sidelobe levels. Also, the sizes of the subreflector and its supports were fixed.

The following sidelobe-reduction technique approaches were undertaken in this study:

- Horn-aperture chokes to reduce the backlobes of the feed horn pattern
- Shroud around subreflector to minimize the edge illumination of the main reflector
- Corrugations attached to the subreflector to impede the wave along the reflector-edge shadow boundary
- Conical flange mounted to the subreflector to divert the energy away from the main-reflector edge
- Absorber ring attached to the subreflector to attenuate the wave along the reflector-edge shadow boundary
- Shroud (with and without absorber material attached) around the main-reflector edge to reduce the edge diffraction
- Plate (i.e., a partial circumferential shroud attached to the main-reflector edge to reduce the edge diffraction in one plane)

II. REFLECTOR GEOMETRY

A. Baseline

The experimental 2-ft diameter Cassegrain antenna is shown in the photograph of Fig. 1. The main reflector (f/D = 1/3) is a spun-aluminum dish with a rolled edge. The 2.919-in. diameter subreflector is supported by a truss spar structure 0.333 in. wide. The spars are located $\pm 45°$ with respect to the principal E and H planes. The conical feed horn is a 1.2-in. diameter by 4.6-in. long with a half-flare angle of 5.415°.

Figure 1. Photograph of experimental 38 GHz, 2-ft diameter reflector antenna

Two subreflector shapes were used in these experiments -- denoted as "oversized" and conventional in Fig. 2. Both subreflectors have the same diameter. The oversized subreflector is arranged to have the main-reflector edge ray strike the central portion of the subreflector as illustrated in Fig. 2a. Since only the central portion of the subreflector is illuminated, it results in a relatively uniform aperture illumination with the specified 1.2-in. diameter feed horn. With this high level of edge illumination, accompanied with high spillover power, the net result is a high sidelobe level over almost the entire angular region, but it yields higher gain (~ 0.7 dB) as compared to the conventional subreflector. Measurements were carried out on both of these subreflectors. The phase center of the horn was chosen to be 0.275 in. inside the horn aperture as determined by focussing tests made with the 2-ft reflector.

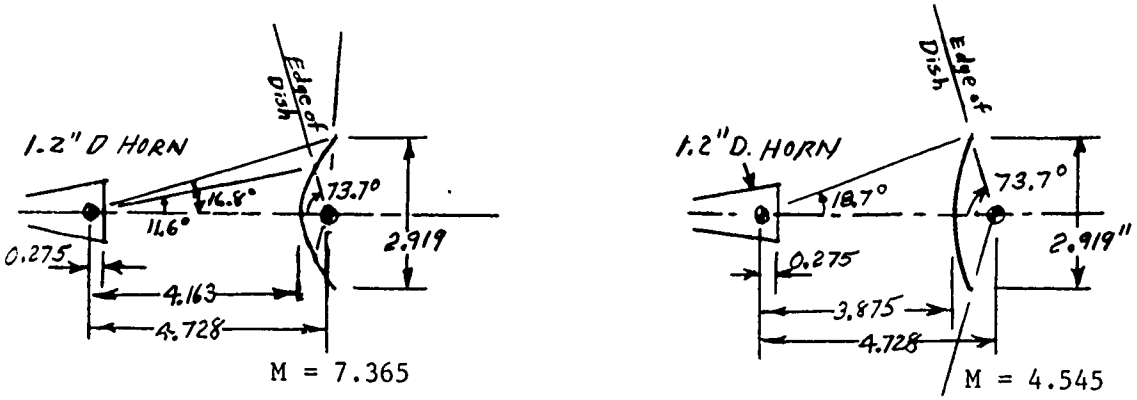

(a) Oversized (b) Conventional

Figure 2. Optics of the horn and the two specified subreflectors

The two focal points of the Cassegrain optics are shown in Fig. 3. With a f/D = 1/3 the primary focal point is 8 in. from the reflector vertex, while the hyperboloidal focal point was fixed at 3.272 in. from the vertex. With these dimensions, the magnification factors of the oversized and conventional subreflectors are 7.365 and 4.545, respectively.

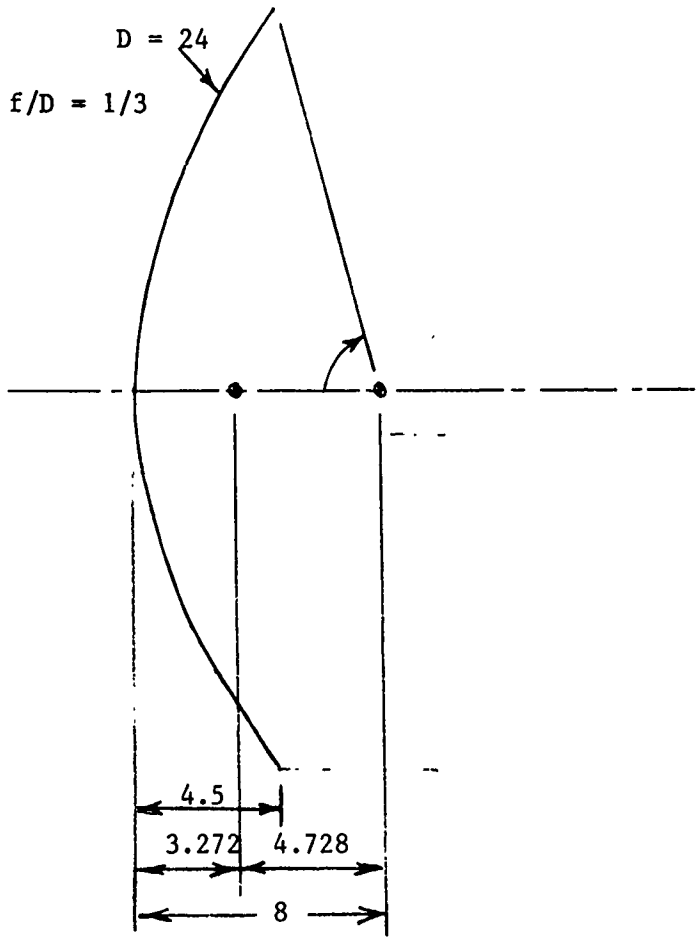

Figure 3. Dimensions of 2-ft paraboloidal reflector

B. Sidelobe Reduction Techniques

Sidelobes in a Cassegrain-reflector system originate from a number of sources, as follows: 1) feed-horn pattern sidelobes, 2) spillover and edge diffraction from the feed horn-illuminated subreflector, 3) spillover and edge diffraction from paraholic reflector illuminated by the subreflector, 4) feed horn and subreflector blockage, and 5) spar blockage and scattering. A 6th source is a function of the aperture illumination, which affects the near-in sidelobes for either a Cassegrain or a prime-focus feed. In addition, poor surface tolerances in the reflector contribute to higher sidelobe levels, but generally, an accurate reflector for the frequency of operation is selected to maximize the gain.

The sidelobe pattern contributions from the various sources are illustrated in the diagram of Fig. 4, with the numbers corresponding to the sources listed above. If these sidelobe contributors can be eliminated or reduced, then lower sidelobe levels can be expected. However, there are fundamental and practical limitations to these sidelobe-reduction techniques that can be employed. In general, if the edge illumination can be reduced resulting in less edge diffraction, then an improvement in the back-region sidelobe levels can be expected. E.g., 5 dB less edge illumination would result in ~ 5 dB sidelobe reduction over an angular region of $\pm 73.7°$ (for f/D = 1/3) or a total angle of 147.4°.

Edge illumination affects all the regions (except for the subreflector blockage region) of the dish pattern shown in the illustration of Fig. 4. Thus, a larger, more directive horn reduces the overall sidelobe levels. However, an increase in feed horn size is accompanied by an increase in aperture taper loss, which reduces the antenna gain. For this sidelobe-reduction study, a 1.2-in. diameter conical feed horn was used, with no experimental

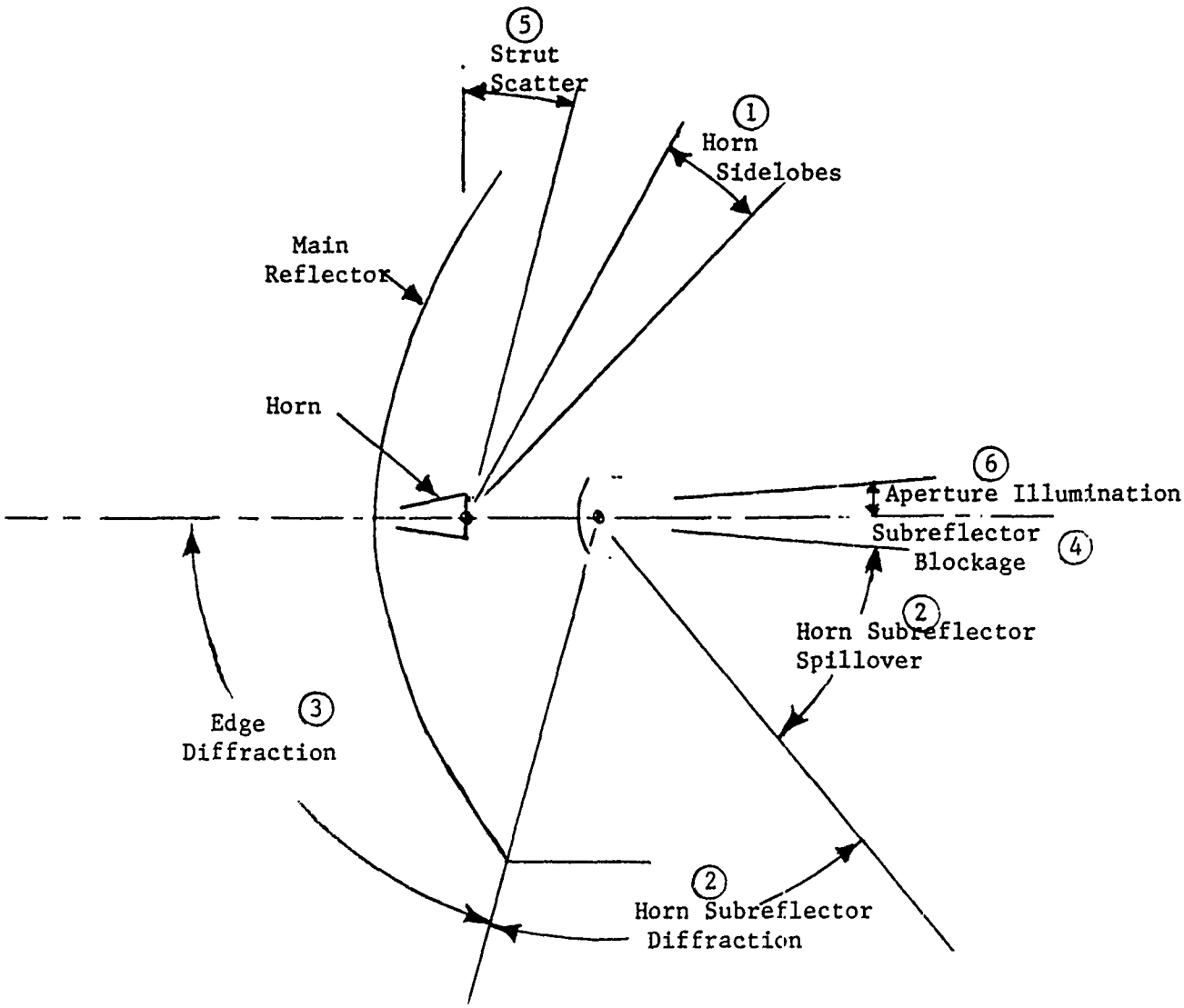

Figure 4. Contributors to radiation pattern sidelobe levels for a Cassegrain reflector antenna

opportunity to optimize the feed horn size for minimum sidelobe levels. However, by computer design as described in Sec. V, Ohio State University (OSU) found that a 1.4-in. diameter corrugated horn is the optimum horn to minimize the reflector sidelobe levels.

The 1.2-in. horn is surrounded by a 4-horn monopulse feed system simulated in the experiments as shown in Fig. 5a. The conical horn patterns were measured with and without the simulated monopulse feeds and also with the shroud of Fig. 5b, to determine the effectiveness in shielding the horn radiation. All of the subsequent horn-subreflector and main reflector pattern measurements were made without the monopulse feed and shroud as these devices did not show any appreciable effect on the conical horn patterns.

Several modifications to the feed horn/subreflector (oversized and conventional) were evaluated for shielding as illustrated in Figs. 6 and 7. For the oversized subreflector, experiments were made on the following shielding techniques:

Figure No.

- 6a Circumferential shroud around subreflector with and without absorbing material
- 6b Corrugations (chokes) along shadow boundary to edge of dish
- 6c Corrugations (chokes) along oversized portion of subreflector
- 6d Conical flange attachment[2]
- 6e Absorber ring along shadow boundary to edge of dish

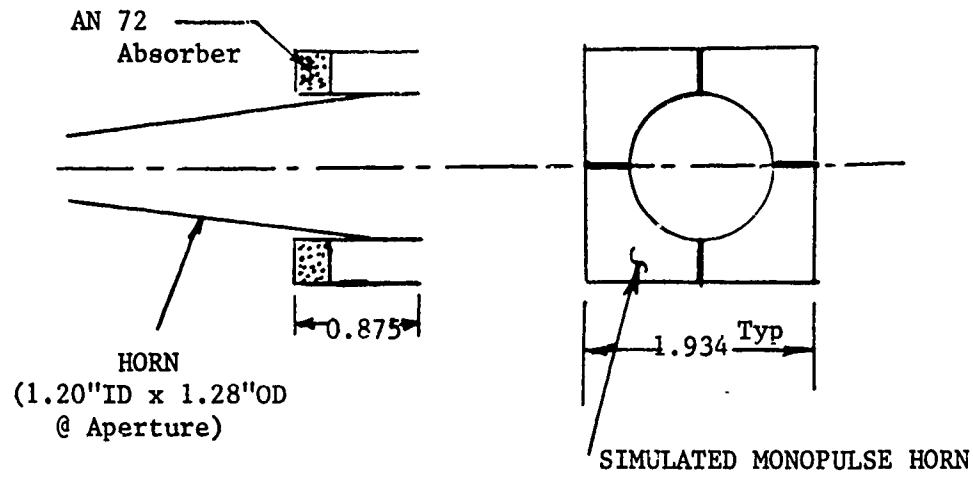

(a) Simulated Monopulse Feed

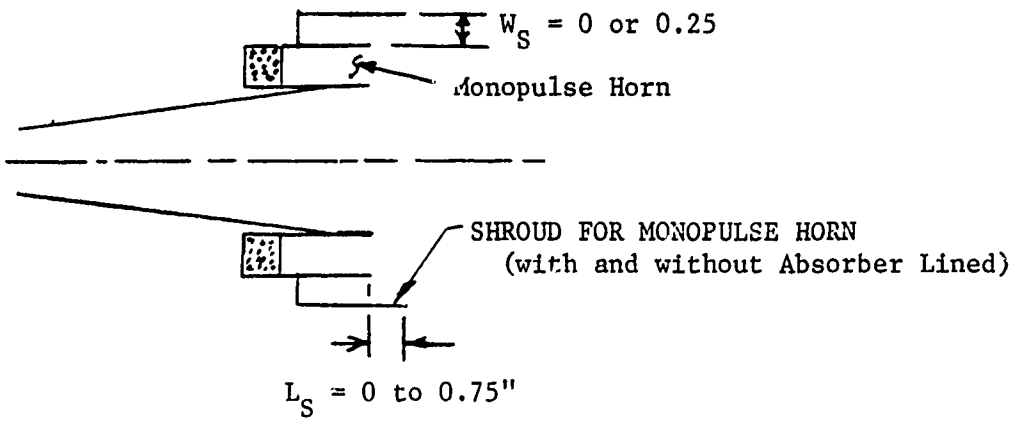

(b) Shielding of Monopulse Feed

Figure 5. Simulated monopulse feed and 1.2-in. conical horn

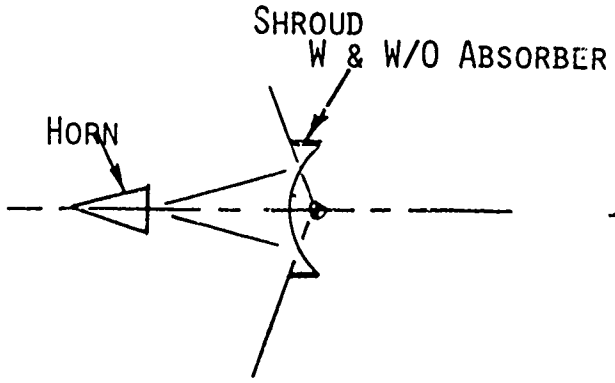

(a) Shroud

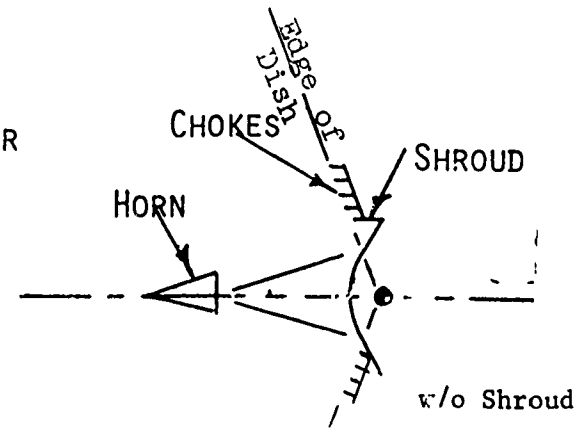

Split view to show with and without shroud

(b) Corrugations Along Shadow Boundary

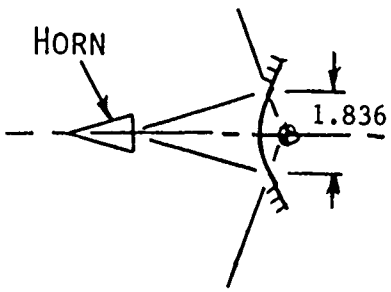

(c) Corrugations Along Reflector

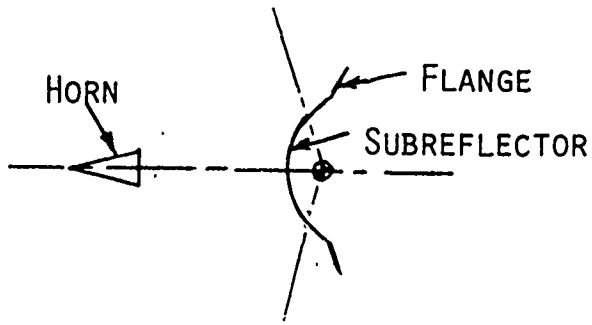

(d) Conical Flange

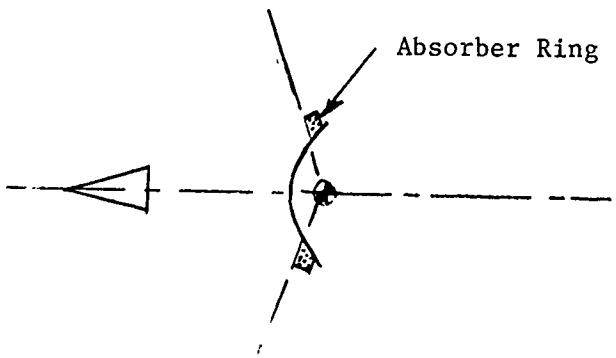

(e) Absorber Ring

Figure 6. Shielding approaches for the oversized subreflector

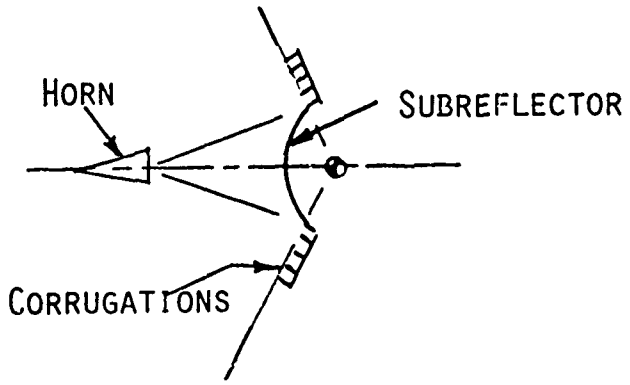

a) Corrugations

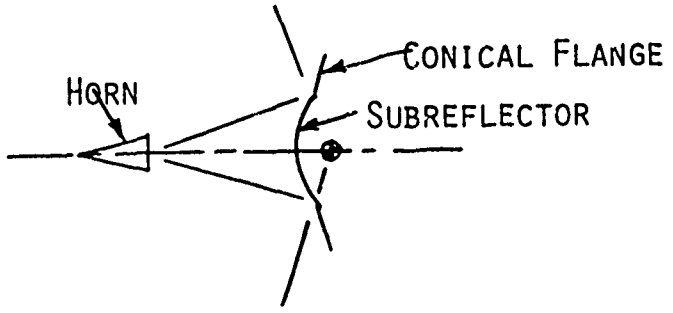

b) Conical Flange

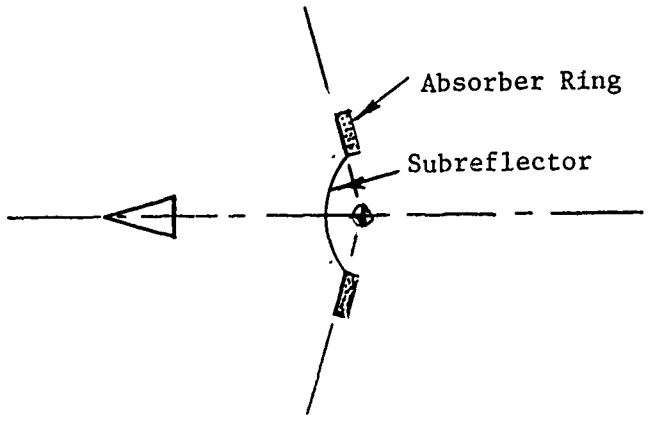

c) Absorber Ring

Figure 7. Shielding approaches for the conventional subreflector

Similarly, experiments were made on the following shielding approaches for the conventional subreflector:

7a Corrugations (chokes) along shadow boundary to edge of dish

7b Conical flange attachment

7c Absorber ring along shadow boundary to edge of dish

Another sidelobe reduction technique consists of a shroud attached to the edge of the main parabolic reflector, as shown in Fig. 8. A 3-in. shroud will reduce the edge diffraction by approximately the amount the horn-subreflector pattern decreases from 73.74° (edge of dish) to 87.61° (ray to edge of shroud). The resultant effect will be a reduction in the backlobe portion of the main reflector (region 3 of Fig. 4). Measurements were made with the shroud (inner and outer surface) lined with microwave absorbing material.

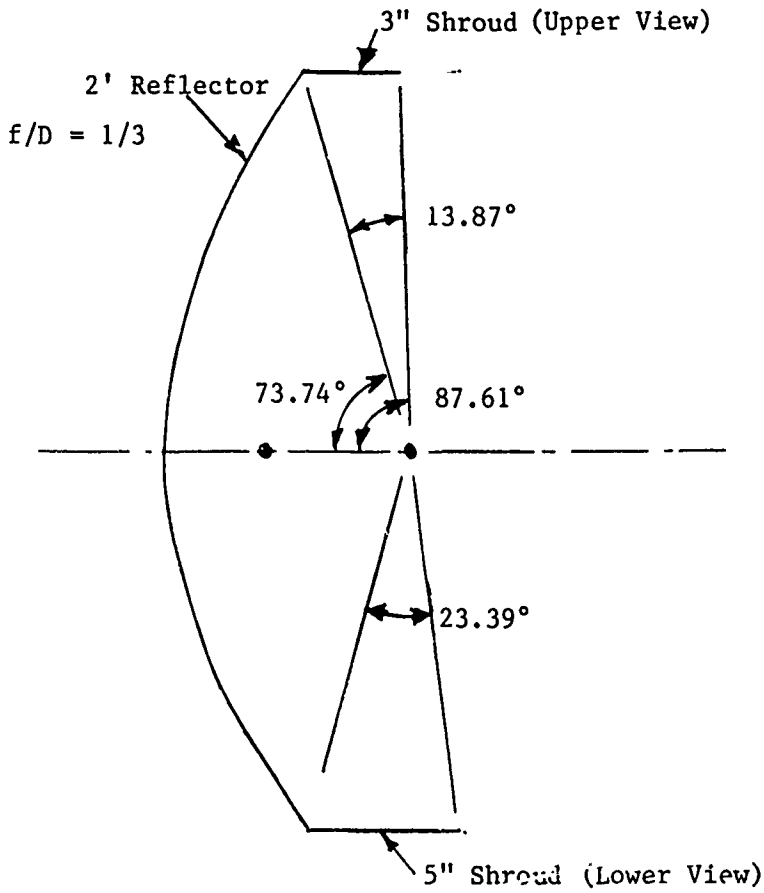

Figure 8. Illustrations of 3-in. and 5-in. shrouds around edge of main reflector

III. FEED SYSTEM MEASUREMENTS

Measured results for the feed horn and the horn-subreflector combinations for sidelobe suppression are presented and evaluated. A range of techniques were examined to identify the most promising techniques for evaluation with the reflector. These horn-subreflector patterns were used as the primary feed patterns (prime-focus feed) to calculate the reflector pattern characteristics using geometrical theory of diffraction (GTD) technique described by Rudduck and Lee. Certain techniques can be discarded without further reflector testing.

A. Measurement Technique

The measurement setup consists of an optical rail with the 38 GHz source at one end and the rotating stage near the other end. The rotating stage has a platform which has two micrometer driven linear stages. One stage adjusts the horn location, the other the subreflector location. The stages have posts with fixtures on top for holding the device under test. The horn is held by a circular clamp at the waveguide flange which allows for rotation about the axis to make measurements in the E and H planes. A photograph of a typical horn-subreflector arrangement is shown in Fig. 9.

B. Feed Horn

The initial measurements were made of the feed horn without a subreflector. The stages were adjusted so that the aperture of the horn was over the axis of rotation of the rotary stage. The E and H plane patterns taken of the 1.2-in. conical horn are shown in Fig. 10. The half-power beamwidths are 15.5° and 19° in the E and H plane, respectively. The subreflector edge tapers for the subreflectors are as follows:

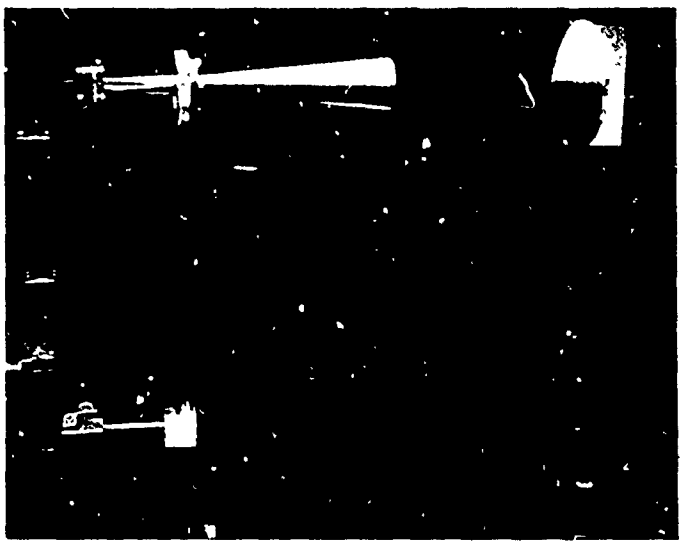

Figure 9. Horn-subreflector pattern measurement setup

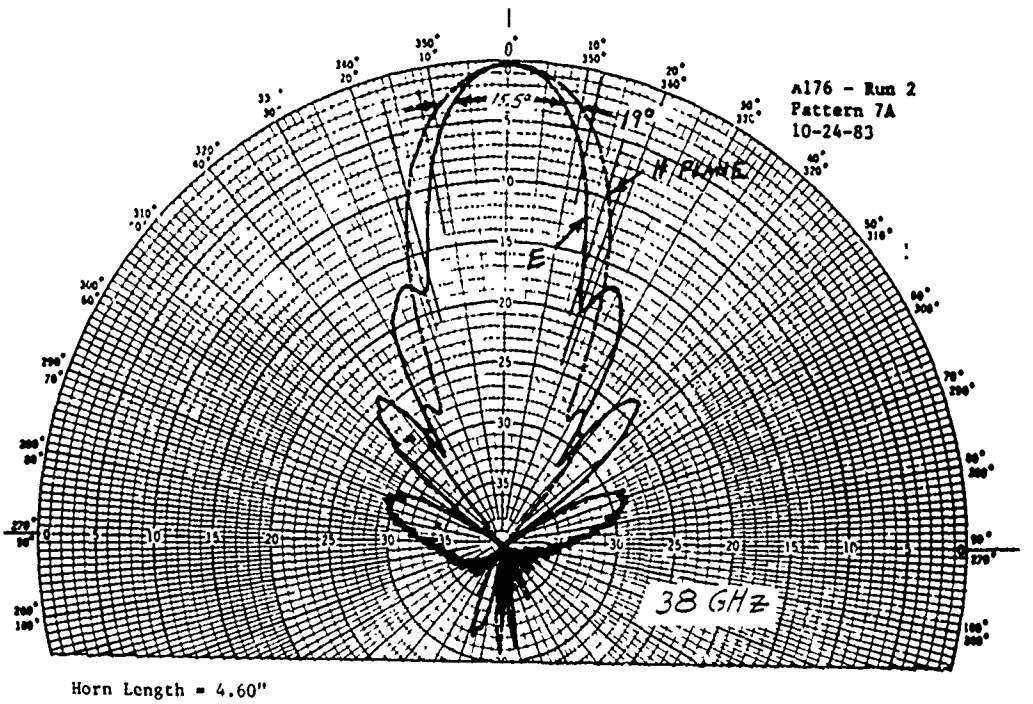

Figure 10. E and H plane patterns of the 1.2-in. diameter conical horn

Oversized 11.6°		Conventional 18.7°	
E	H	E	H
7.7	4.5 dB	19.5	11.5 dB

The oversized subreflector will have a relatively uniform aperture illumination as compared to the conventional subreflector. The 1.2-in. diameter horn is close to optimum with the E-plane first null illuminating the edge and with 11.5 dB edge taper in the H plane.

The monopulse horn was simulated by constructing a box around the horn as illustrated in Fig. 5. The box is divided into 4 quadrants and is terminated in back by absorber. The central horn patterns with the monopulse-horn simulator were first measured with the patterns shown in Fig. 11a. Then a shroud, which extends 0.75 in. beyond the monopulse horn, was added with the patterns shown in Fig. 11b. Finally, the shroud was lined on the inside with absorber and its patterns recorded in Fig. 11c. The purpose of the shroud was to determine if it would provide any shielding of the horn-pattern sidelobes to reduce the reflector sidelobes, as shown in zone 1 of Fig. 4. Although the monopulse horn/shroud patterns show minor improvements in sidelobes, no major changes of 10 to 20 dB reduction in reflector sidelobe levels were anticipated; thus, subsequent pattern measurements were made without the peripheral horns.

In an attempt to shield the horn-pattern sidelobes and backlobes, aperture chokes were added. They consist of concentric rings which produce $\lambda/4$ grooves in the aperture plane. E and H plane pattern measurements were made for 1 to 5 grooves, with little variation in the pattern characteristics. The patterns of the horn with 5 grooves are shown in Fig. 12. There was no significant change in sidelobes with only a slight improvement in the backlobes. Thus, no major changes in reflector sidelobes would be expected. The use of the aperture chokes would also yield additional aperture blockage

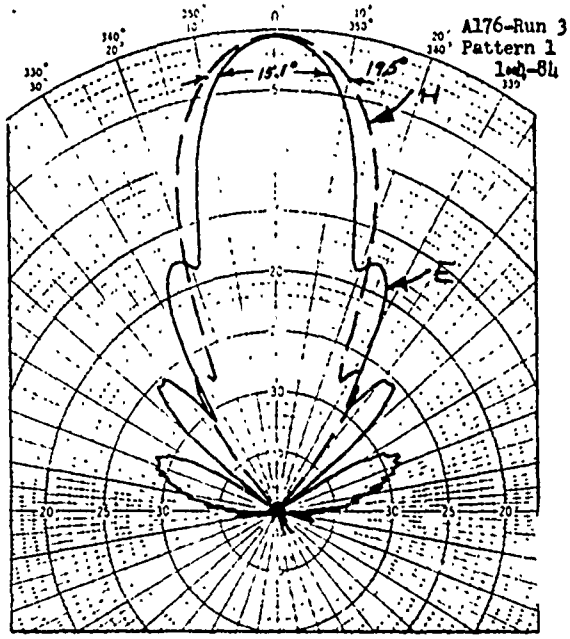

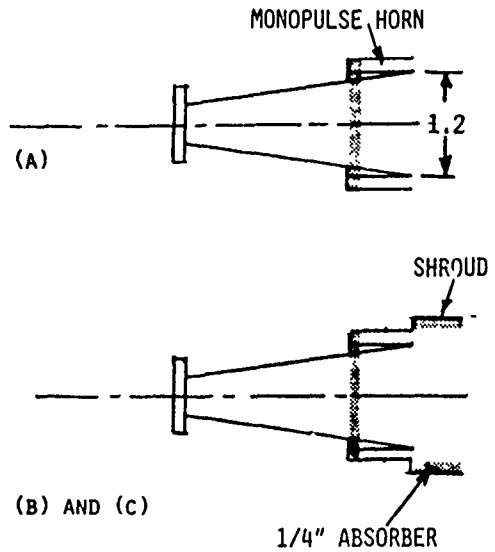

(A) With monopulse horn

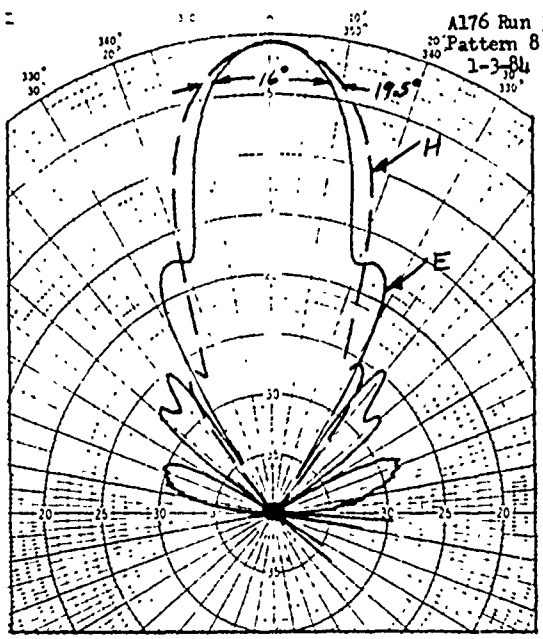

(B) With shroud around monopulse horn

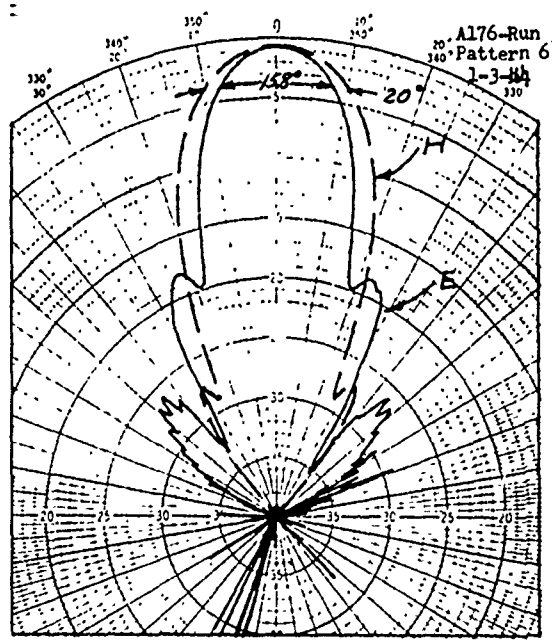

(C) With absorber-lined shroud around monopulse horn

Figure 11. Patterns of 1.2-in. diameter horn with monopulse horn

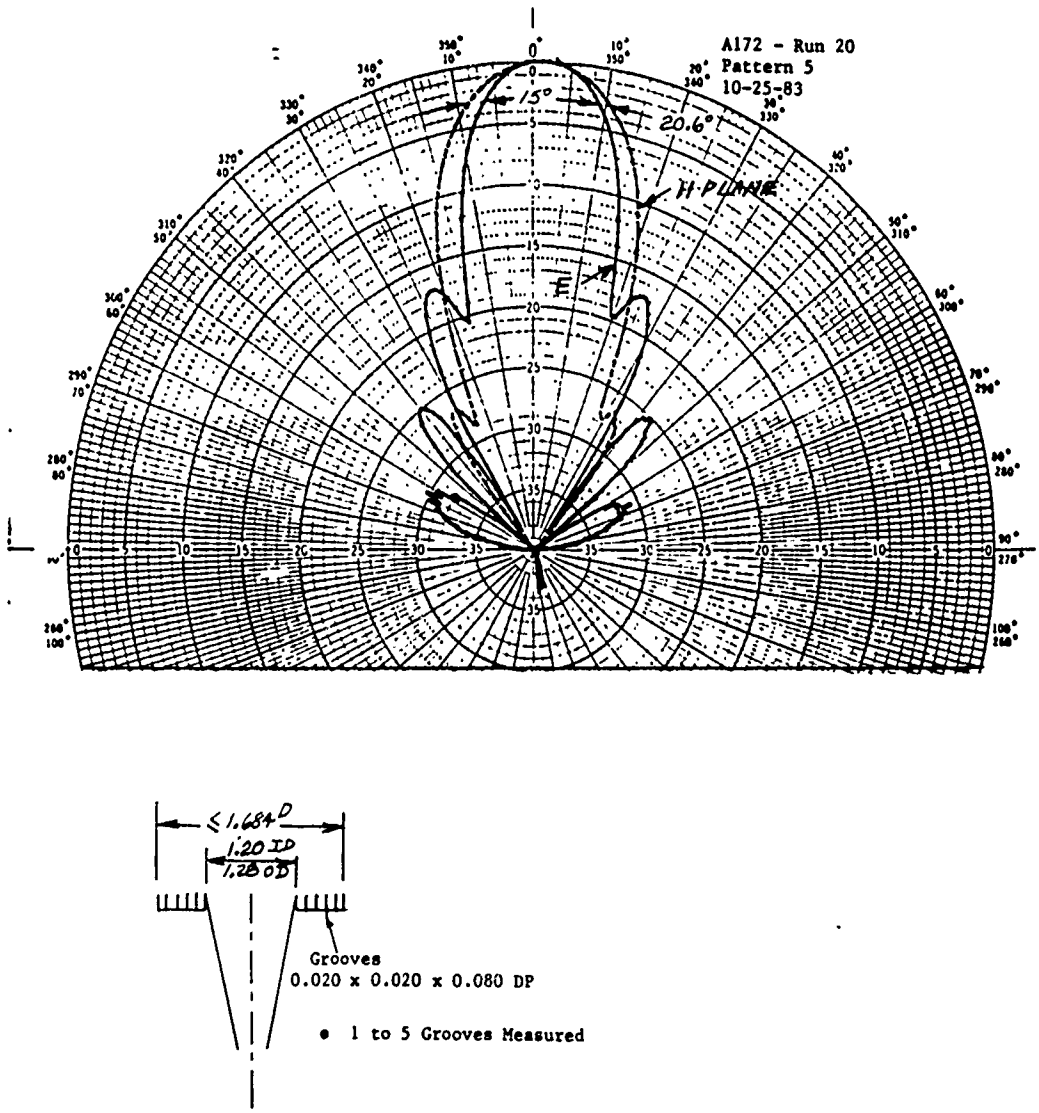

Figure 12. Patterns of 1.2-in. diameter horn with aperture chokes

leading to reduced reflector gain (few tenths dB) and an increase in the near-in sidelobes. Incorporating the aperture chokes for sidelobe reduction appears to have little value.

C. Feed horn-Oversized Subreflector Patterns

1. Basic Subreflector

Horn-subreflector combinations were measured using two posts on the linear stages. The center of rotation for these measurements is the vertex of the subreflector. The stage moving the horn was then adjusted for the proper horn-to-subreflector spacing, as illustrated in Fig. 2. The phase center of the conical horn lies 0.275 in. behind the aperture plane based on the secondary reflector patterns.

The oversized subreflector patterns with the 1.2-in. diameter horn are shown in Fig. 13. The upper portion of the polar plot illuminates the reflector. The "edge of dish" angle is $\pm 73.7°$. The pattern indicates a relatively uniform aperture illumination. The region near $\psi = 180°$ represents spillover in the forward direction, which adds to the secondary pattern sidelobe levels. The 0 dBi level was established by integrating the measured patterns to determine directivity.

2. Oversized Subreflector with Attachments

Attachments added to the oversized subreflector were examined for horn-subreflector primary patterns that would yield lower reflector sidelobe levels. Referring to Fig. 4, zones 2 and 3 represent regions where sidelobe reduction can be achieved. If the edge illumination can be reduced, then the horn-subreflector spillover and reflector-edge diffraction can be reduced. A

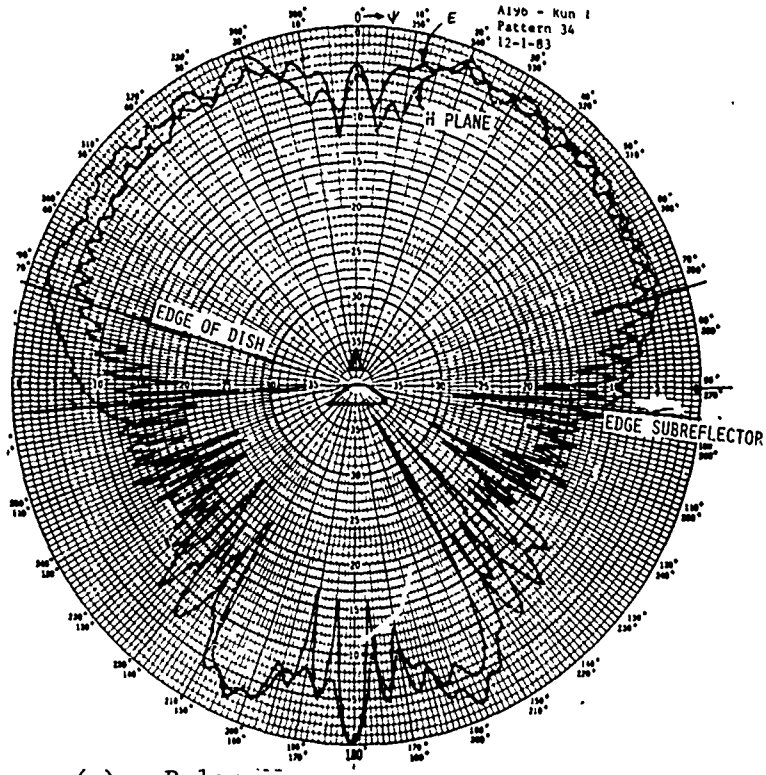

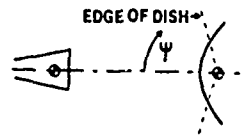

(a) Polar

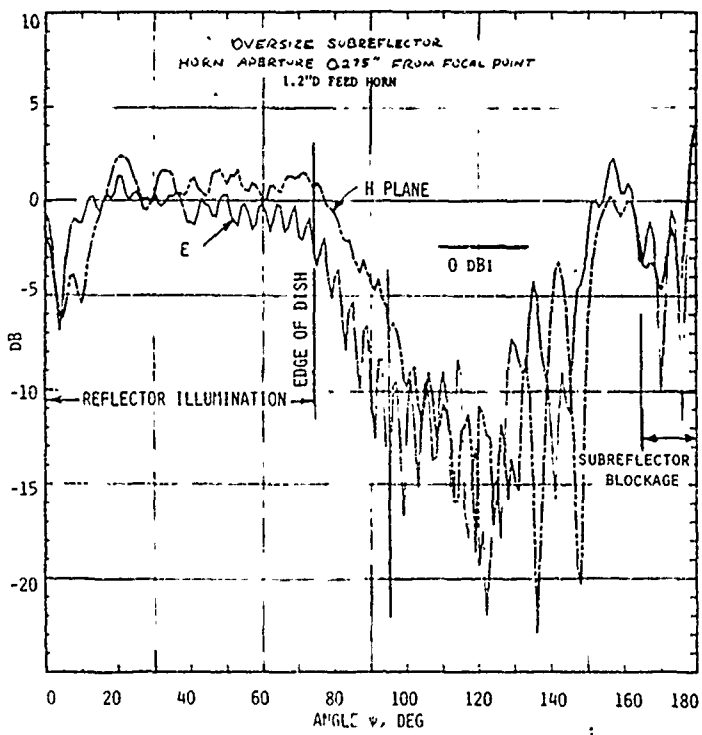

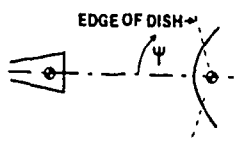

(b) Rectangular

Figure 13. Baseline patterns of 1.2-in. horn/oversized subreflector

10 dB reduction in edge illumination results in ~10 dB lower reflector backlobes (zone 3). If the forward spillover ($100 < \psi < 180$, Fig. 13) can be reduced, then the reflector sidelobes could also be reduced. Horn-subreflector attachment patterns were recorded for the combinations shown in Fig. 6.

a. Shroud

A cylindrical shroud was placed on the oversized subreflector to intersect the shadow boundary of the dish. The 0.618-in. length shroud has a diameter 0.5 in. greater than the subreflector, as illustrated in the inset of Fig. 14a. (The horn used in all the shroud measurements was a conical horn with an aperture diameter of 0.855 in. with a half flare angle of 6.40°, instead of the 1.2-in. horn, because of the availability of the smaller horn in the early stages of the measurements program. The smaller horn provides a few dB more edge illumination, but similar consequences were anticipated with the 1.2-in. horn). E and H plane patterns are shown in Fig. 14a. Notice that the aperture illumination is non-uniform in amplitude; thus, as a pattern for illuminating a reflector it is useless.

The inner surface of the 0.618 in. length shroud was filled with 1/4 in. AN 72 flat absorber up to the shadow boundary, with the resultant pattern shown in Fig. 14b. The aperture fields are more uniform than those of Fig. 14a but would most likely provide no improvement in reflector sidelobe levels as compared to the bare subreflector (Fig. 13).

An 0.545-in. length shroud with the same diameter as the subreflector (2.919 in.) extending to the dish shadow boundary was installed and the horn-subreflector pattern recorded as shown on Fig. 15. The pattern without absorber shows deep holes in the portion that illuminates the reflector. By

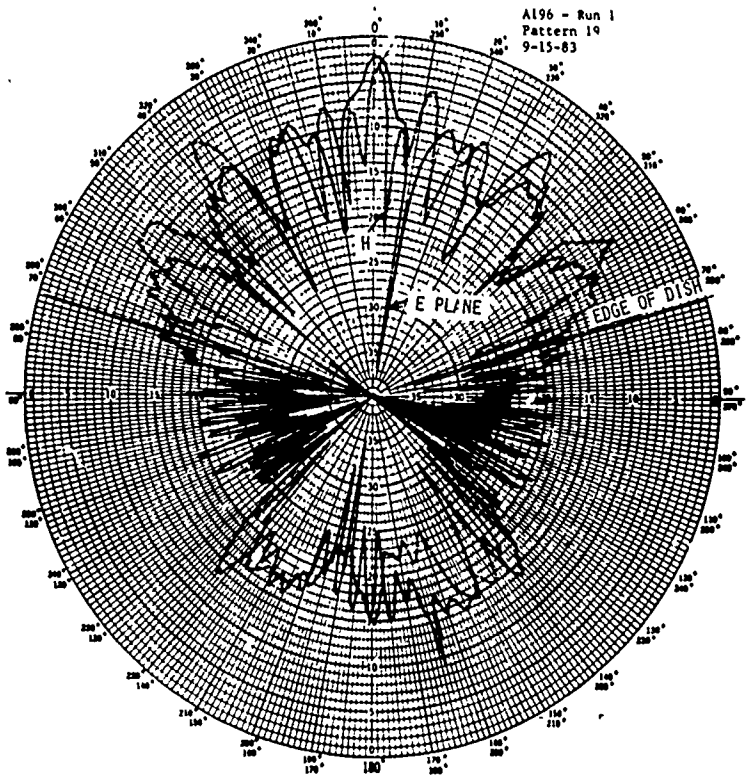

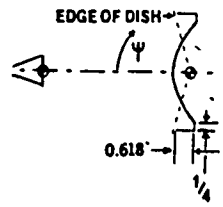

(a) Without absorber

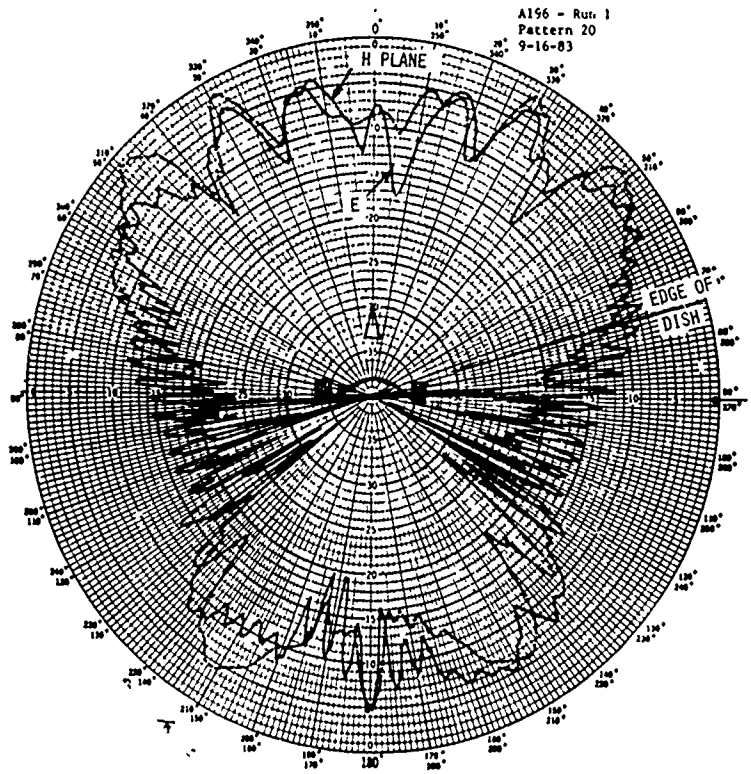

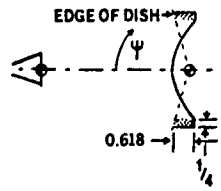

(b) With absorber

Figure 14. Patterns of horn/oversized subreflector with cylindrical shroud (with and without absorber on shroud inner surface)

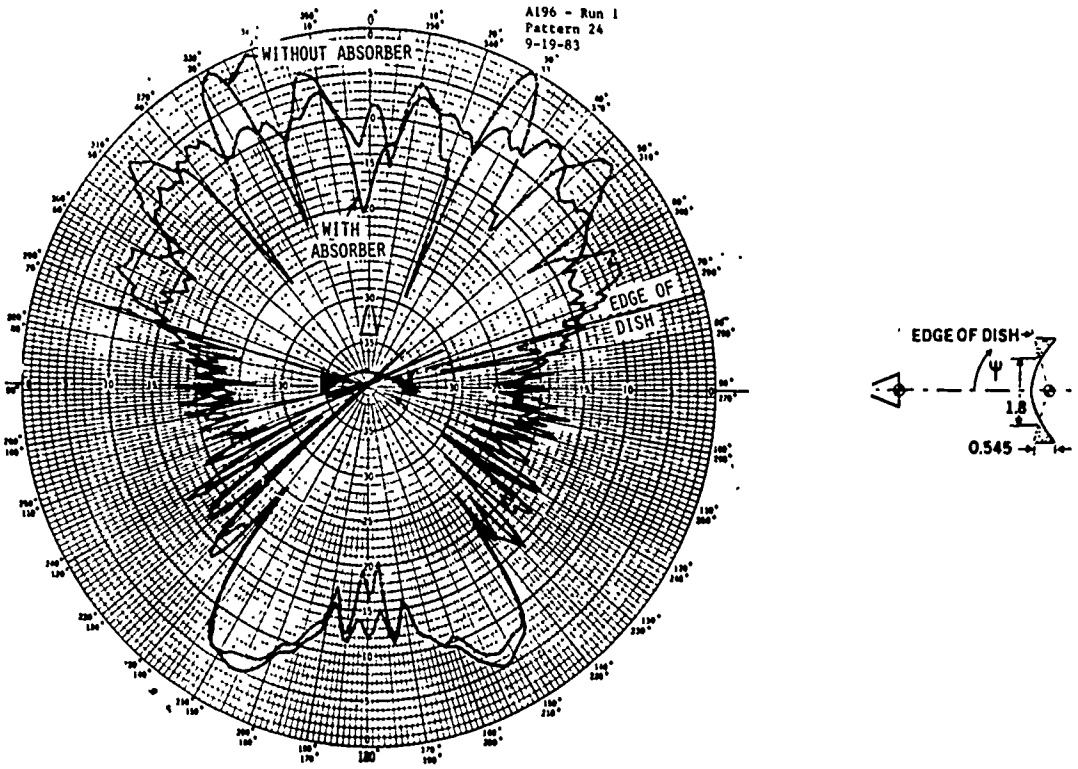

Figure 15. Oversized subreflector with cylindrical shroud with and without absorber along the surface of the oversized portion of the subreflector.

placing absorber along the oversized portion of the subreflector and up to the dish shadow boundary, leaving an exposed area of the subreflector of 1.8 in. diameter, the pattern (with absorber, Fig. 15) uniformity improved considerably. The large variation in amplitude with the shrouds (Figs. 14 and 15) may have been caused by overmoding in a cavity consisting of the shroud and subreflector surface. To illustrate this point, as shown in Fig. 15, the absorber in the oversized portion of the subreflector tends to dampen out the large fluctuations in amplitude.

b. Corrugations

A corrugated ring with 11 grooves along the dish shadow boundary was placed on the oversized subreflector. The grooves are 0.02-in. wide and 0.078-in. deep. The E and H plane patterns shown in Fig. 16a were measured using the 1.2-in. diameter conical horn. Figure 16b shows the horn-subreflector patterns with the corrugated ring moved back so that the corrugations are recessed 0.05 in. from the shadow boundary. The corrugations do not yield uniform aperture fields but the edge taper is down 10 to 15 dB which is beneficial for lower sidelobes.

Corrugations were placed above and along the oversized portion of the subreflector. The corrugated section had 11 circumferential grooves, each groove 0.02-in. wide and 0.078-in. deep. The measured patterns are reasonably uniform as shown in Fig. 17. The "hole" in the H plane ($\psi < 15°$) is not expected to be significant because it is in the region of the subreflector aperture blockage. Since the edge illumination is relatively high, the edge-diffracted radiation will be high and spillover is high, so the corrugations are not expected to be beneficial for sidelobe reduction. Note that these corrugations were not flush with the subreflector surface.

A review of Figs. 16 and 17 shows that none of the patterns have adequate prominent sidelobe-reduction features to warrant further studies.

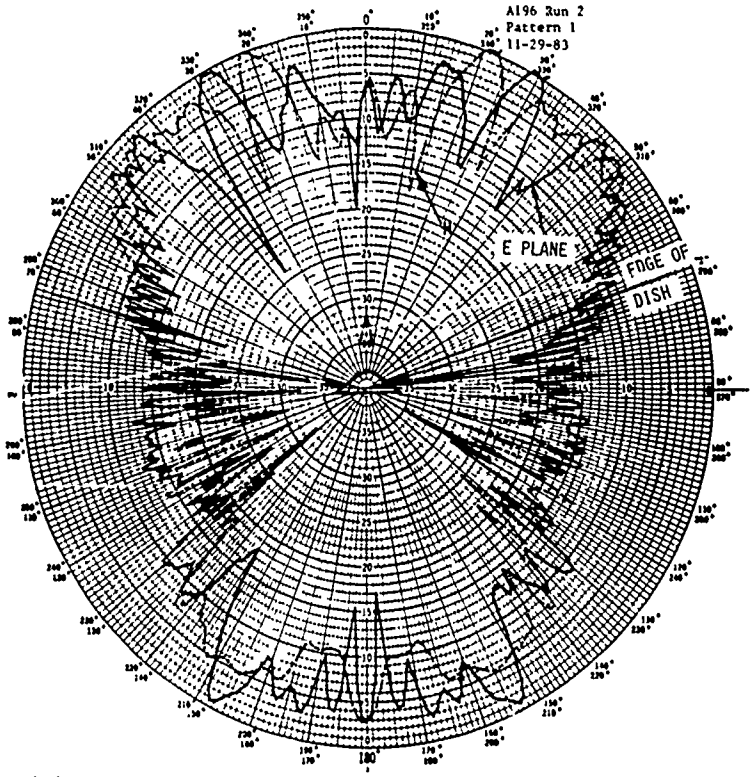

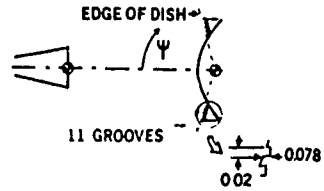

(a) Corrugations along shadow boundary

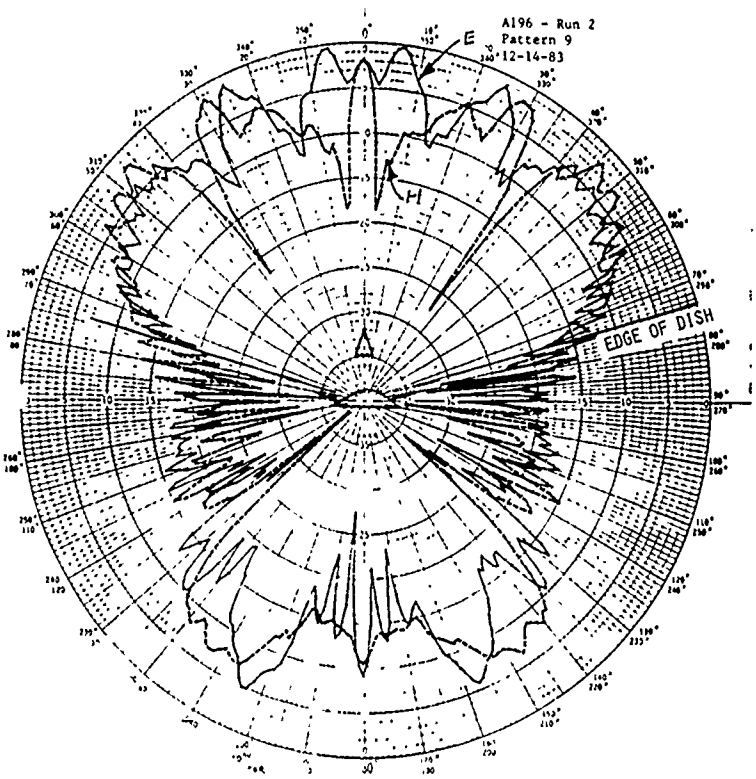

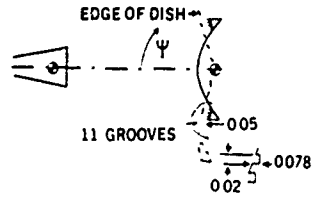

(b) Corrugations recessed 0.05 in. from shadow boundary

Figure 16. Horn/oversized subreflector patterns with corrugations parallel to dish shadow boundary

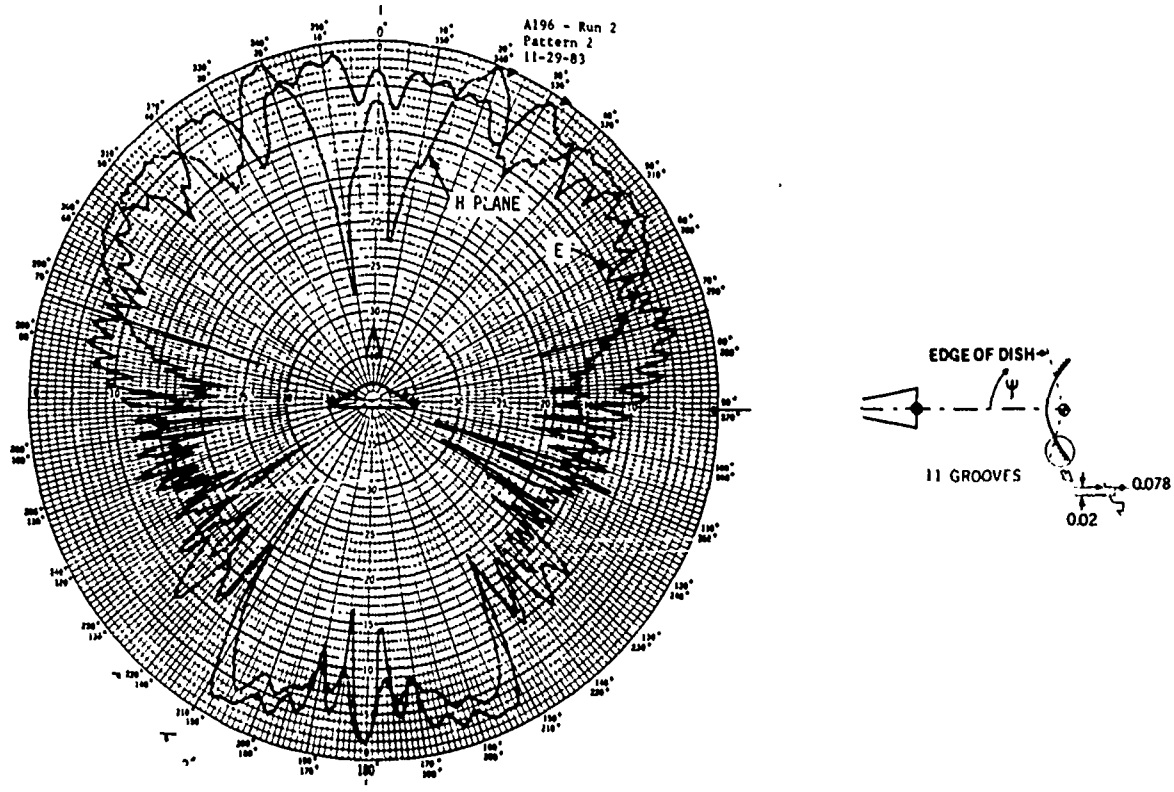

Figure 17. Horn/oversized subreflector patterns with corrugations along the surface of the oversized-portion of the subreflector

c. Conical Flange

Three conical flanges (1, 1.5 and 2λ wide) were evaluated; however, only the 1λ and 2λ data are shown. The patterns for 1λ wide ring with an angle 17° from vertical are shown in the rectangular representation of Fig 18a. The patterns of Fig. 18b are for the 2λ wide flange with an angle 21.3°. As compared to the baseline horn-subreflector patterns of Fig. 13b, the conical flange patterns yield less forward spillover and less radiation in the $\psi \approx 120°$ region. However, as a net result on the reflector secondary pattern only a slight reduction (probably 1 or 2 dB) in the forward-region sidelobe levels is expected.

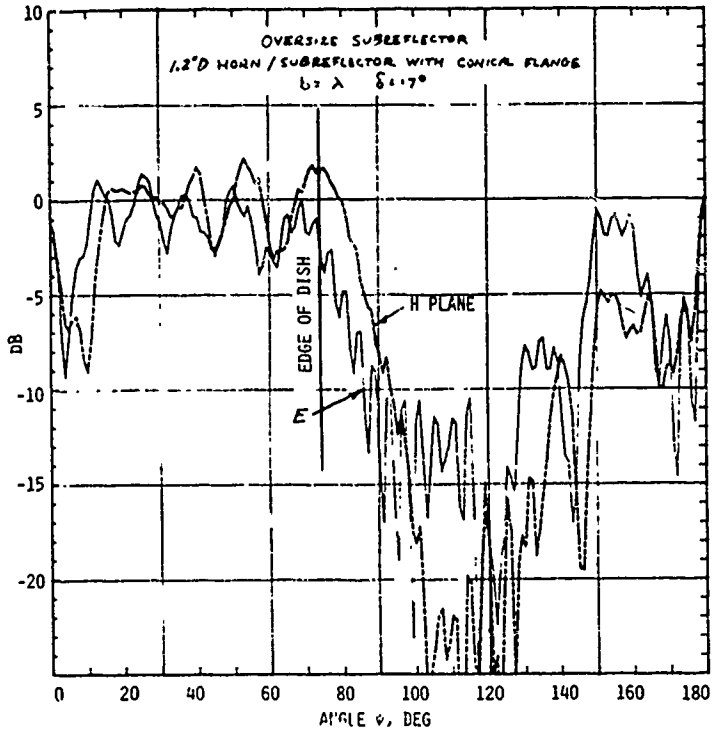

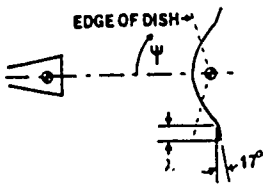

(a) 1λ

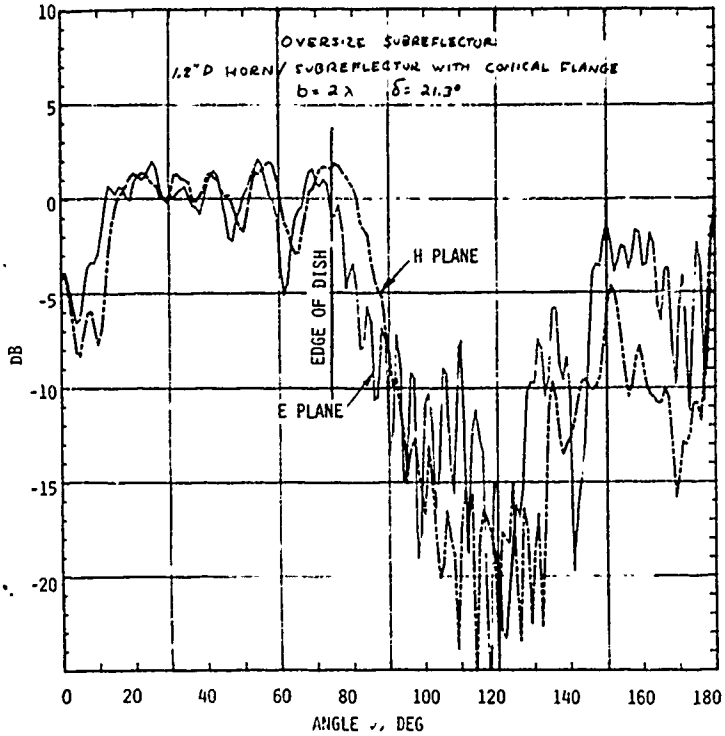

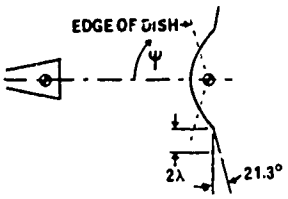

(b) 2λ

Figure 18. Horn/oversized subreflector patterns with 1λ and 2λ wide conical flange

d. Absorber Ring

A ring of 1/4-in. flat absorber (AN 72) was placed on the oversized subreflector along the shadow boundary. The absorber leaves an exposed area of the subreflector with a diameter of 1.8 in. The E and H plane patterns are shown in Fig. 19. The spillover power level is about the same high level as the baseline pattern of Fig. 13. The absorber ring has an advantage because of the reduced edge illumination, which will yield lower backlobe levels in the secondary pattern. Thus, the absorber ring may be useful as a sidelobe-reduction technique if one is limited to the use of an oversized subreflector. The use of an absorber ring may raise the noise temperature of the antenna as horn spillover power is being absorbed. Also, for high-power transmit antennas, dissipation of the absorbed power may be a consideration.

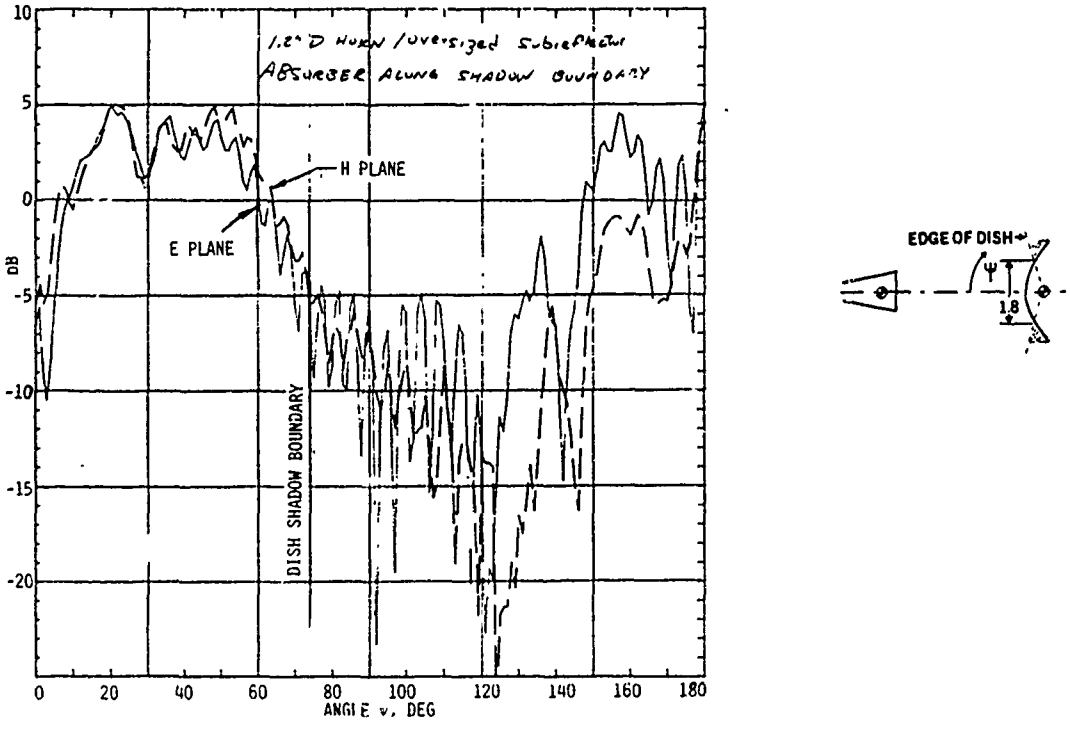

Figure 19. Horn oversized subreflector patterns with absorber ring along dish shadow boundary

D. Feed Horn/Conventional Subreflector Patterns

The geometry of the horn-subreflector is illustrated in Fig. 2b. The 1.2-in. diameter horn was used with all the conventional subreflector measurements.

1. Basic Subreflector

The conventional subreflector and the horn as an assembly was measured with the patterns shown in the rectangular plot of Fig. 20. The 0 dBi level was determined by integrating the measured patterns to determine directivity. As compared to the oversized subreflector (Fig. 13), the conventional subreflector yields ~ -15 dB edge taper and less spillover power which would result in lower secondary pattern sidelobes. The improvement will be shown in Sec. IV (Experimental) and Sec. V (Theoretical).

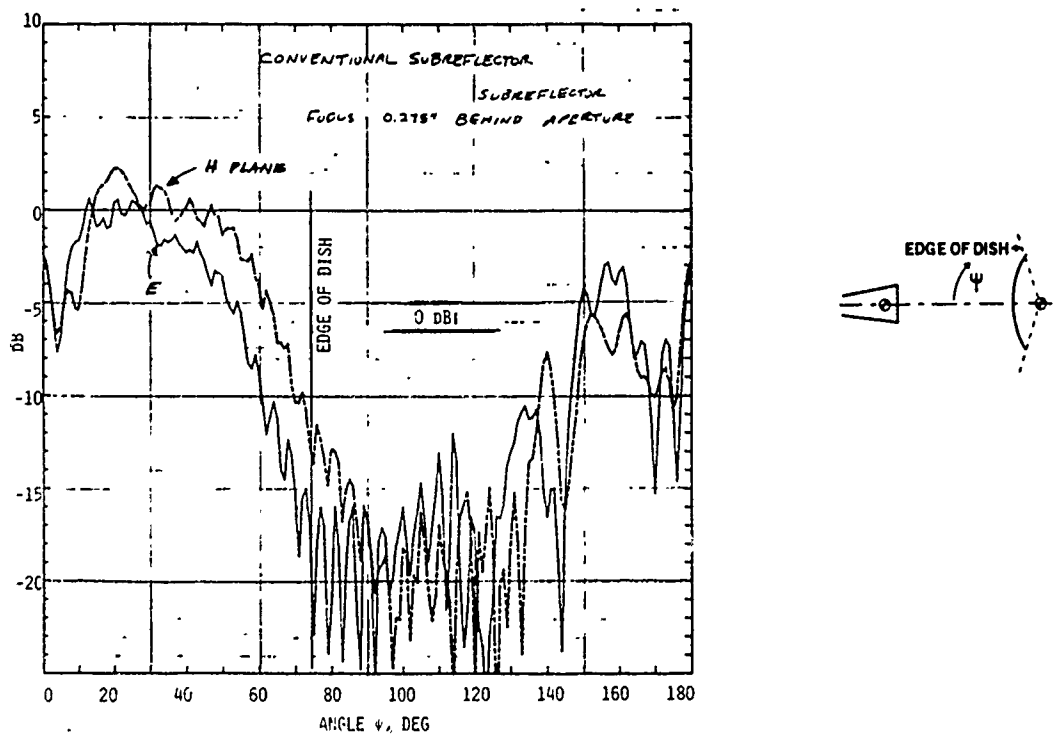

Figure 20. Baseline patterns of 1.2-in. horn/conventional subreflector

2. Conventional Subreflector with Attachments

To reduce the sidelobes for a conventional subreflector, three techniques were evaluated as illustrated in Fig. 7 -- a conical flange, corrugations and an absorber ring.

a. Conical Flange

The same conical flanges used with the oversized subreflector were also used with the conventional subreflector. The horn/conventional-subreflector patterns with the 1λ and 2λ wide flanges are shown in Fig. 21. Although the conical flanges provide some reduction (a few dB) in the edge illumination and slightly less spillover power, as compared to the baseline pattern of Fig. 20, the net improvement in the secondary pattern is a few dB (see Sec. V). Any sidelobe reduction will be at the expense of increased aperture blockage, but probably with an insignificant loss in gain.

b. Corrugations

An arrangement of circumferential corrugated rings was attached to the conventional subreflector. One to four grooves were fabricated and measured. The grooves are 0.02-in. wide, 0.085-in. deep with 0.020-in. gaps aligned along the shadow boundary. The patterns for the 4-groove case are shown in Fig. 22a. It shows an edge taper of ~18 to 20 dB which should be beneficial for lower secondary-pattern sidelobes. With the corrugated ring moved back so that the corrugations were recessed 0.05 in. from the shadow boundary, the resultant patterns are shown in Fig. 22b. The edge illumination is higher compared to the corrugations flush with the shadow boundary.

In comparing the horn-subreflector patterns for the conical flanges and the corrugations, the corrugated patterns (Fig. 22a) have a slight advantage

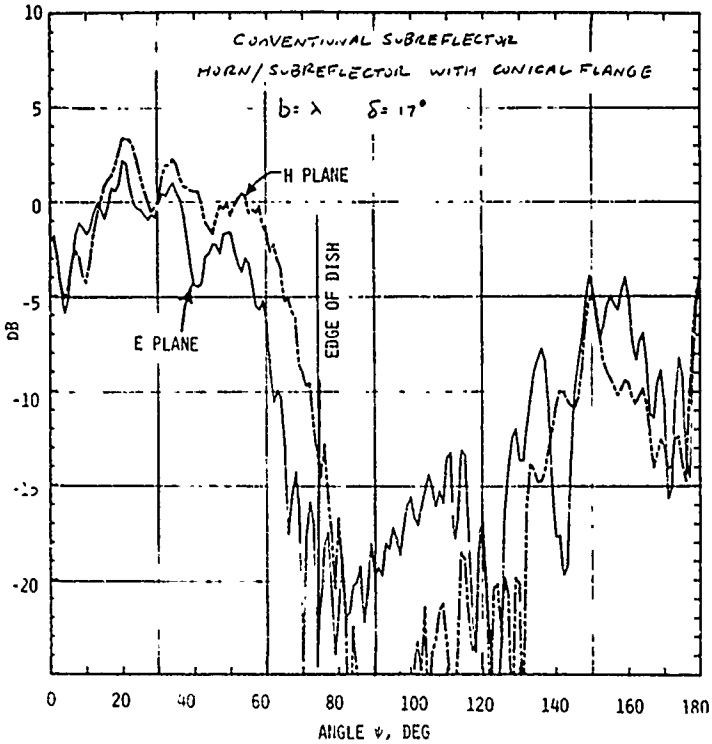

(a) 1λ

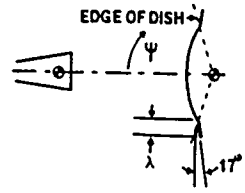

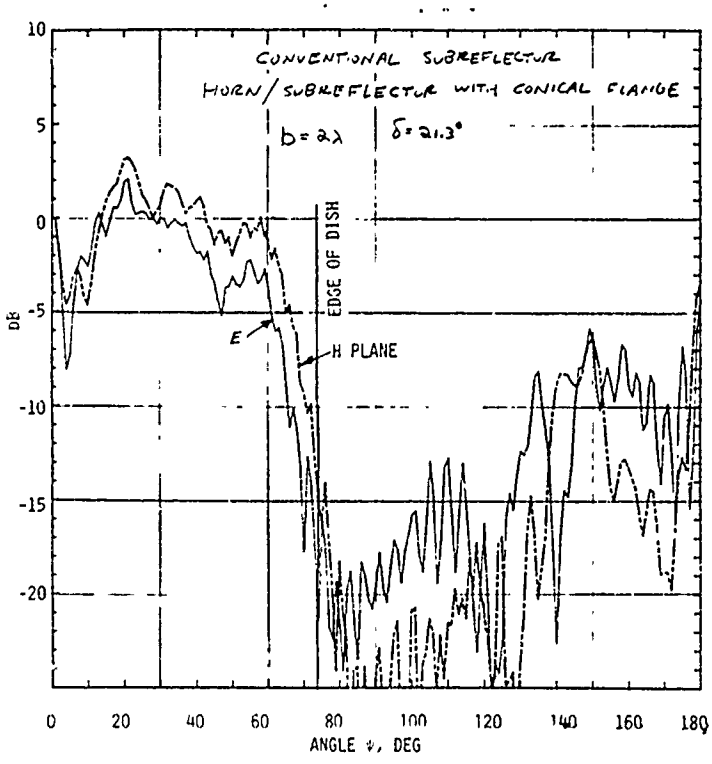

(b) 2λ

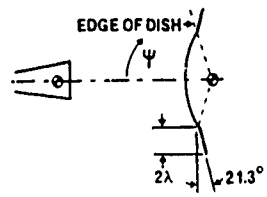

Figure 21. Horn/conventional subreflector patterns with 1λ and 2λ wide conical flange

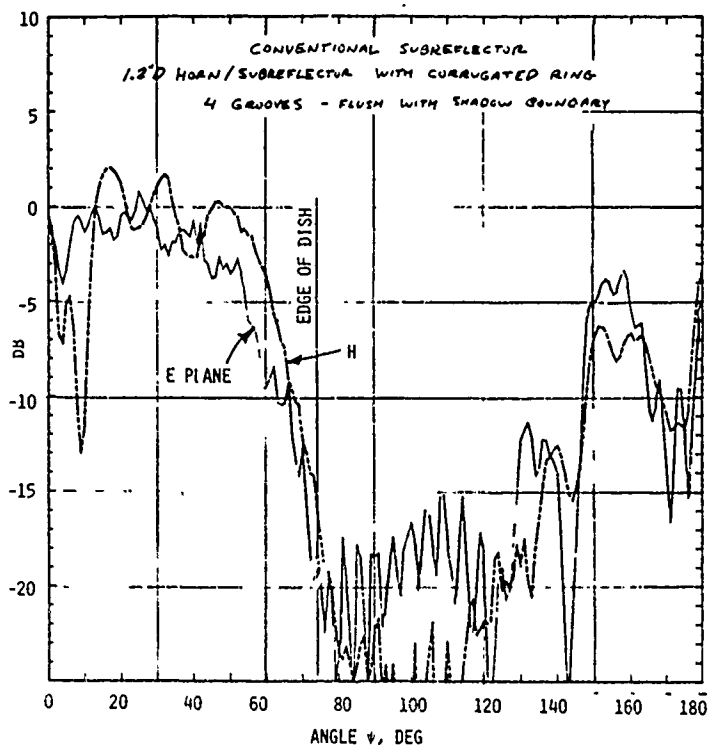

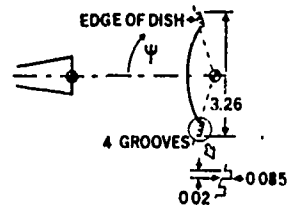

(a) Corrugations along shadow boundary

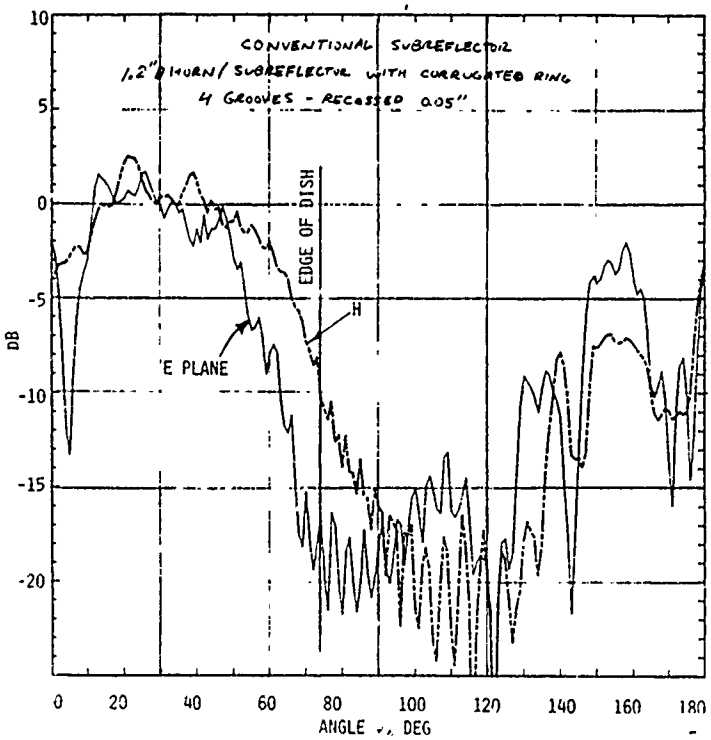

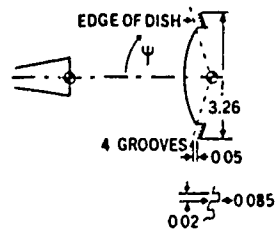

(b) Corrugations recessed 0.05 in. from shadow boundary

Figure 22. Horn/conventional subreflector patterns with corrugations parallel to dish shadow boundary

over the conical flange case. Although the corrugations are more difficult to construct, they will reduce reflector backlobe levels compared to the baseline conventional subreflector and a smaller improvement as compared to the conical-flanged subreflector.

c. Absorber Ring

An absorber ring (~ 2λ wide) of 1/4-in. flat absorber (AN 72) placed on the conventional subreflector with the absorber along the dish shadow boundary did not provide significant horn-subreflector pattern (Fig. 23) improvement over the basic pattern of Fig. 20. This is in contrast to the oversized subreflector with the absorber ring, which reduced the edge illumination by 7 to 8 dB.

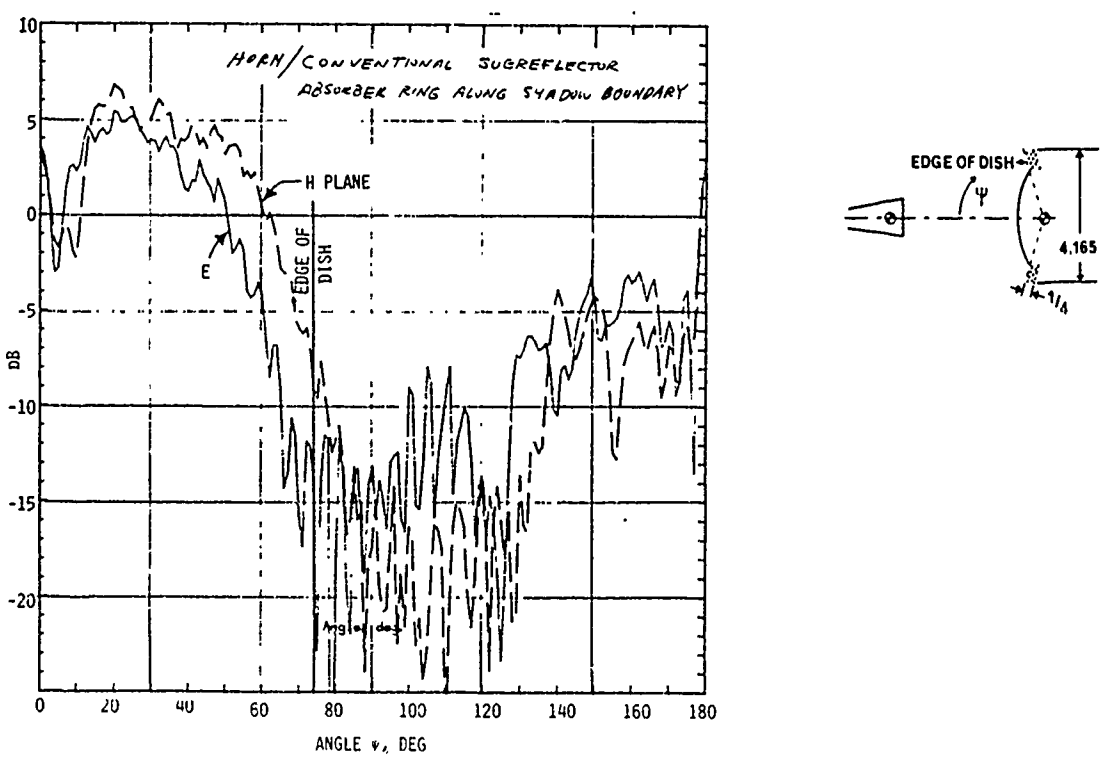

Figure 23. Horn/ conventional subreflector patterns with absorber ring along dish shadow boundary

E. Conclusions

The shrouds, corrugations, conical flanges and absorber rings evaluated for both the oversized and conventional subreflectors indicated that no one feature will produce significant reflector sidelobe level reduction. As Sec. V will illustrate, a reduction of 20 dB in the forward spillover power reduces the reflector forward-region sidelobes 5 to 10 dB. Although this is an improvement, it is difficult to reduce the forward spillover power to a -20 dB level.

The conventional subreflector yields lower edge illumination and spillover power, as compared to the oversized subreflector; thus, the best main-reflector sidelobe characteristics will be obtained with the conventional subreflector.

IV. MEASURED REFLECTOR PATTERNS

The 2-ft reflector pattern measurements are described. A 95 dB dynamic range was achieved in these measurements and the instrumentation and range requirements are described. Pattern measurements with oversized and conventional subreflectors are presented along with the patterns for the reflector shroud and fence. The fence is merely a partial circumferential shroud in the plane for which the sidelobes are to be reduced. Not all of the shielding combinations depicted in Figs. 6 and 7 were measured. Since the dish patterns can be computed accurately with the measured horn-subreflector patterns, comparison of sidelobe variations can be done by evaluating computed reflector patterns. Section V will demonstrate the agreement between the measured and computed reflector patterns.

A. Measurement Technique

The minimum sidelobe levels of the 2-ft reflector antenna without control were expected to be approximately -75 dB below the beam peak. For the anticipated sidelobe reduction techniques, measurements over a 95 dB or greater dynamic range are required. The instrumentation for these measurements was developed in-house[3] based on a Scientific-Atlanta (SA) wideband receiver (Model 1742) used with a phase-locked Gunn diode local oscillator and transmitter. The modified receiver has a sensitivity of -120 dBm or a 30 dB enhancement in sensitivity with the phase-locked circuitry as compared with the conventional instrumentation. In the past, we have been able to make antenna pattern measurements over a 120 dB dynamic range with this system; however, during this study the mixer-preamplifier circuit was degraded by ~20 dB. With the short program schedule, the receiver could not be repaired in a timely manner, so our dynamic range was limited to 90 to 95 dB.

In conventional antenna pattern measurements, the antenna under test is usually rotated in azimuth. However, with ground multipath and reflections from surrounding buildings, the 2-ft reflector was rotated in elevation so that the antenna boresight axis is always pointing upwards to the sky. The photograph of Fig. 24 shows the antenna mounted for elevation-plane measurements, utilizing the polarization axis of the SA test mount.

RF shielding of the electronics enclosures and the reflector surface is a necessity for low-sidelobe antenna measurements to eliminate leakage components. The seams of the box housing the 38 GHz receiver were sealed with aluminum tape. Waveguide joints were taped and often wrapped with absorber material. The four small openings in the reflector for the passage of the four subreflector-support struts also had to be taped, since their contributions exceeded the noise level by about 10 dB. Figure 25 shows a photograph of the electronics box which houses the RF front end. The system noise and leakage levels shown in Fig. 26 were recorded with the feed horn aperture filled with absorber material and sealed with copper tape. These levels are ~ - 95 dB below the peak gain level. Larger dynamic range could have been achieved if the mixer-preamplifier unit was repaired.

The main lobe and the first few sidelobes were measured with 20 or 30 dB of attenuation inserted in the system to preserve linearity. The far-out sidelobes were measured with the attenuator removed. This technique results in two pattern levels on the recording chart with a scale for the main-beam portion and a second scale for the far-out sidelobes appearing on the pattern recordings. These scales represent the absolute gain values of the antenna. The peak gain of the 2-ft antenna is ~ 45.5 dBi. Linearity was achieved over the entire dynamic range, except for a 1 or 2 dB compression at the higher power levels causing a nonlinear beam peak recording. This correc-

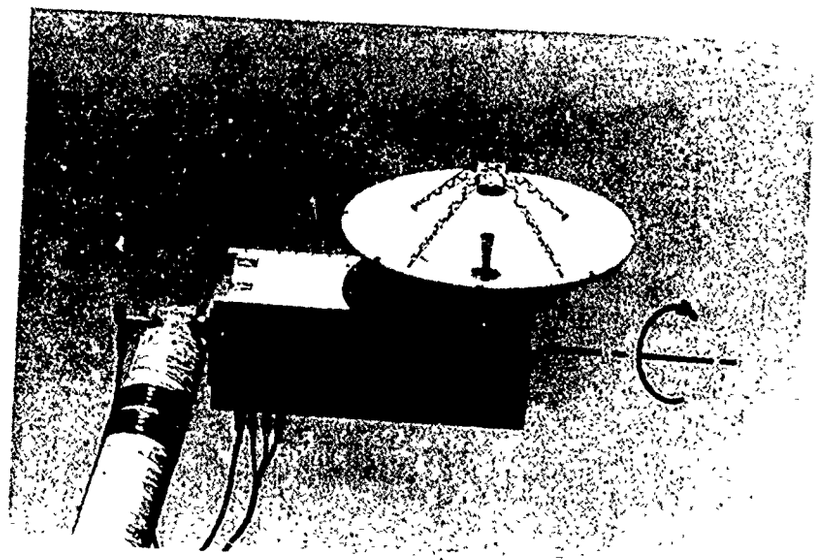

Figure 24. 2-ft reflector mounted for elevation-plane pattern measurements

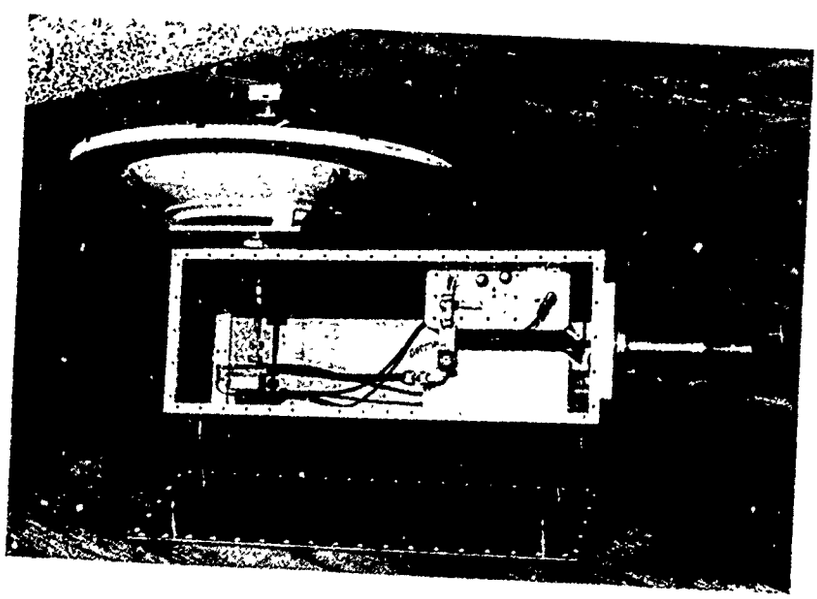

Figure 25. 38 GHz receiver and enclosure

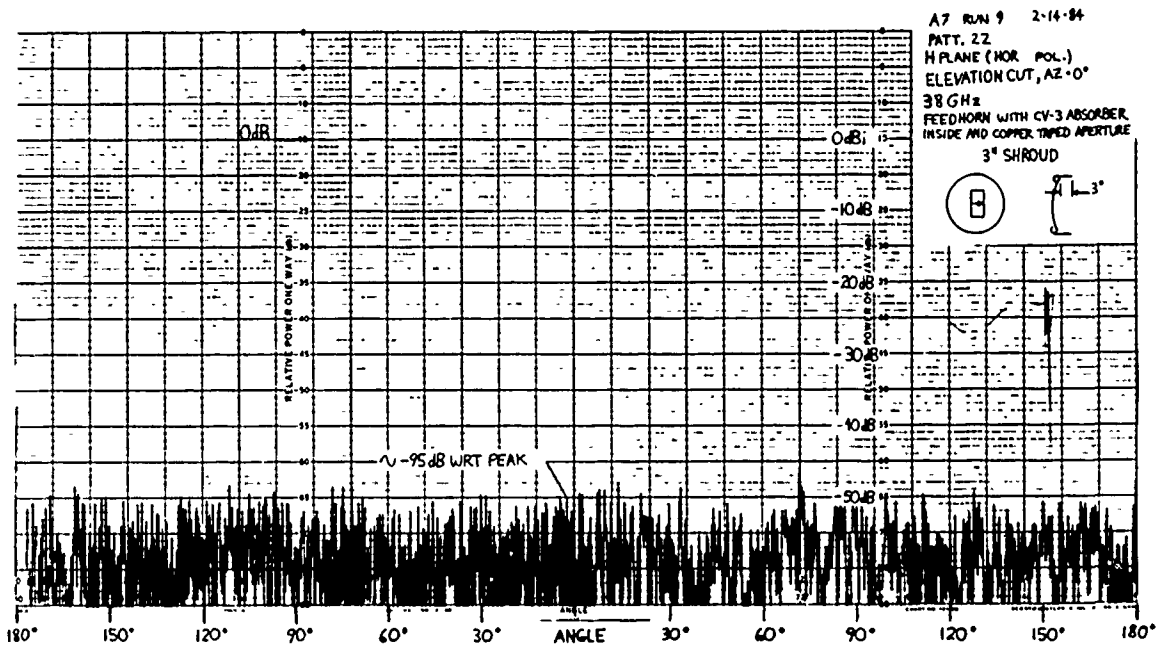

Figure 26. System noise level

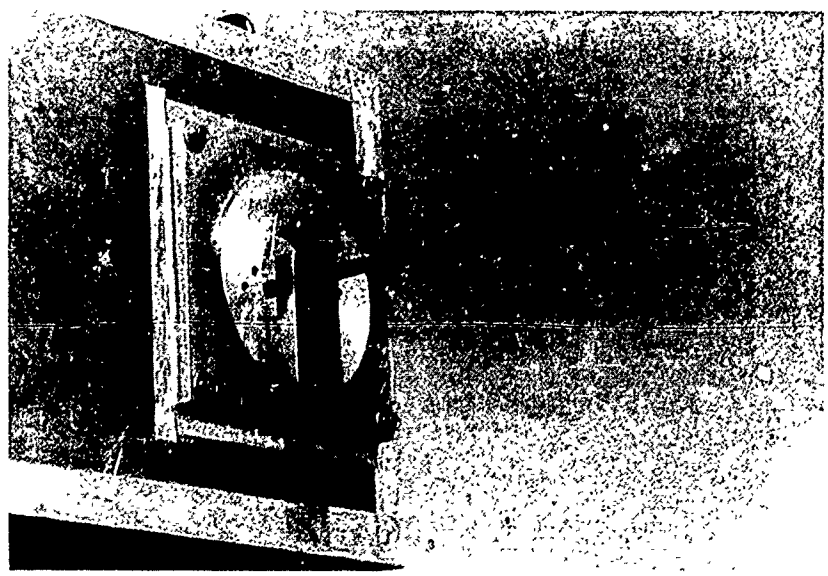

Figure 27. Standard gain horn connected for establishing the absolute gain level

tion for nonlinearity was not made because the absolute sidelobe levels are the most important data to be extracted from the patterns. Gain measurements were done by substituting a standard-gain horn for the 2-ft antenna and comparing the difference in power levels. Figure 27 shows the reference horn connected to the receiver.

B. Oversized Subreflector

Patterns of the 2-ft reflector (oversized subreflector, Fig. 2a) with and without a circumferential metallic shroud (3 in. and 5 in.) and with the shroud bare and lined with absorber were recorded. The 3-in. shroud used 1/4 in. thick (flat) absorber (Emerson and Cuming AN-72) while the 5-in. shroud was measured with both the AN-72 and 1-in. thick pyramidal absorber (Rantec EHP-1).

The 1.2-in. diameter (3.86λ) conical feedhorn and the subreflector yields almost uniform aperture illumination as depicted in the horn-subreflector patterns of Fig. 13. Thus, a significant amount of spillover past both the main and subreflectors contributes to high sidelobe levels.

The patterns reported are tabulated as follows:

Figure	Description
28	Baseline patterns of 2-ft reflector
30	3-in. circumferential metal shroud
31	3-in. shroud with 1/4-in. thick absorber on inside of shroud
32	3-in. shroud with 1/4-in. thick absorber on outside of shroud
33	3-in. shroud with 1/4-in. thick absorber on both sides of shroud
34	5-in. circumferential metal shroud
35	5-in. shroud with 1/4-in. thick absorber on inside of shroud

36	5-in. shroud with 1/4-in. thick absorber on outside of shroud
37	5-in. shroud with 1/4-in. thick absorber on both sides of shroud
38	5-in. shroud with 1-in. pyramidal absorber on inside of shroud
39	5-in. shroud with 1-in. pyramidal absorber on outside of shroud
40	5-in. shroud with 1-in. pyramidal absorber on both sides of shroud

Figure 28 shows the baseline E and H plane patterns of the 2-ft reflector with an oversized subreflector.* The forward-region sidelobes ($\theta < 75°$) are attributed primarily to the horn-subreflector spillover. The prominent lobes at approximately $\pm 100°$ are caused by the main reflector edge diffraction. The back region is caused by the diffracted wave from the dish edge. The principal method to reduce the sidelobe levels in both the forward and rearward regions is to reduce the edge illumination. If there were freedom to enlarge the horn, then the beamwidth can be narrowed to reduce the edge illumination. Techniques using subreflector shroud, corrugations and conical flange did not appear attractive based on the horn-subreflector patterns of Figs. 14 through 18.

*Beam peak of patterns has been compressed

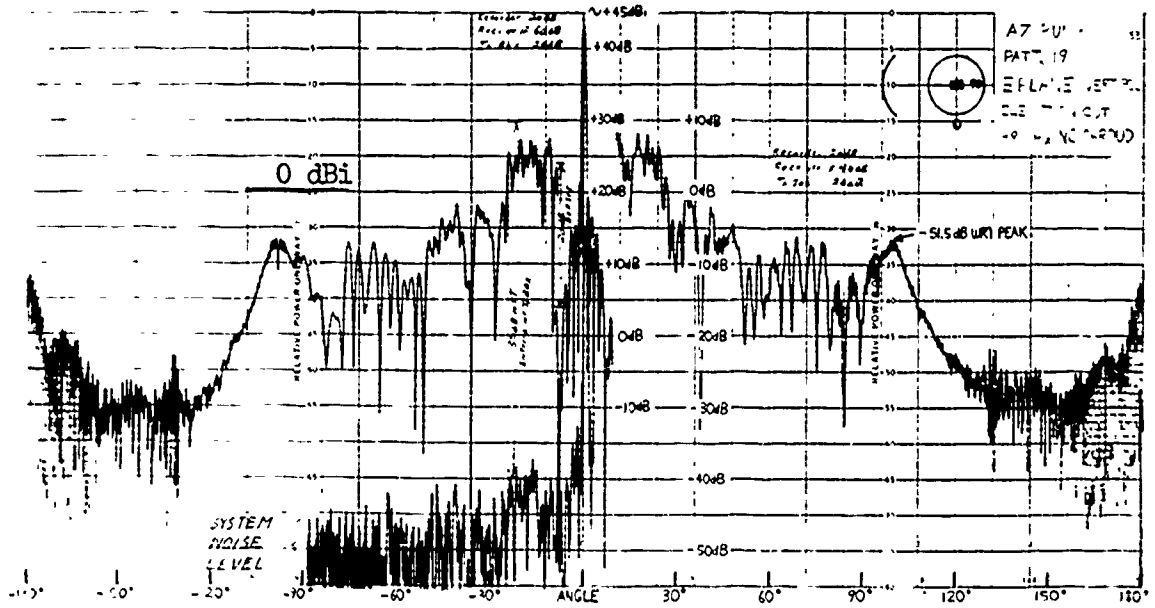

a) E Plane

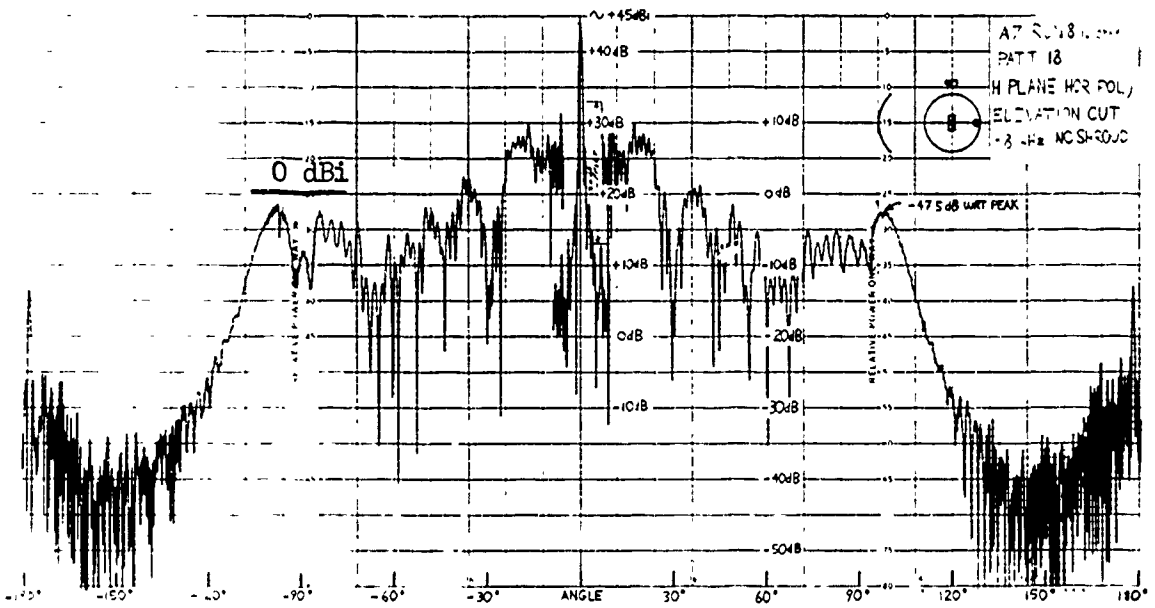

b) H Plane

12-28-83

Figure 28. Baseline patterns of 2-ft reflector with oversized subreflector

The circumferential shroud around the main reflector, as illustrated in Fig. 8 and the photograph of Fig. 29, was expected to reduce the main-reflector edge diffraction. In addition, tne angle from the boresight axis to the edge shadow boundary is reduced, thus, containing the forward radiation to a smaller angular region. (For example, a tunnel or long shroud would restrict the radiation over a narrow angle.) Figures 30 to 40 illustrate this point. The gain levels > -20 dBi are contained within the following angles from the main beam:

Shroud	Angle
None	$\pm$110°
3 in.	$\pm$ 95°
5 in.	$\pm$ 85°

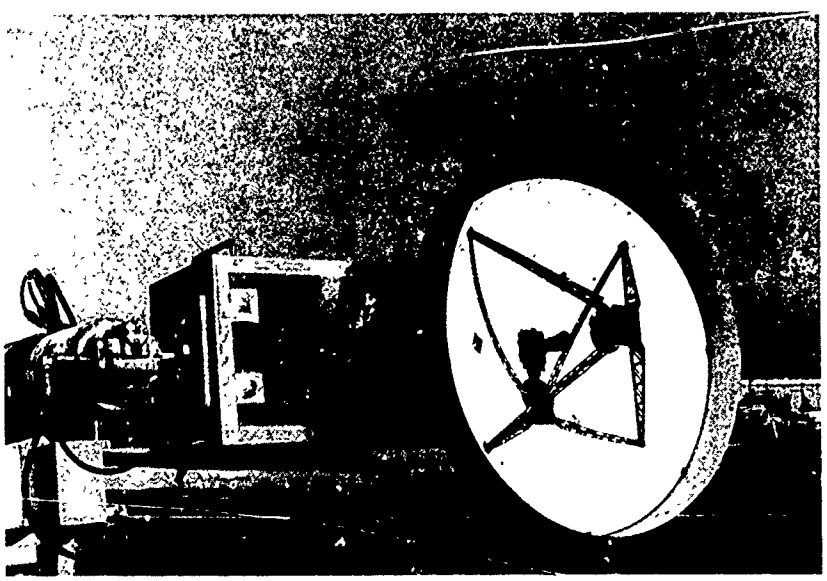

Figure 29. 2-ft reflector with 3-in. shroud

Or, we can say that pattern levels < -20 dBi have been increased 30° and 50° by using a 3 and 5 in. shroud, respectively.

The pattern characteristics of Figs. 30 to 40 can be summarized as follows:

- The forward-region sidelobes are unaffected by the shroud
- A bare metal shroud reduces the back lobes by ~ 10 dB
- Absorber on both sides of the shroud reduced the 180° backlobe (caustic) by ~ 10 dB
- Patterns in the -40 dBi levels may be questionable as they were close to the system noise level
- No apparent advantage whether the absorber is inside or outside of the shroud
- The 1-in. pyramidal absorber appears to be better than the 1/4-in. thick flat absorber
- Sidelobe reduction is better in the E plane

C. Conventional Subreflector

The patterns of the 2-ft reflector with the conventional subreflector were measured with a metallic circumferential shroud (3 in.) and a partial shroud (referred to as a plate). Elevation pattern cuts were made as well as azimuth pattern cuts to provide correlation between the two measurement techniques. Great circle cuts were also made by tilting the antenna at 35° and 45° elevation angles and rotating the antenna in azimuth.

The 1.2-in. conical horn provides a subreflector-edge taper of 19.3 and 11.3 dB, for the E and H planes, respectively (see the feedhorn patterns of Fig. 10 and the optics arrangement in Fig. 2b). In contrast to the oversized subreflector, the conventional subreflector yields the typical edge taper for reflector antenna system, thus, minimizing the spillover power and providing less edge illumination.

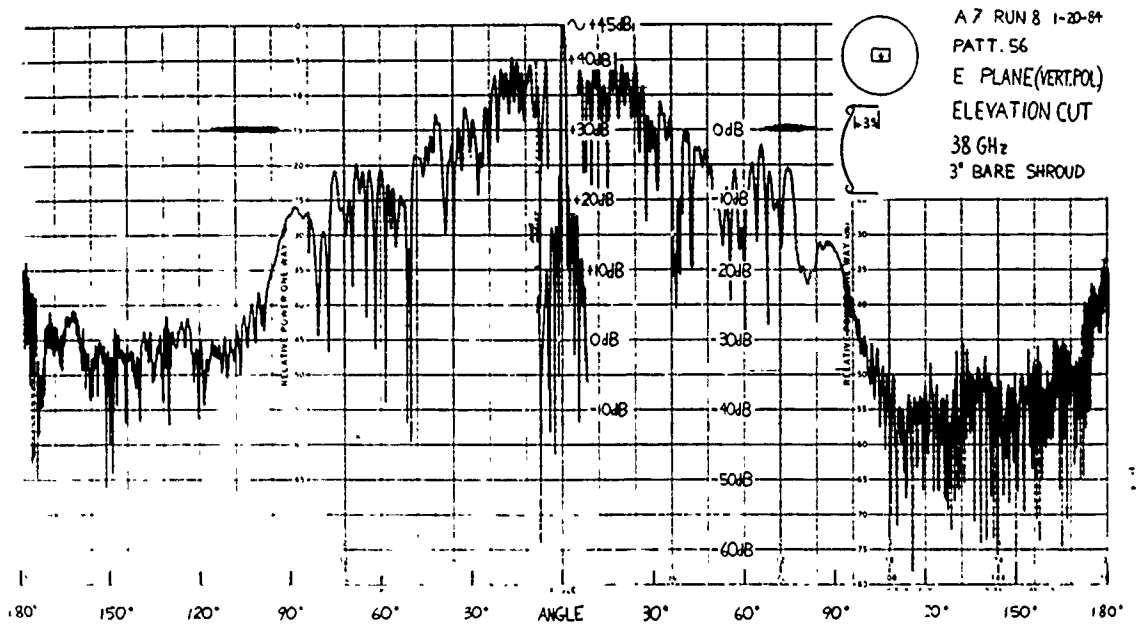

a) E Plane

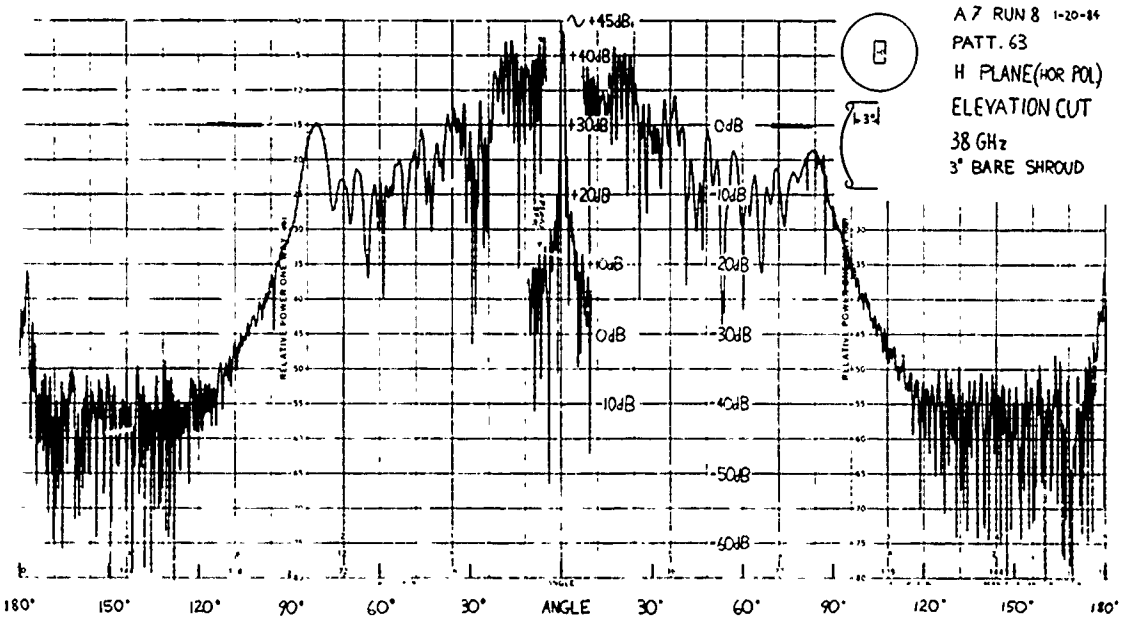

b) H Plane

1-25-84

Figure 30. 2-ft reflector (oversized subreflector) with 3-in. circumferential metal shroud patterns.

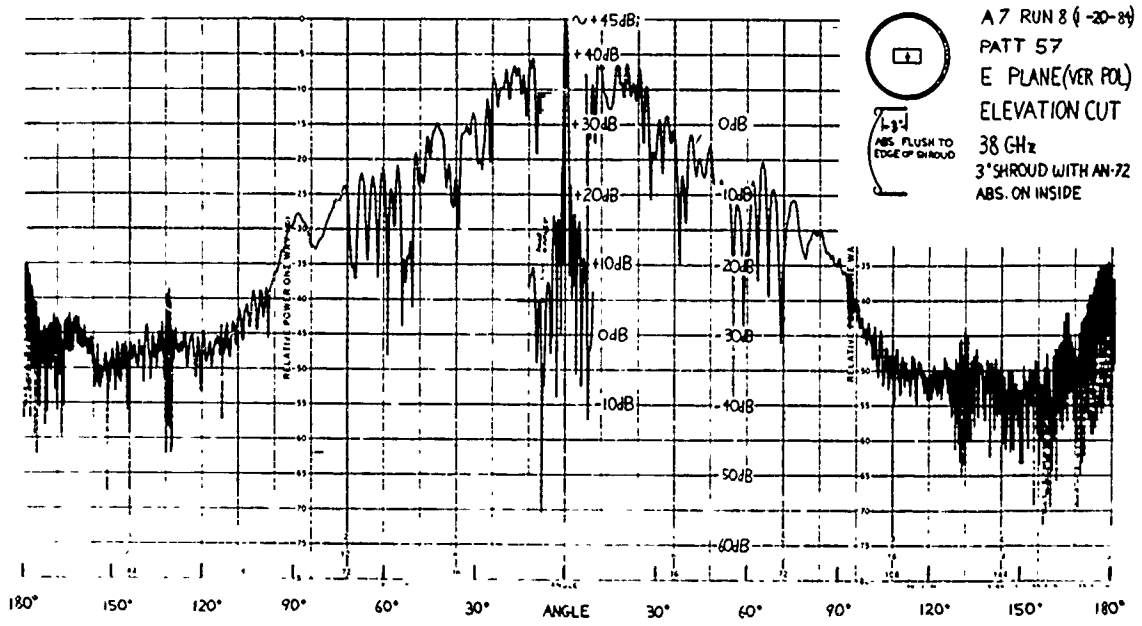

a) E Plane

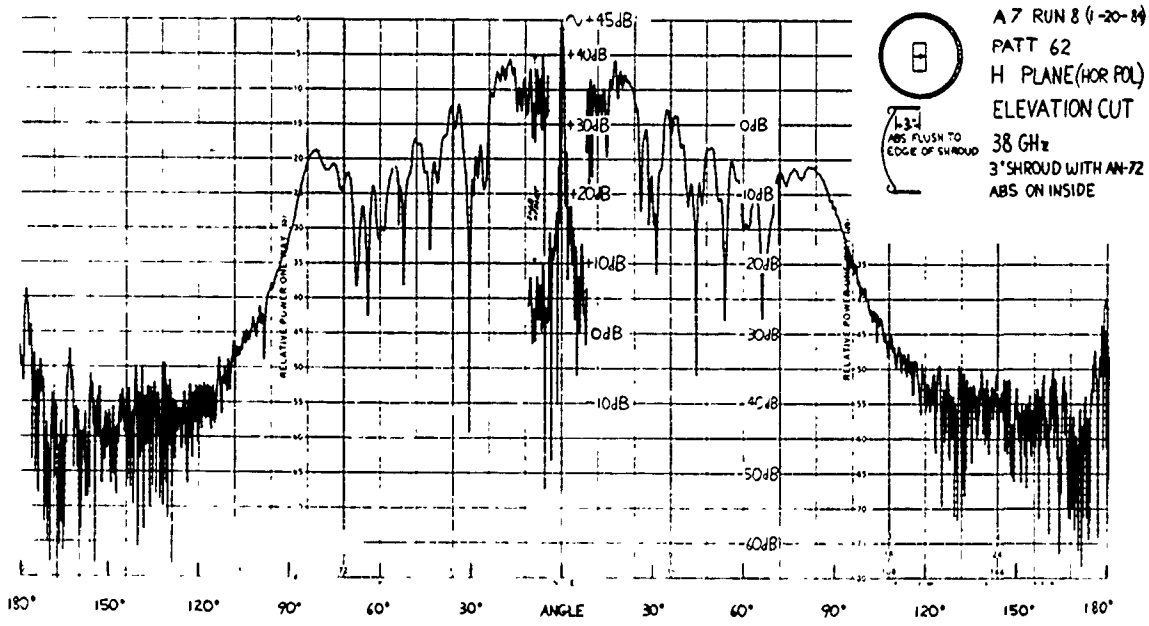

b) H Plane

1-25-84

Figure 31. 2-ft reflector (oversized subreflector) with 1/4 in. thick absorber on inside of 3-in. metal shroud patterns

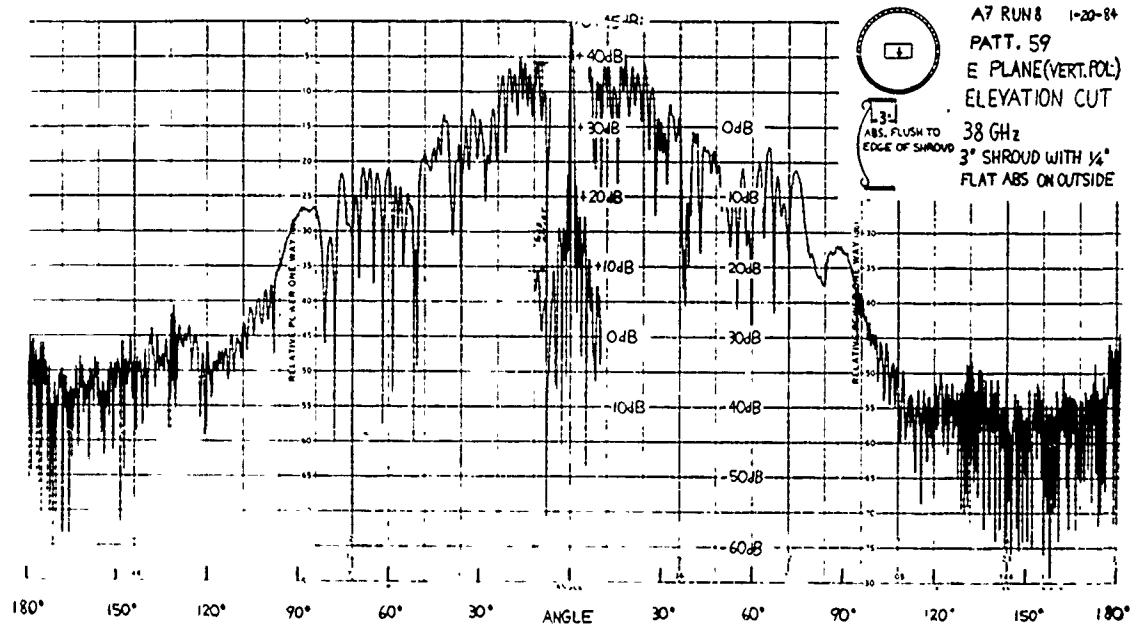

a) E Plane

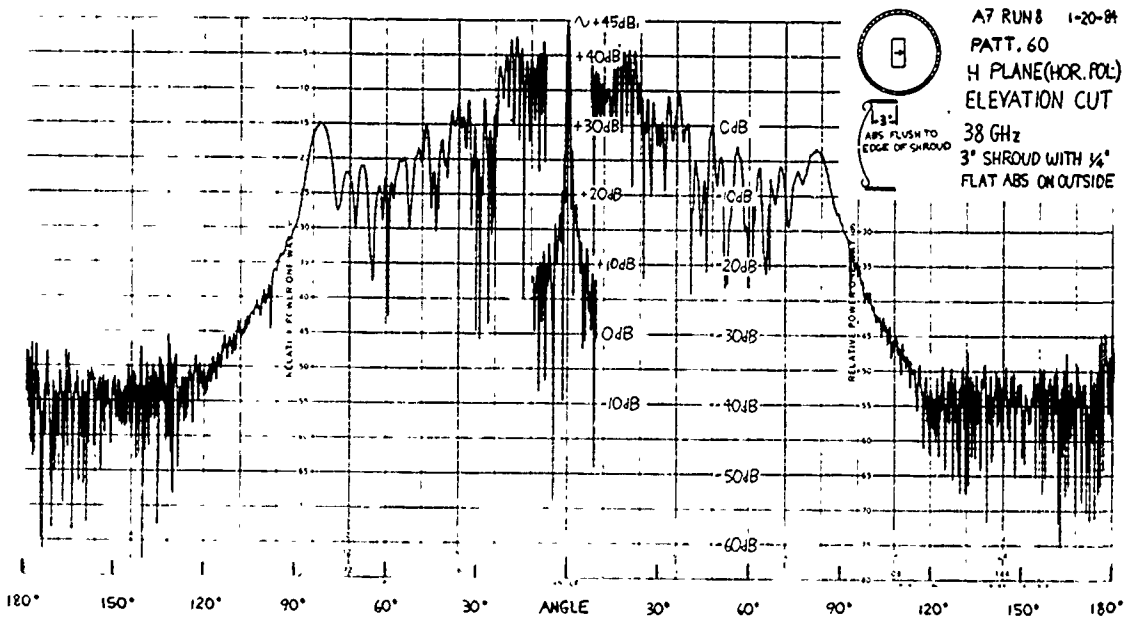

b) H Plane

1-25-84

Figure 32. 2-ft reflector (oversized subreflector) with 1/4 in. thick absorber on outside of 3-in. metal shroud patterns

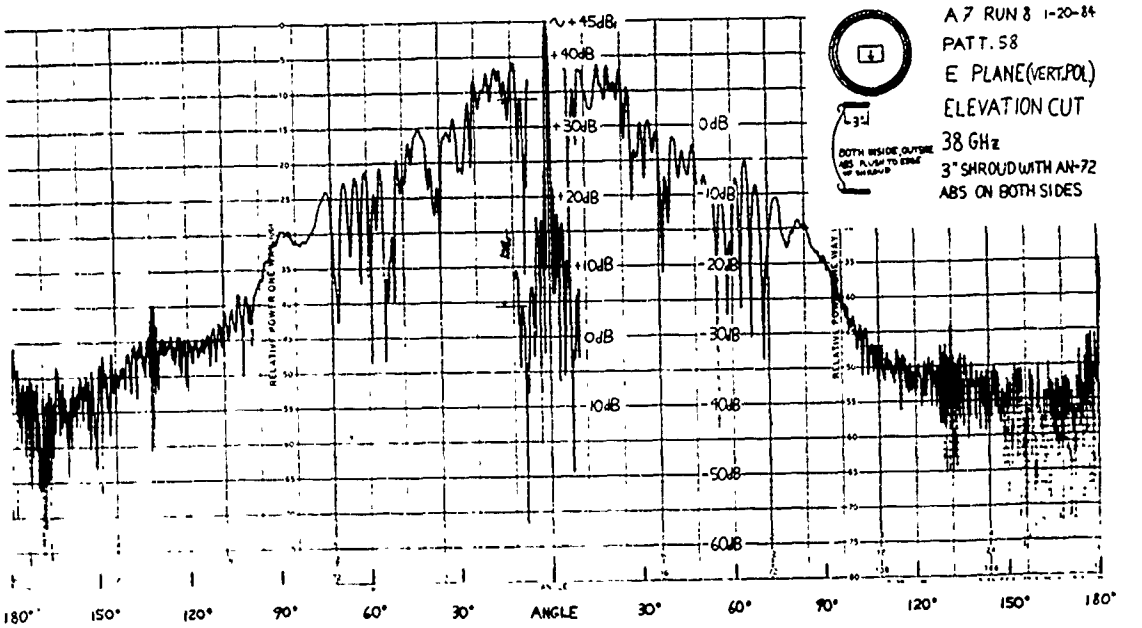

a) E Plane

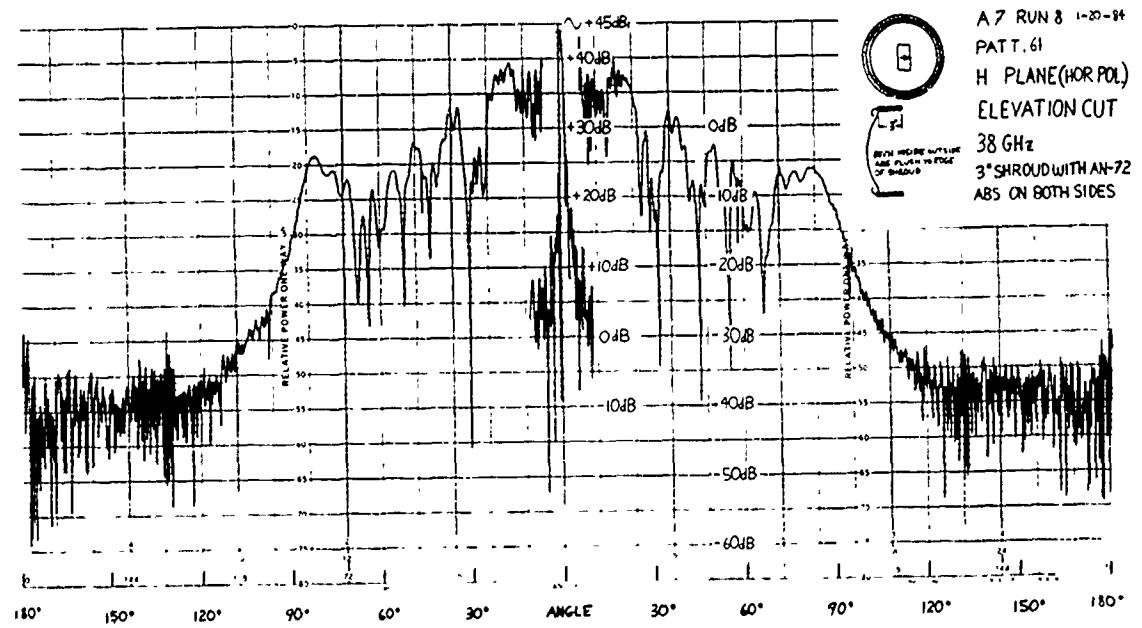

b) H Plane

Figure 33. 2-ft reflector (oversized subreflector) with 1/4 in. thick absorber on both sides of 3-in. metal shroud patterns

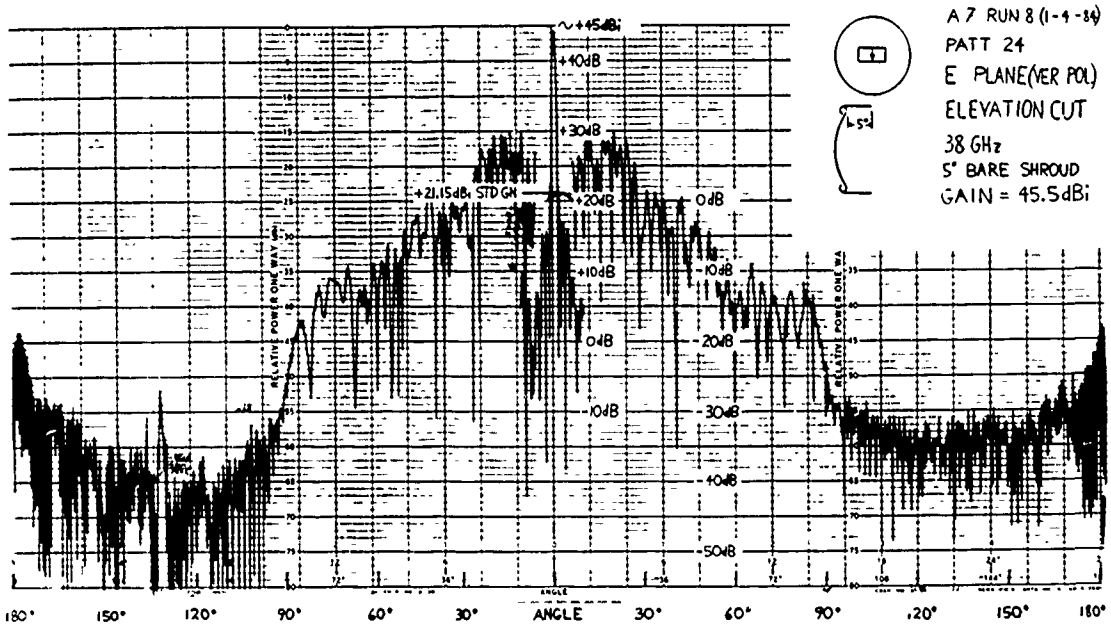

a) E Plane

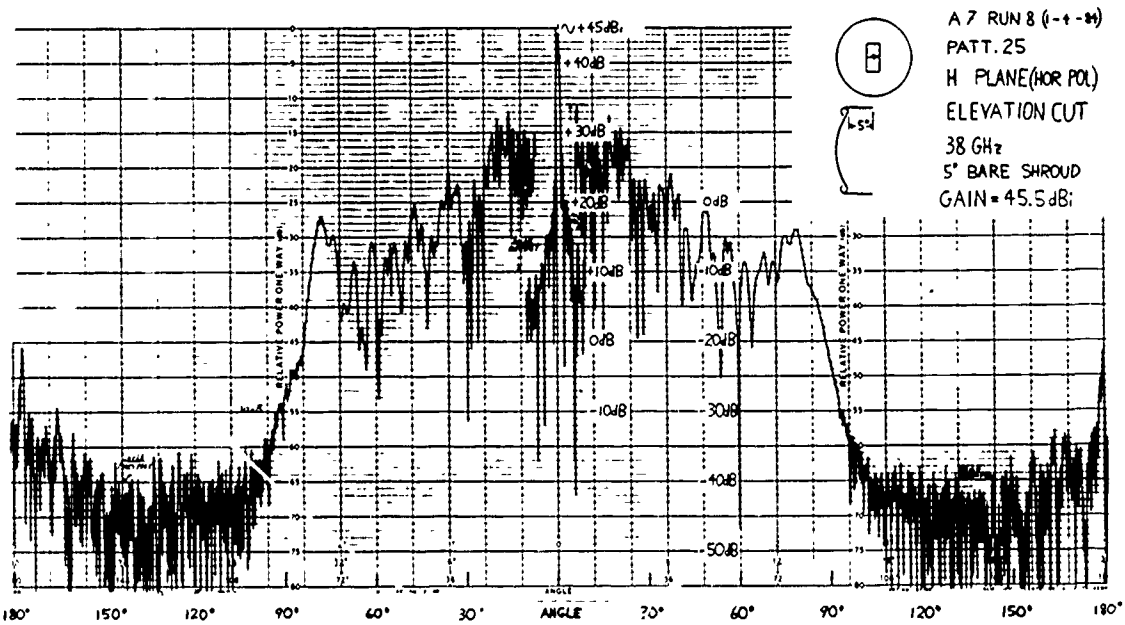

b) H Plane

1-9-84

Figure 34. 2-ft reflector (oversized subreflector) with 5-in. circumferential metal shroud patterns

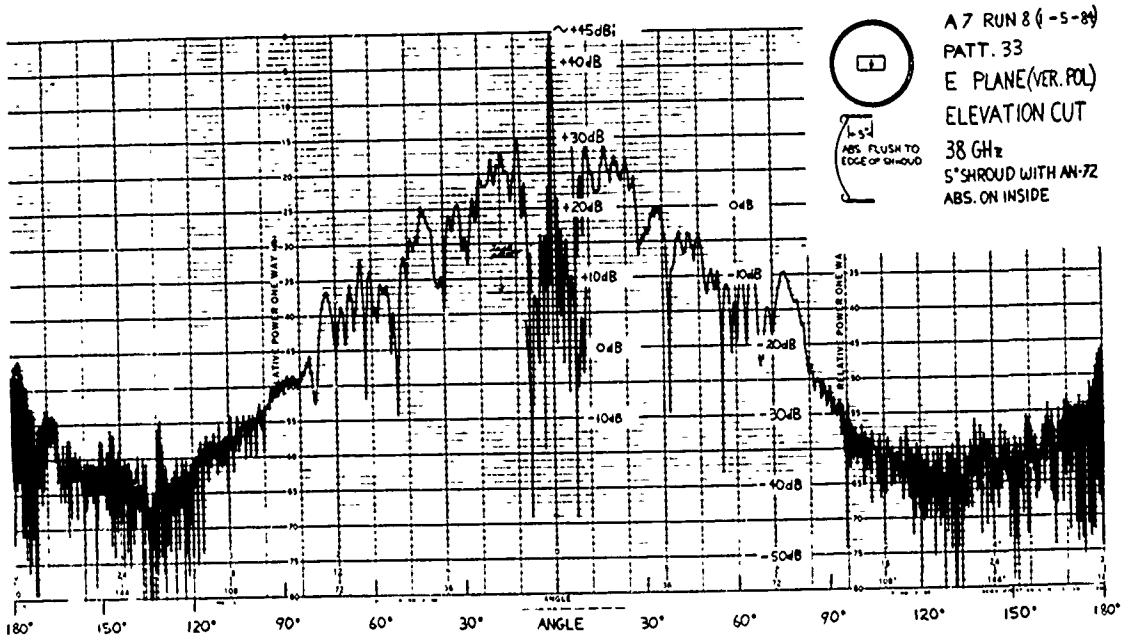

a) E Plane

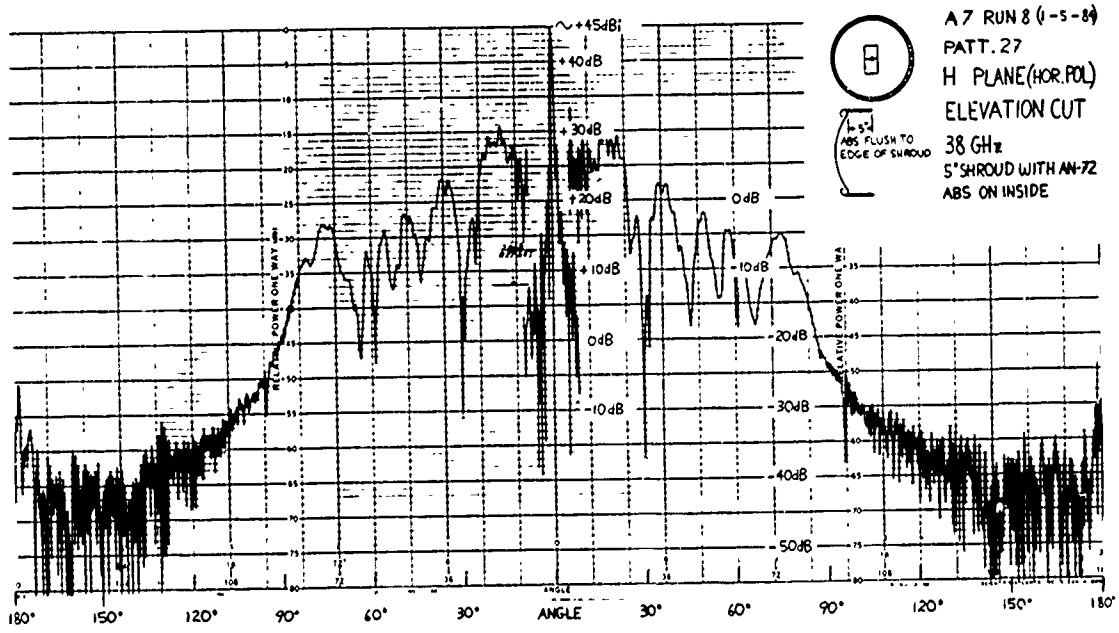

b) H Plane

1-9-84

Figure 35. 2-ft reflector (oversized subreflector) with 1/4 in. thick absorber on inside of 5-in. metal shroud patterns

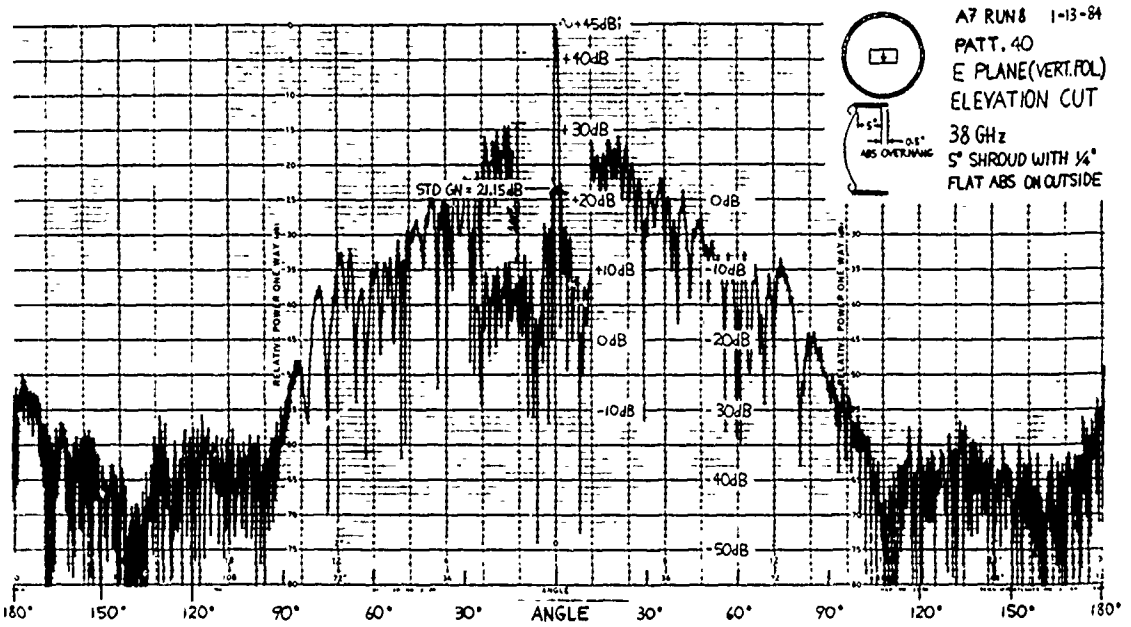

a) E Plane

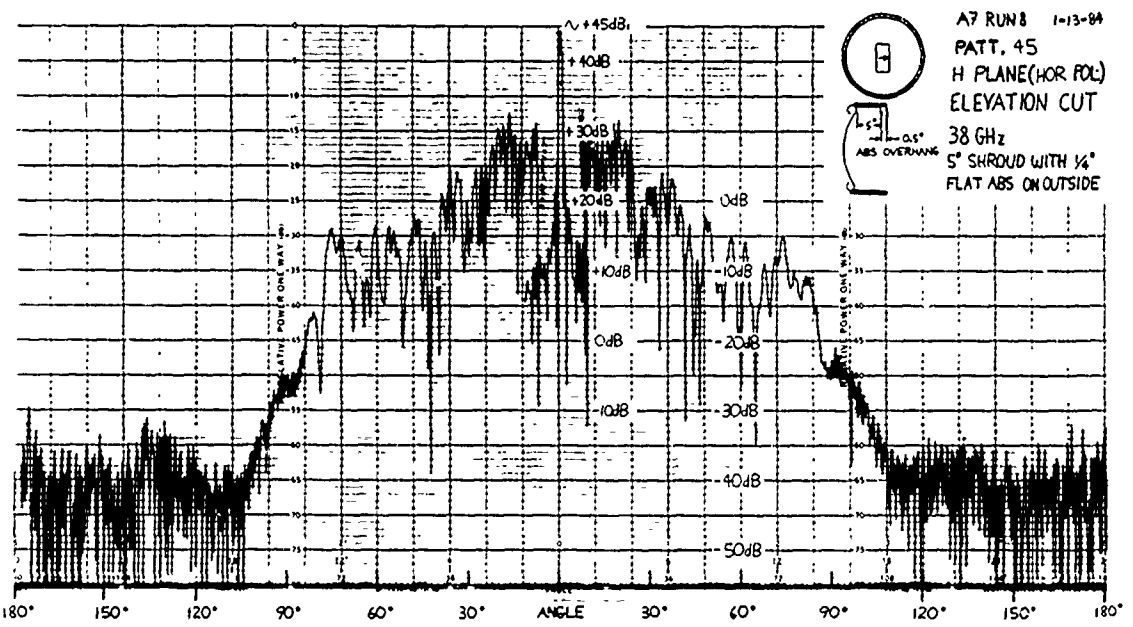

b) H Plane

1-17-84

Figure 36. 2-ft reflector (oversized subreflector) with 1/4 in. thick absorber on outside of 5-in. metal shroud patterns

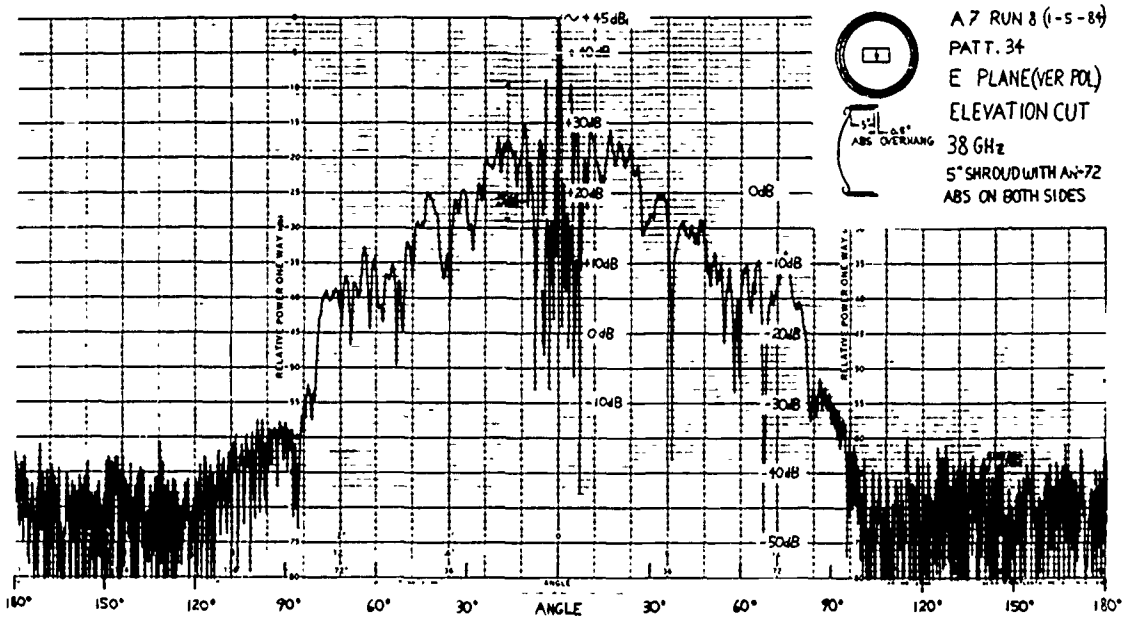

a) E Plane

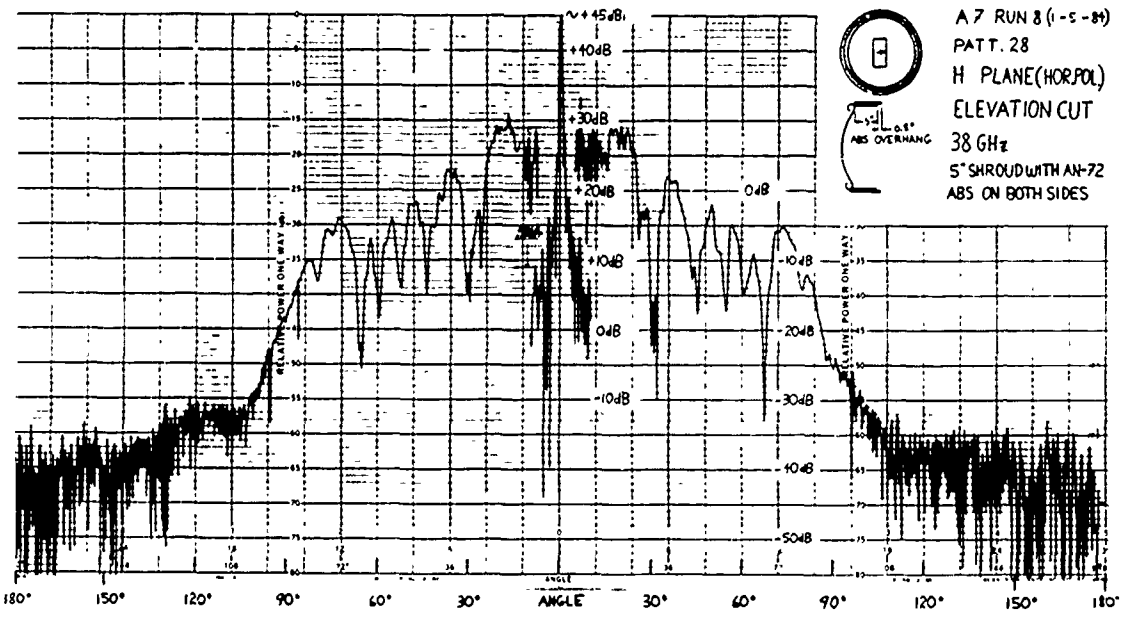

b) H Plane

1-9-84

Figure 37. 2-ft reflector (oversized subreflector) with 1/4 in. thick absorber on both sides of 5-in. metal shroud patterns

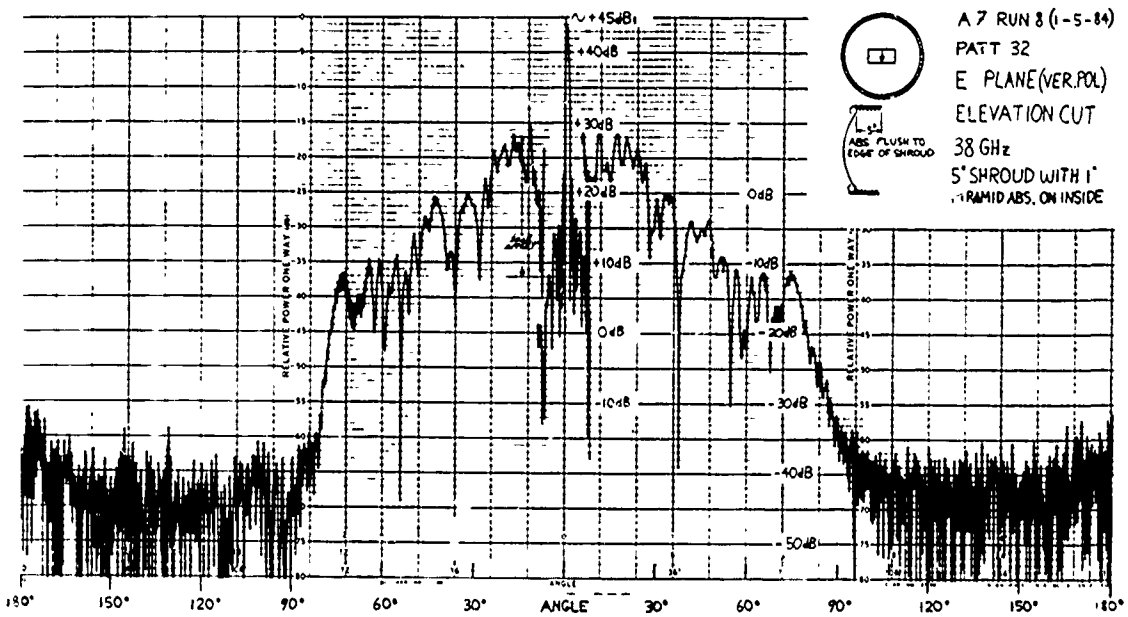

a) E Plane

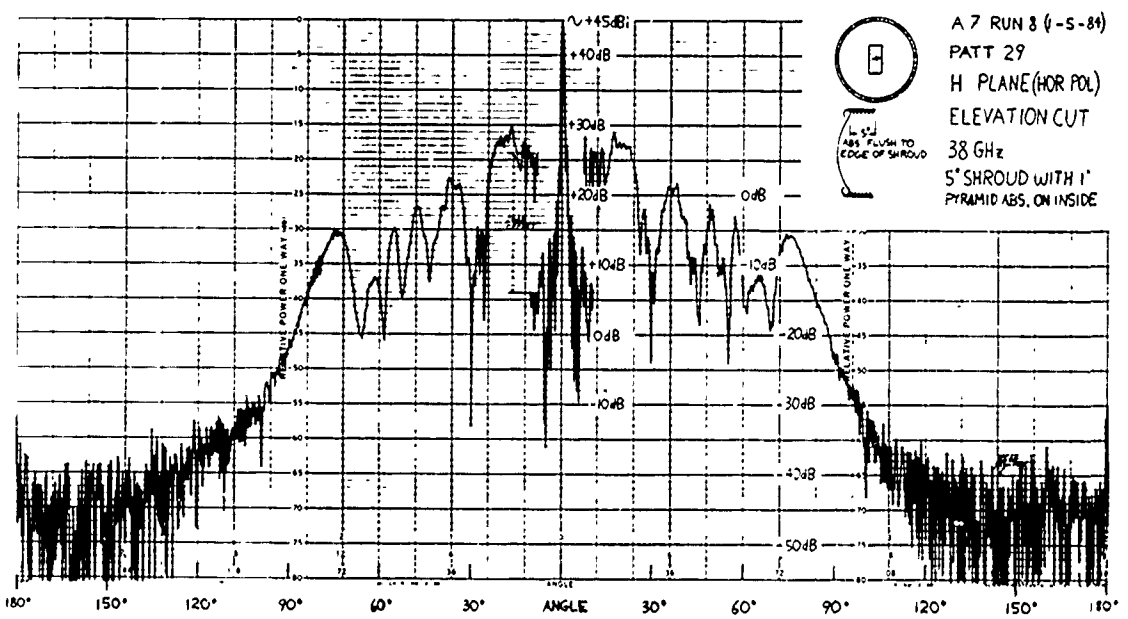

b) H Plane

Figure 38. 2-ft reflector (oversized subreflector) with 1-in. pyramidal absorber on inside of 5-in. metal shroud patterns

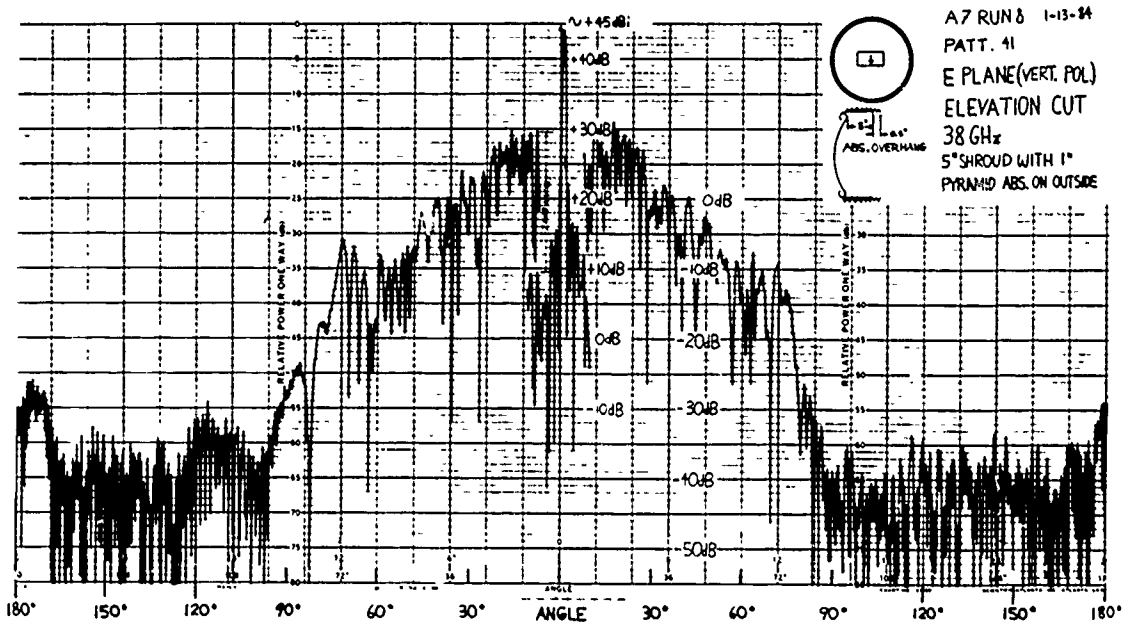

a) E Plane

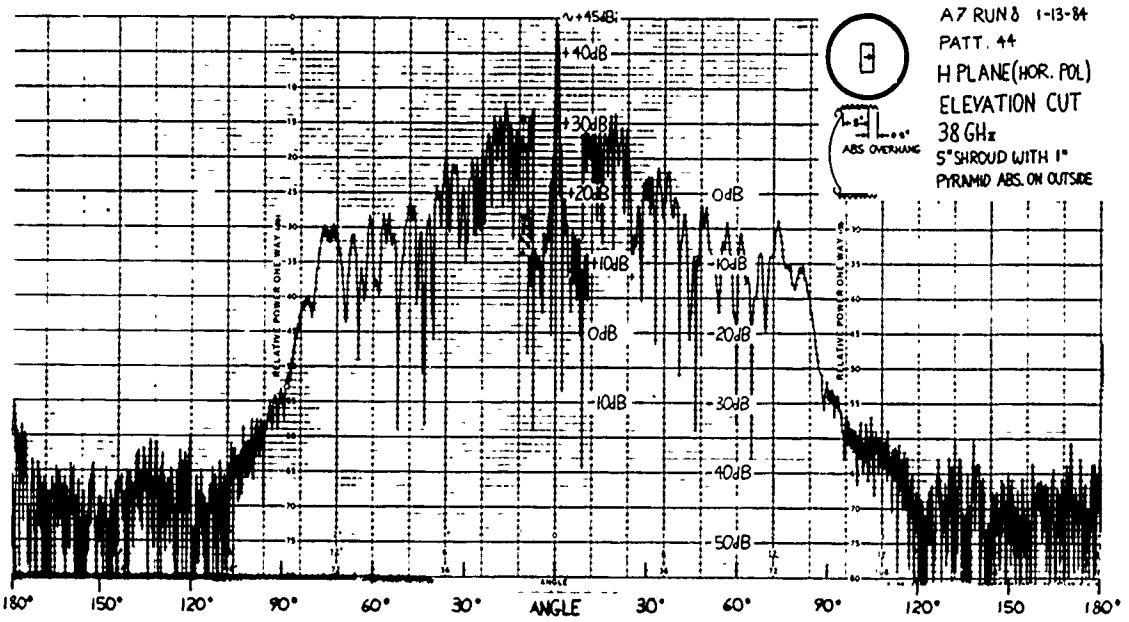

b) H Plane

Figure 39. 2-ft reflector (ovesized subreflector) with 1-in. pyramidal absorber on outside of 5-in. metal shroud patterns

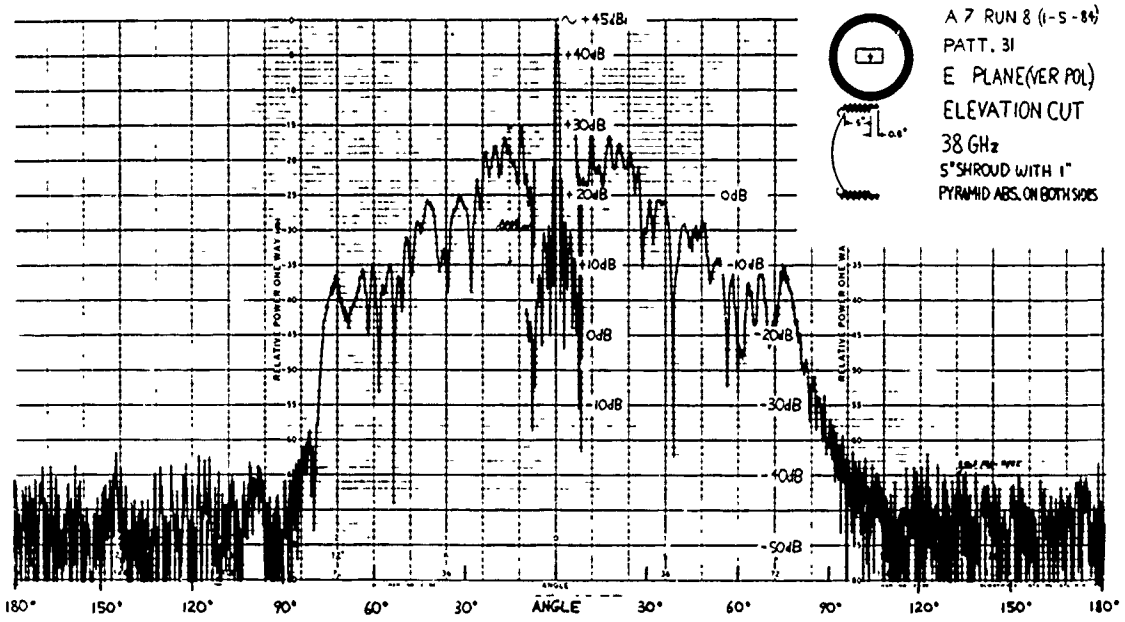

a) E Plane

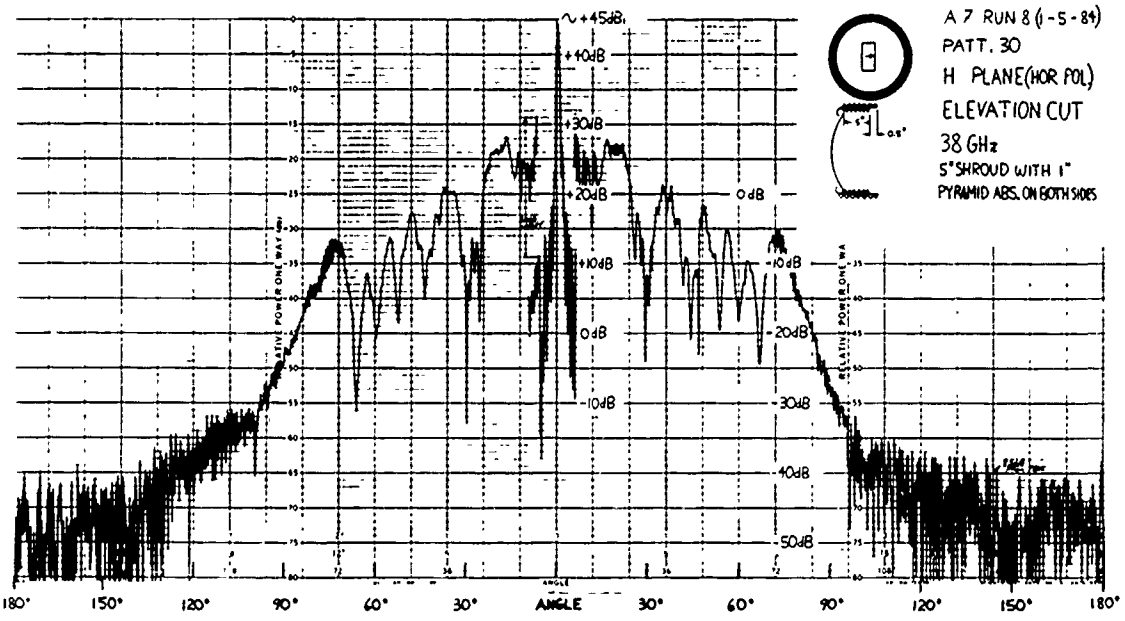

b) H Plane

1-9-84

Figure 40. 2-ft reflector (oversized subreflector) with 1-in. pyramidal absorber on both sides of 5-in. metal shroud patterns

Figure 41 shows the baseline E and H plane patterns* of the 2-ft reflector with a conventional subreflector. The forward-region ($\theta < 75°$) sidelobes are attributed primarily to the horn-subreflector spillover. The edge-diffracted lobe at $\sim \pm 100°$ is noticeable in the H plane, but the E plane pattern shows some unaccountable asymmetry. In contrast to the oversized subreflector, the conventional subreflector patterns of Fig. 41 reveal lower backlobes due to the reduced subreflector and main-reflector edge illumination. Techniques using the conical flange, corrugations and absorber ring as illustrated in Fig. 7 to reduce sidelobes 10 to 20 dB did not appear promising, after a review of the horn-subreflector patterns of Figs. 16 and 21 to 23; thus, the main-reflector measured patterns of these techniques are not reported.

A number of diagnostic-type measurements were made in an attempt to find the unsymmetrical anomaly in the E plane of Fig. 41. By moving the subreflector closer to the dish vertex by 0.025 in., better symmetry was obtained as illustrated in Fig. 42; however, the backlobes appear to be higher by $\sim$ 5 dB. Again, this condition cannot be explained. Nevertheless, we proceeded to make additional measurements with the main-reflector shroud and fence with the defocussed subreflector.

Figure 43 shows the main-reflector patterns with a 3-in. high circumferential metallic shroud. In contrast to the bare reflector, the shroud reduced the -20 dBi beamwidth (half angle) from 180° to 85° (E plane) and to 92° (H plane) or gain levels $\leq$ -20 dBi have increased a total of 46° and 32° in the E plane and H plane, respectively. In addition, the shroud reduced the backlobes by 10 to 20 dB.

---

*Patterns at the beam peak have been compressed.

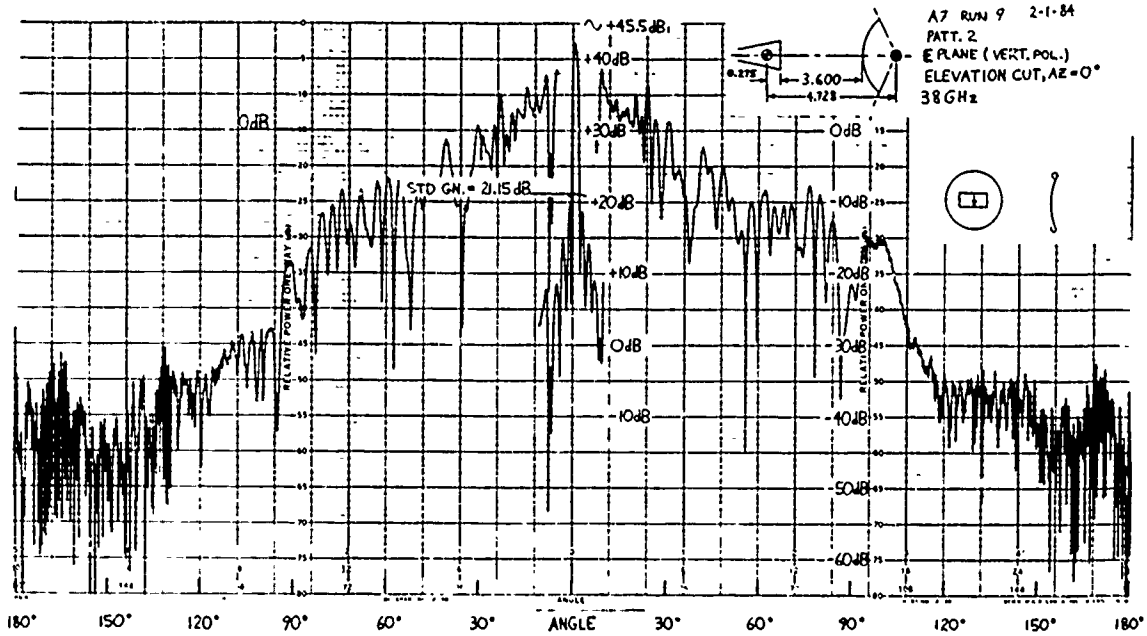

a) E Plane

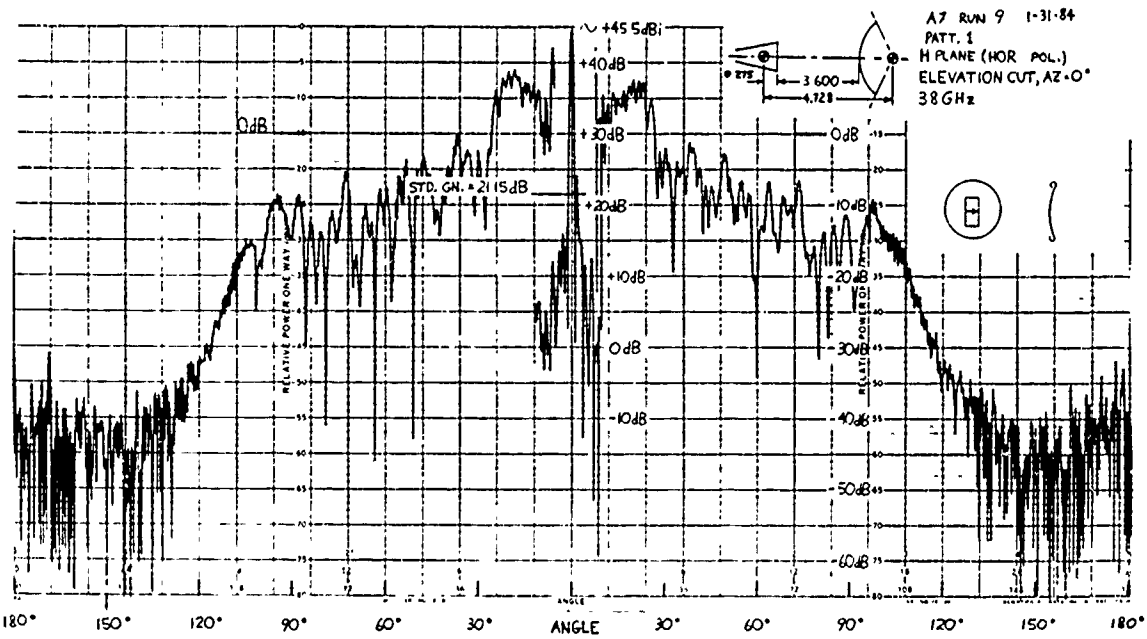

b) H Plane

Figure 41. Baseline patterns of 2-ft reflector with conventional subreflector

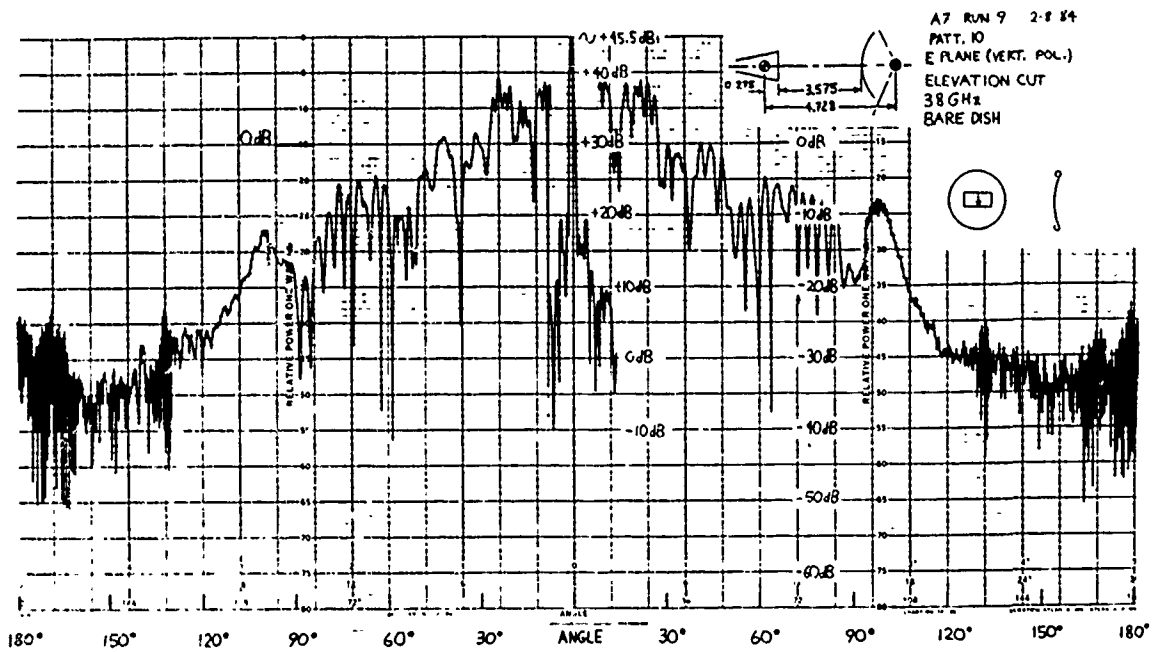

a) E Plane

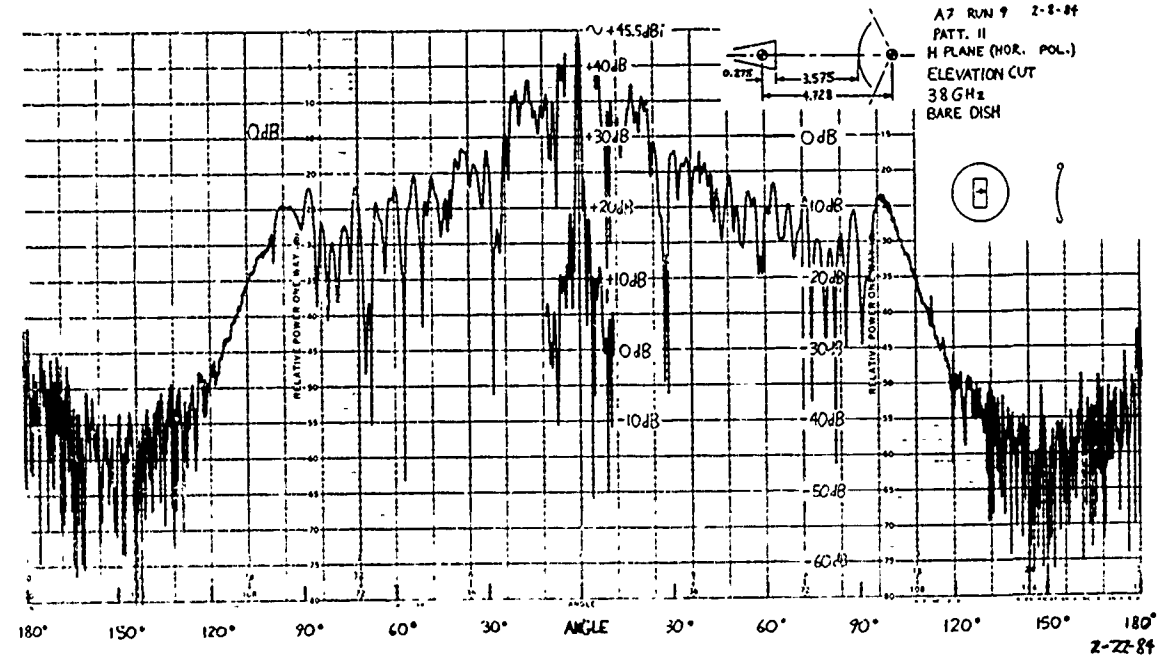

b) H Plane

Figure 42. Patterns of 2-ft reflector with conventional subreflector moved toward dish vertex 0.025 in.

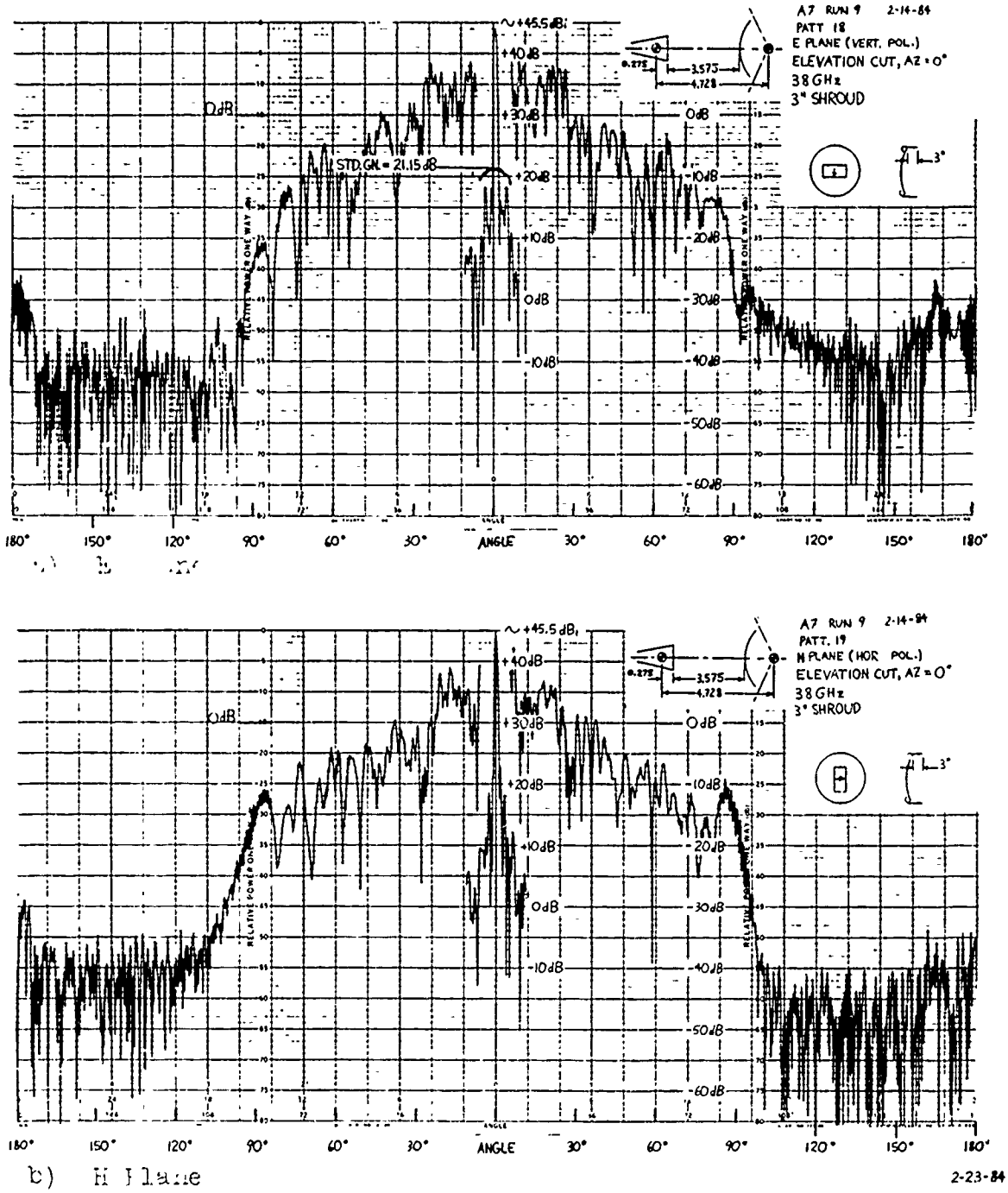

b) H Plane

Figure 43. Patterns of 2-ft reflector (conventional subreflector) with 3-in. circumferential metallic shroud

The antenna user also has a need to know the pattern characteristics in a great-circle cut --i.e., antenna tilted up at a specified elevation angle and rotating the antenna in azimuth while recording the pattern. Prior to making the great-circle pattern measurements, an azimuth cut pattern (with shroud) was taken to compare it with the elevation-cut patterns, as shown in Fig. 44, which compares reasonably well with the elevation-cut pattern of Fig. 43. Great circle patterns were recorded for elevation angles of 35° and 45° as shown in Figs. 45 and 46, respectively. Corresponding great-circle patterns for the bare reflector are shown in Figs. 47 and 48 for comparison. The dish shroud, as compared to the bare reflector, primarily reduces the reflector-edge diffraction lobe by ~ 20 dB (over a 20° to 30° angular sector near $\theta = 100°$) and with minimal improvement in the forward and rear sidelobes.

To place a complete circumferential shroud around the edge may not be practical, depending upon the application. Experiments were made with a partial shroud -- referred to as fences or plates which were 3-in. high and 6-in. long, with the 6-in. dimension along the edge of the dish as shown in the photograph of Fig. 49. In the plane desiring sidelobe reduction, the plates only one fourth the dish diameter were found to be as effective as a circumferential shroud by comparing the fence patterns of Fig. 50 with the shroud patterns of Fig. 43.

With the fence not in the plane of the pattern cut, the patterns (Fig. 51) show approximately the same radiation characteristics as for the reflector without a shroud. This result is expected as the fence is not effective in reducing edge diffraction orthogonal to the plane of interest.

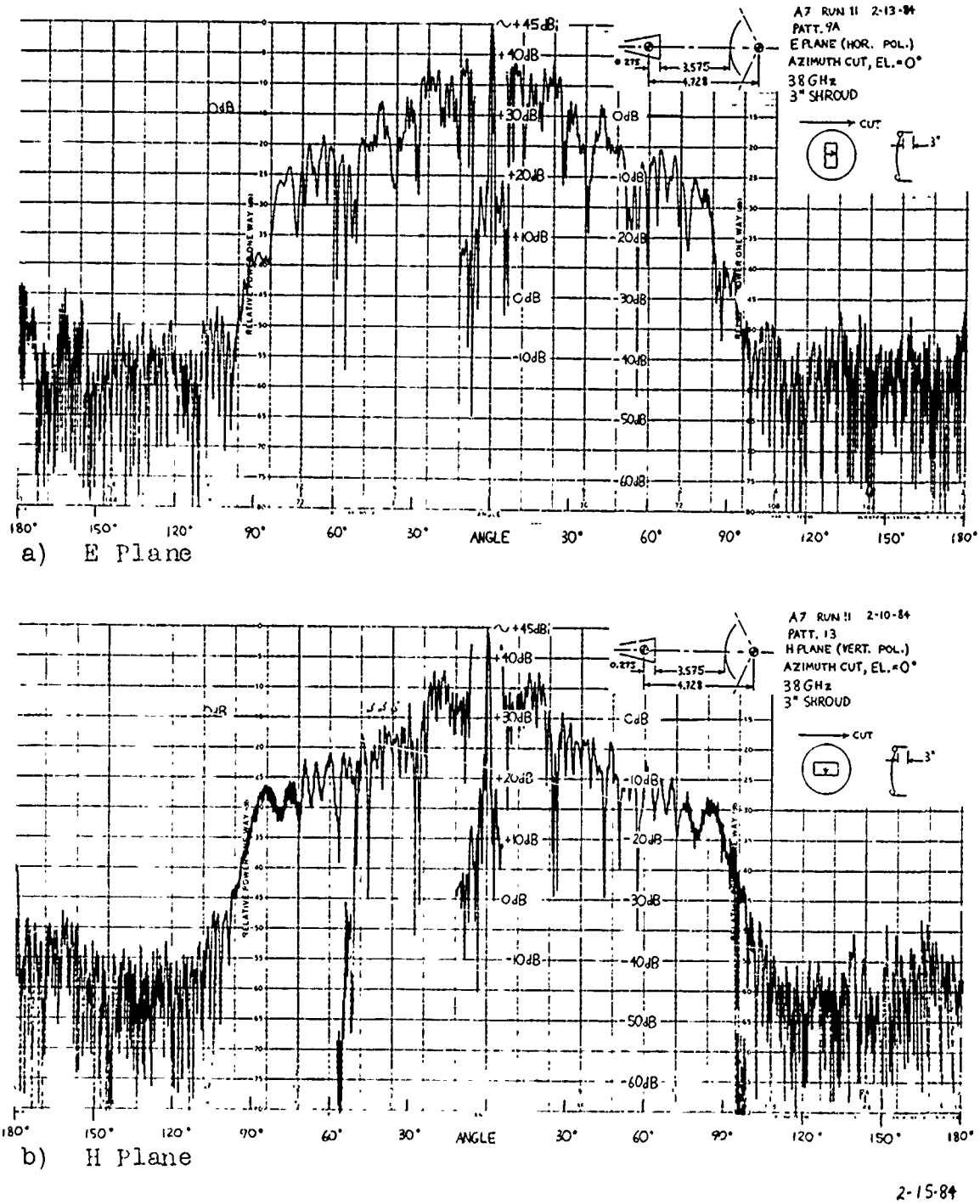

Figure 44. Patterns of 2-ft reflector (conventional subreflector) with 3-in. circumferential metallic shroud -- azimuth cut

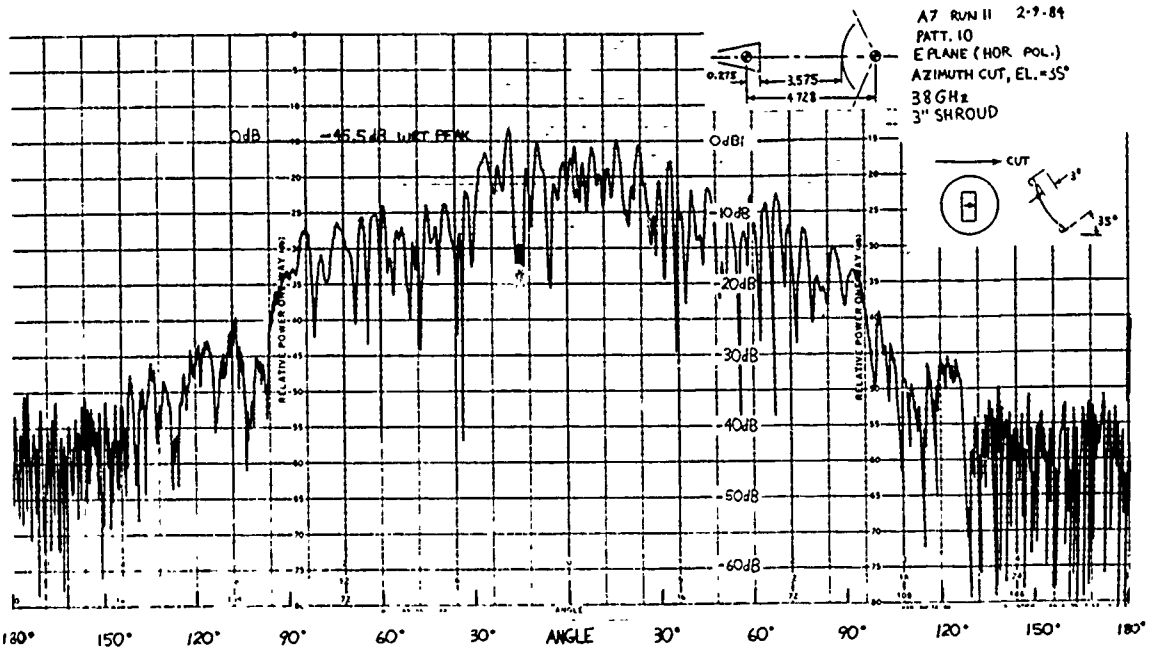

a) E Plane

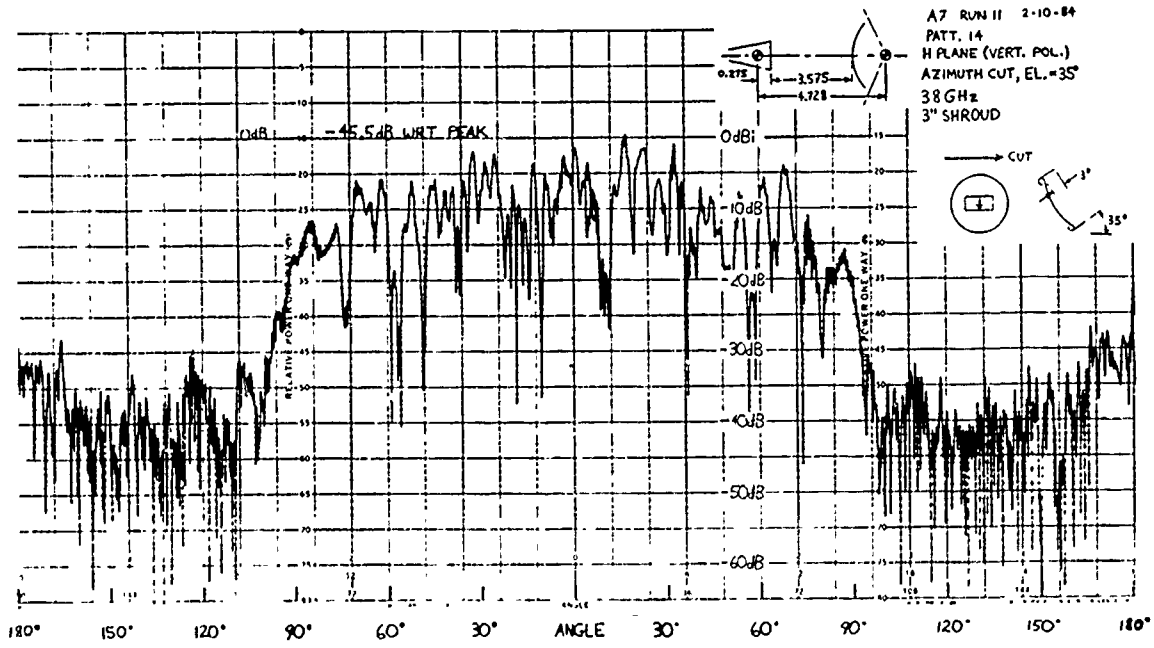

b) H Plane

2-15-84

Figure 45. Great-circle cut patterns of 2-ft reflector (conventional sub-reflector) with 3-in. circumferential metallic shroud -- elevation angle = 35°

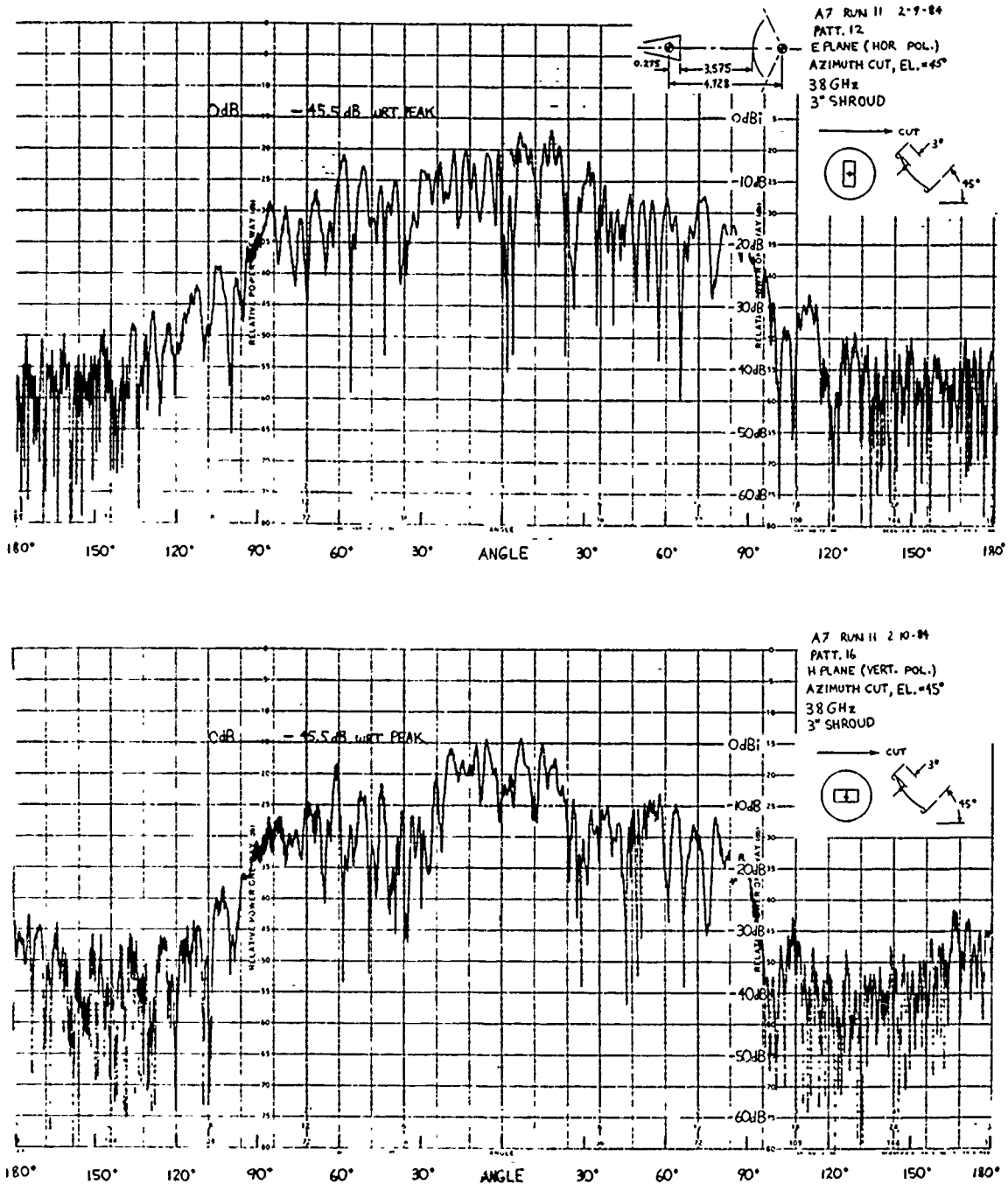

Figure 46. Great-circle patterns of 2-ft reflector (conventional sub-reflector) with 3-in. circumferential metallic shroud -- elevation angle = 45°

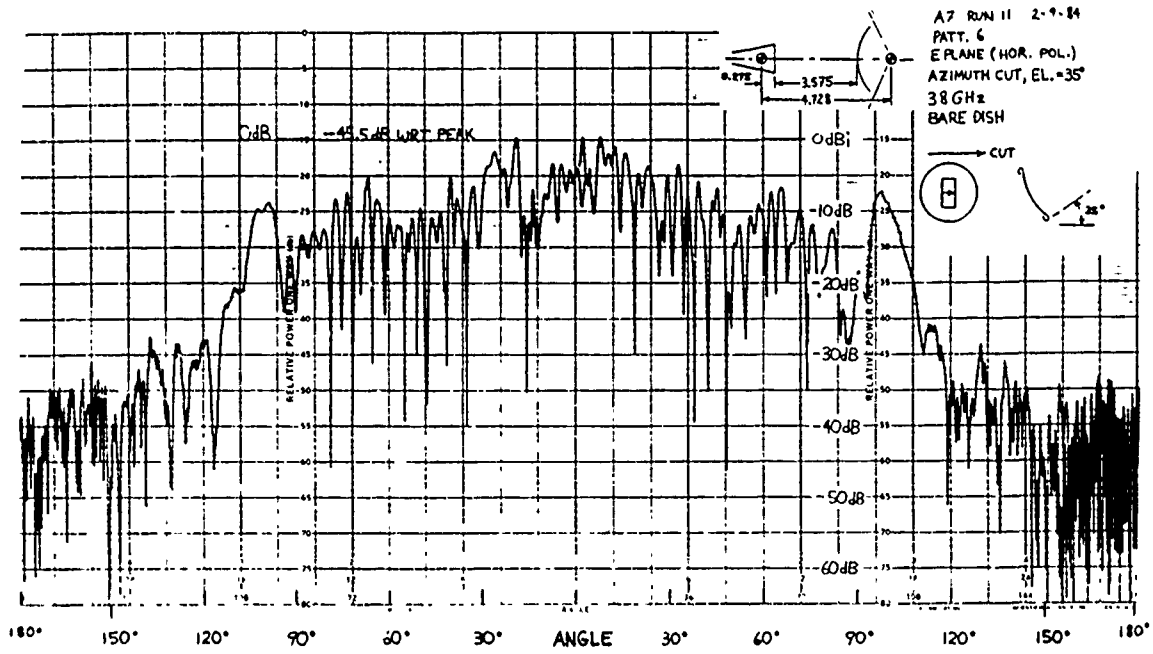

a) E Plane

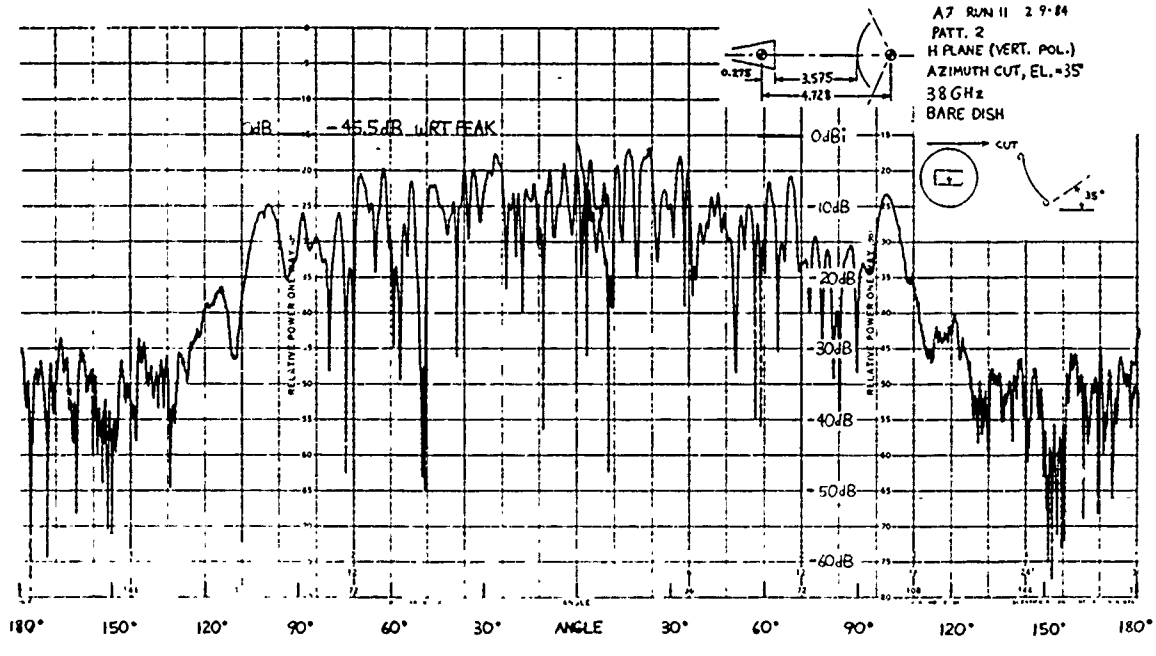

b) H Plane

2-15-84

Figure 47. Great-circle cut patterns (35°) of bare 2-ft reflector (conventional subreflector)

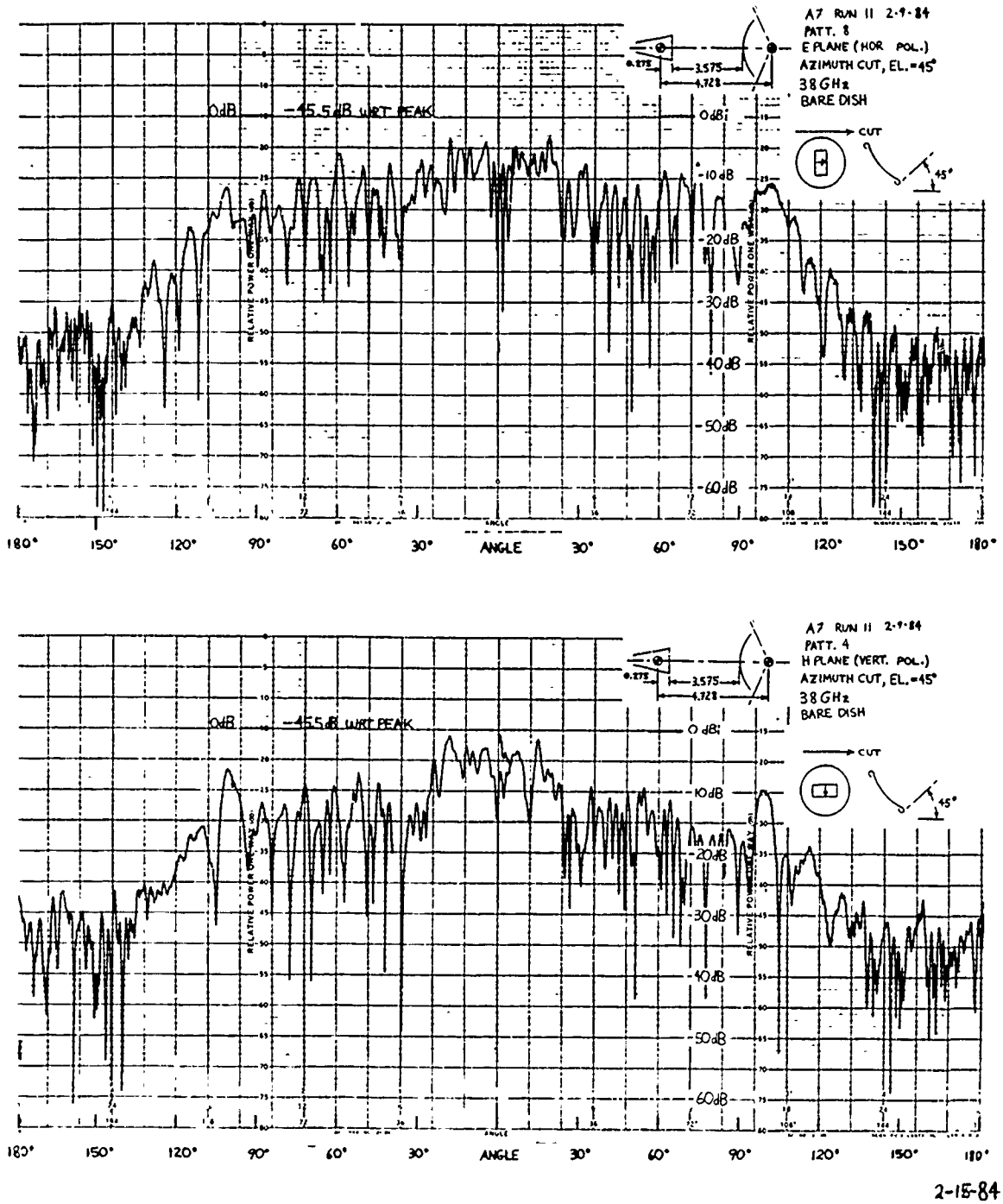

Figure 48. Great-circle cut patterns (45°) of bare 2-ft reflector (conventional subreflector

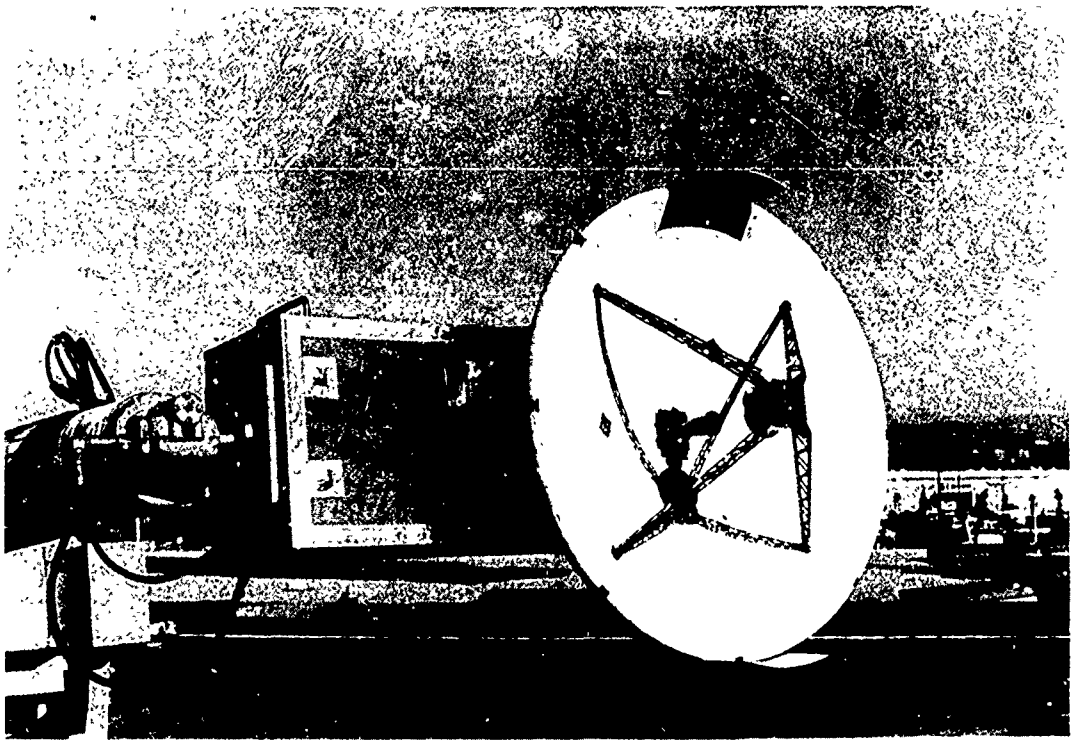

Figure 49. Photograph of 2-ft reflector with 3-in. x 6-in. long plates on edge of dish

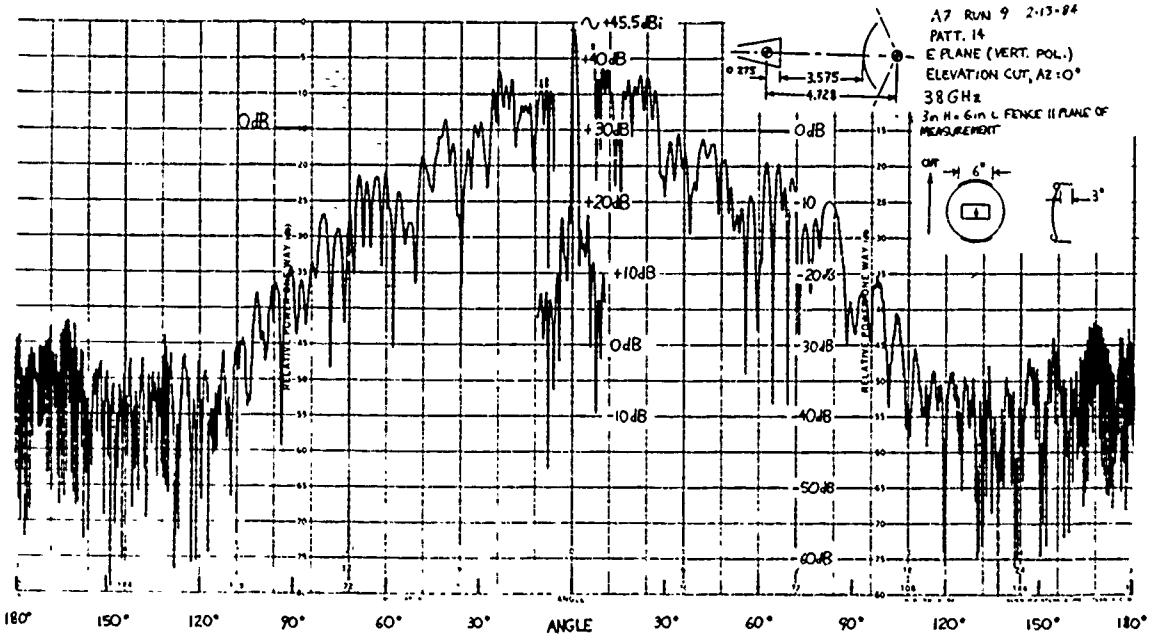

a) E Plane

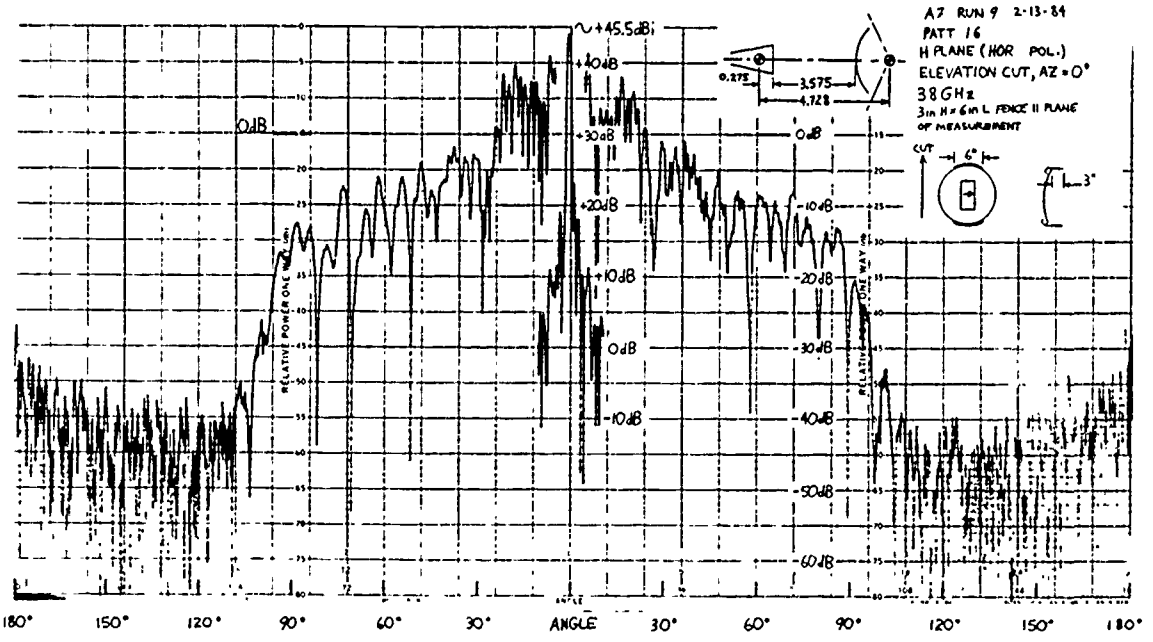

b) H Plane

2-24-84

Figure 50. Pattern cut through the 3 x 6-in. plates for 2-ft dish (conventional subreflector)

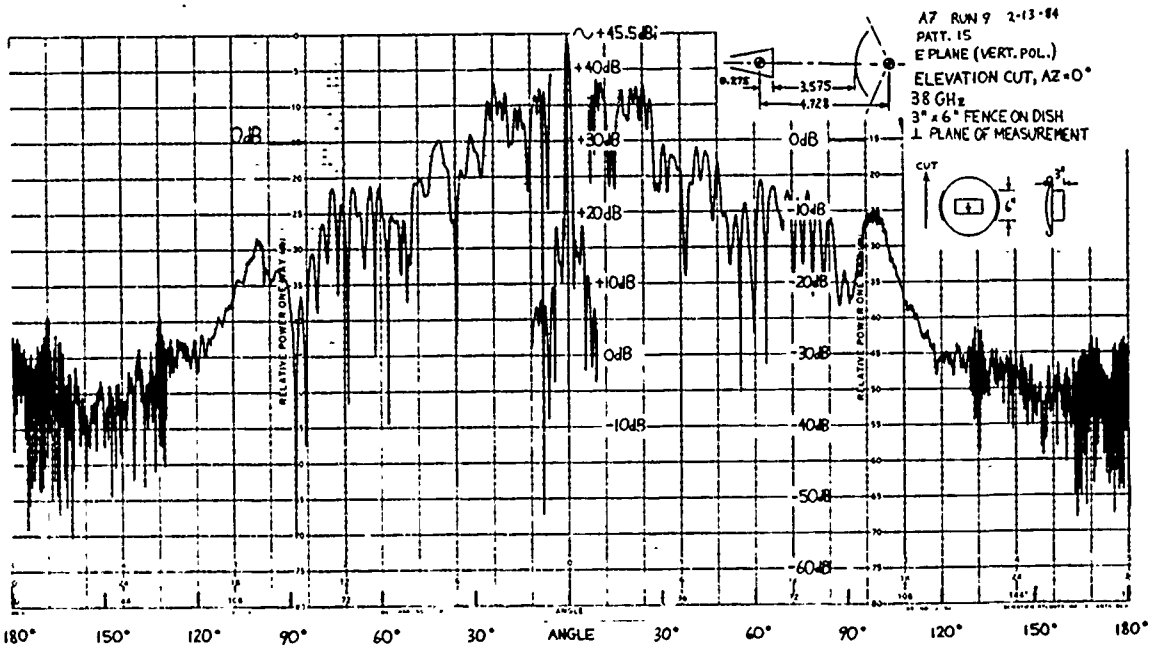

a) E Plane

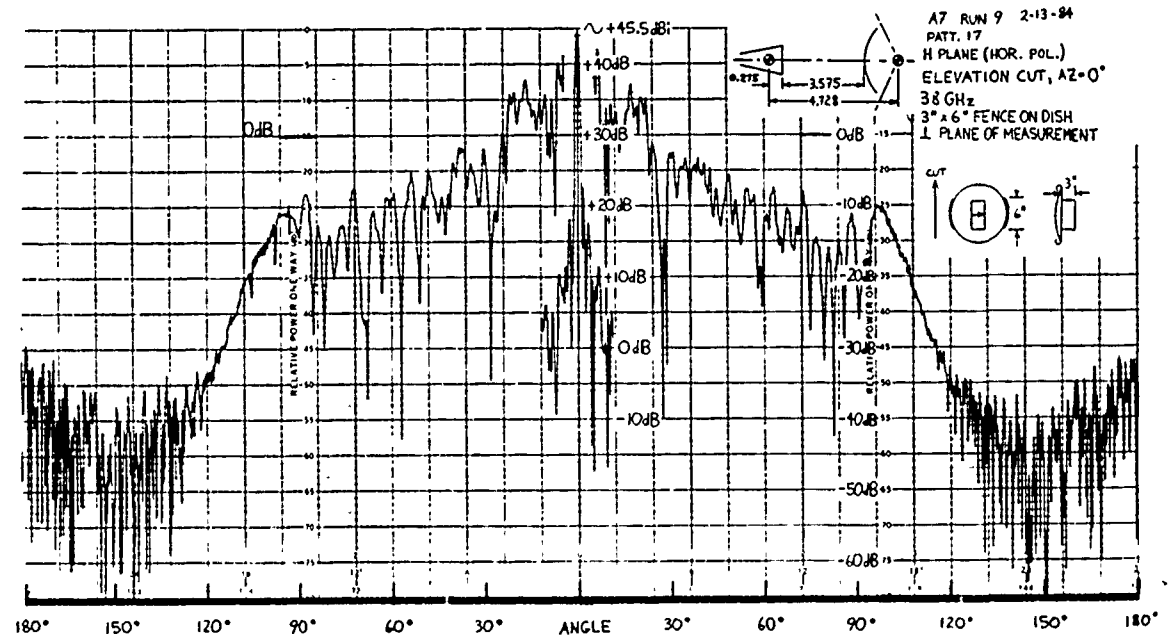

b) H Plane

Figure 51. Patterns of 2-ft reflector (conventional subreflector) with 3 x 6-in. plate not in the plane of the pattern cut

Great-circle pattern cuts for elevation angles of 35° and 45° with the 3 x 6 in. fence are shown in Figs. 52 and 53, respectively. In comparison with the complete shroud (Figs. 45 and 46) the fence is not as effective in reducing sidelobes off the principal plane of the fence. Nevertheless, the fence provides improvement over a bare reflector. Thus, depending on the mechanical difficulty or costs of installing a circumferential shroud, a fence could be a compromise in mechanical consideration and likewise a compromise in sidelobe reduction.

The cross polarization levels (Fig. 54) are generally 15 to 20 dB lower than the principal polarization patterns (Fig. 42).

Patterns for the 2-ft reflector with the conventional subreflector have been presented in Figs. 41 to 52. The pattern characteristics are summarized as follows:

- The sidelobes in the rear region (0 > 100°) are ~10 dB lower as compared to the reflector employing the oversized subreflector.
- Sidelobe levels in the forward region are comparable in level to those of the 2-ft reflector with the oversized subreflector.
- A 3-in. circumferential metallic shroud on the 2-ft reflector edge reduces the backlobes by 10 to 20 dB, as compared to the bare reflector case.
- With the shroud, the angular region with gain levels <-20 dBi increased 46° and 32° in the E and H planes, respectively.
- A partial shroud, or two plates 6-in. long (1/4th dish diameter) diametrically opposite on the dish edge, yield similar pattern characteristics as a complete circumferential shroud, with a pattern cut made through the plates.
- Great-circle pattern cuts made 35° off the main lobe show that two plates provide worse sidelobe levels than the complete shroud.

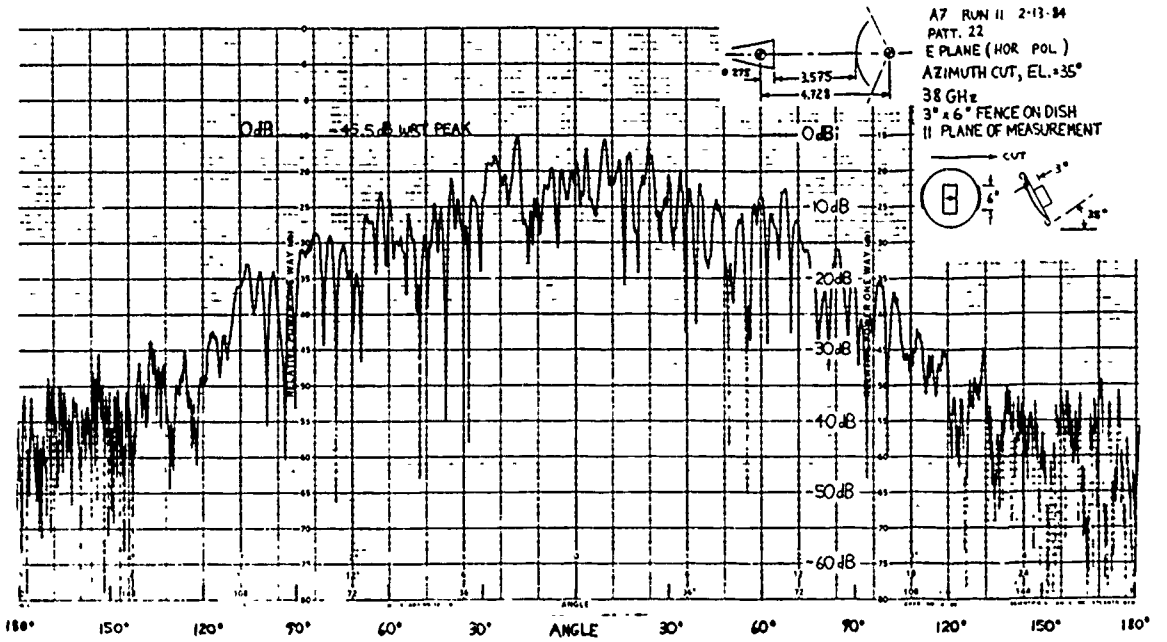

a) E Plane

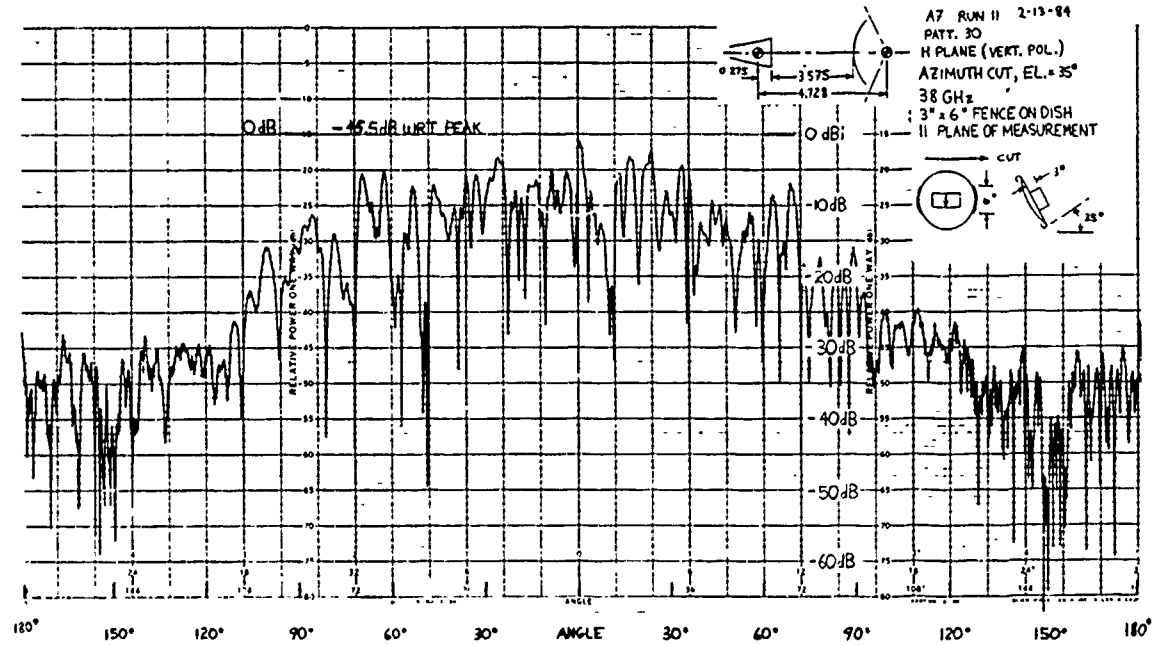

b) H Plane

2-15-84

Figure 52. Great-circle pattern cut of 2-ft reflector (conventional sub-reflector) with 3 x 6-in. plates -- elevation angle = 35°

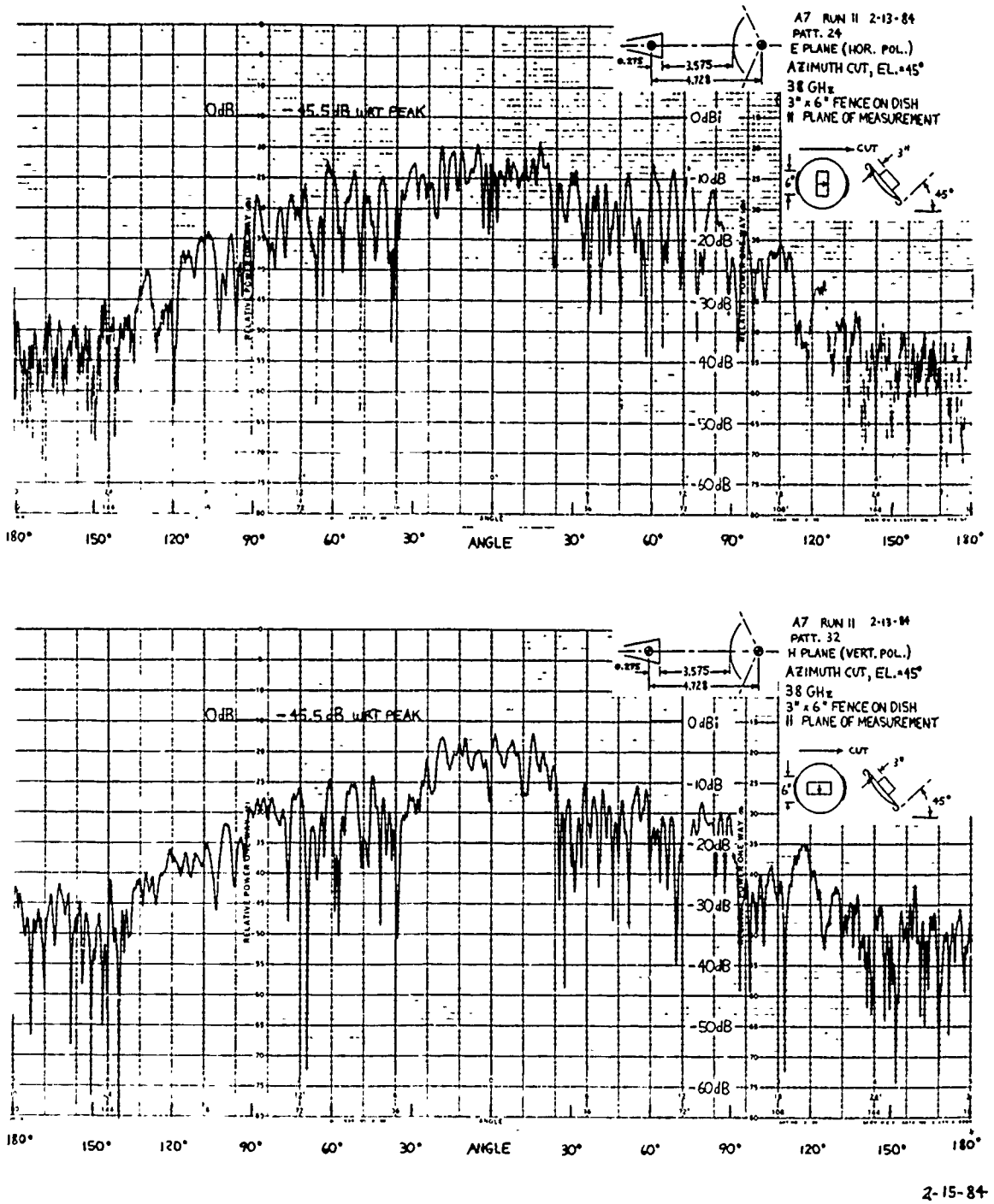

Figure 53. Great-circle pattern cut of 2-ft reflector (conventional sub-reflector) with 3 x 6-in. plates -- elevation angle = 45°

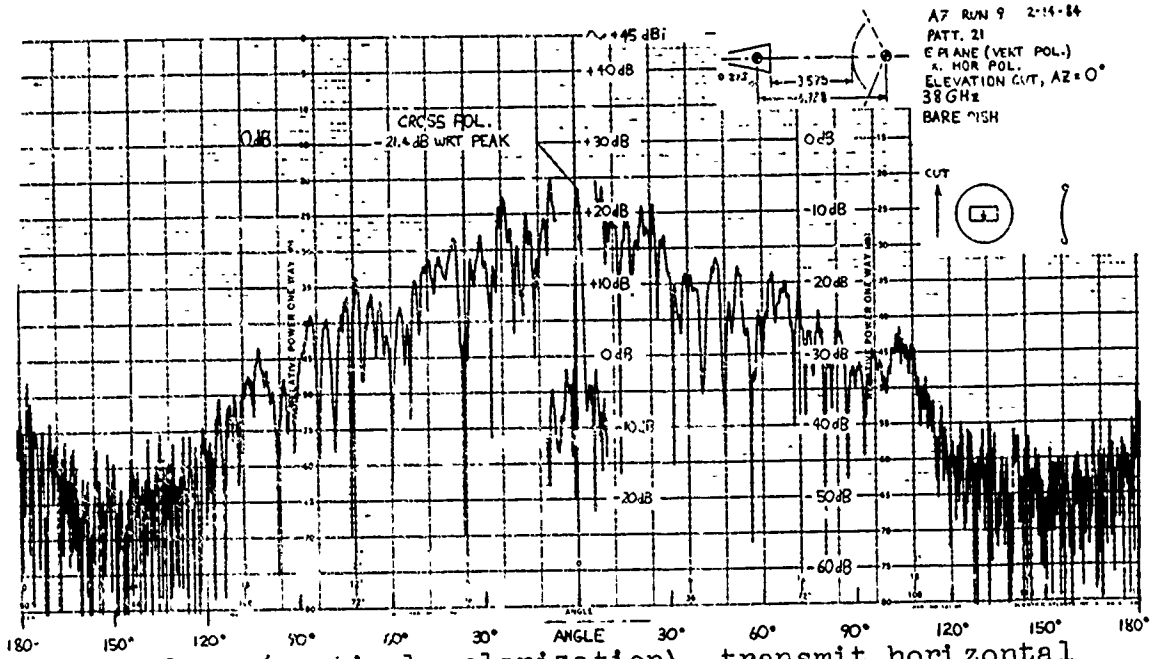

a) E Plane (vertical polarization), transmit horizontal

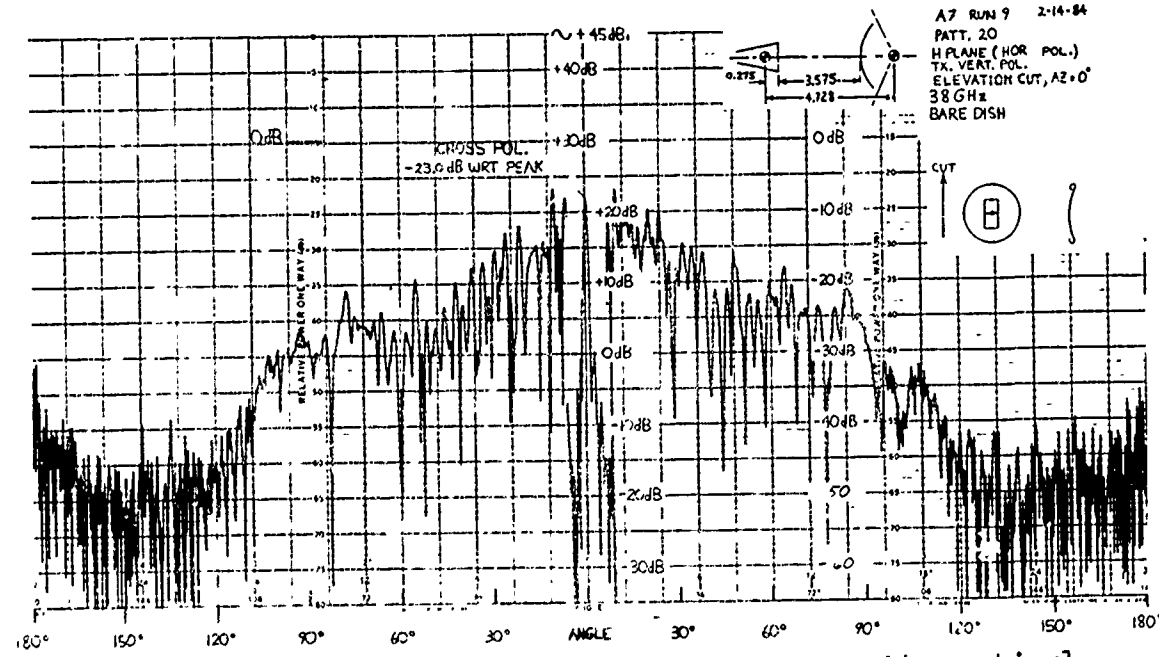

b) H plane (Horizontal polarization), transmit vertical 2-16-84

Figure 54. Cross polarization patterns of 2-ft reflector (conventional subreflector)

V. COMPUTED PATTERNS

Concurrent with the experimental studies (described in Sections III and IV), theoretical analyses of the Cassegrain antenna system were being done in-house and by Prof. Roger Rudduck, of the Ohio State University ElectroScience Laboratory. Our approach is empirical whereby we use the measured horn-subreflector patterns of Section III as the primary pattern for a prime-focus feed. This approach was necessary as we do not have the computer codes for Cassegrain antennas. With the measured horn-subreflector patterns for the various attachments, such as shrouds, corrugations, flanges and rings, the secondary patterns can be obtained quicker by computations than by measurements. With these computed reflector patterns the sidelobe level changes are more discernable as compared to the measured reflector patterns. A comparison of the computed and measured reflector patterns will be shown to illustrate the good correlation.

Rudduck's objectives were different than our analytical approach. He had the task of generating computer codes to calculate the patterns of the Cassegrain antenna system. With this tool he would be able to determine techniques to reduce the sidelobe levels. He has the capabilities of simulating a shroud around the dish and other shielding techniques described in Section II. Also, the effects of a metal space frame radome on the antenna sidelobe characteristics were computed. The results of OSU's horn, horn-subreflector, Cassegrain reflector (with and without the edge plates), and space-frame radome will be summarized in Section V. Details of their mathematical procedures will be written up in a subsequent report by Rudduck.

A. Aerospace Analysis

Using the measured E and H plane patterns of the horn-subreflector as a primary pattern for a prime-focus feed, we were able to compute the secondary patterns. The computer code (after Lee, Rudduck, et al.,[1]) is a GTD (geometrical theory of diffraction) analysis which includes the effects of the feed and strut scattering. A number of secondary reflector patterns were calculated using the horn-subreflector measured primary patterns. The oversized and conventional subreflectors show the major changes from an almost uniform aperture illumination (with high edge diffraction levels) to a conventional 10 to 20 dB edge taper. A few of the secondary patterns will be shown for the horn-subreflector shielding techniques.

1. Oversized Subreflector

With the horn/oversized subreflector patterns of Fig. 13 the computed 2-ft reflector patterns are shown in Fig. 55. The sidelobes in the region around 84° are attributed to the scattering from the four spars that support the subreflector. The backlobes in the angular region >100° are generated by the reflector-edge diffraction. The horn-subreflector spillover power primarily affects the forward sidelobes in the 10° to 70° zone.

To illustrate the effects of the spillover power from the horn-subreflector pattern, the backlobe (ψ >100°) was reduced to a constant -20 dB level (-17.5 dBi level of Fig. 13), and the computed 2-ft reflector patterns are shown in Fig. 56. The forward sidelobes (10° to 70°) are reduced by ~10 dB -- an encouraging result. Evaluation of the Fig. 56 patterns illustrate that it requires a considerable reduction in the horn-subreflector forward spillover power to significantly reduce the forward-region reflector sidelobes. Unfortunatly, it is physically difficult to reduce the spillover power to a -17.5 dBi level.

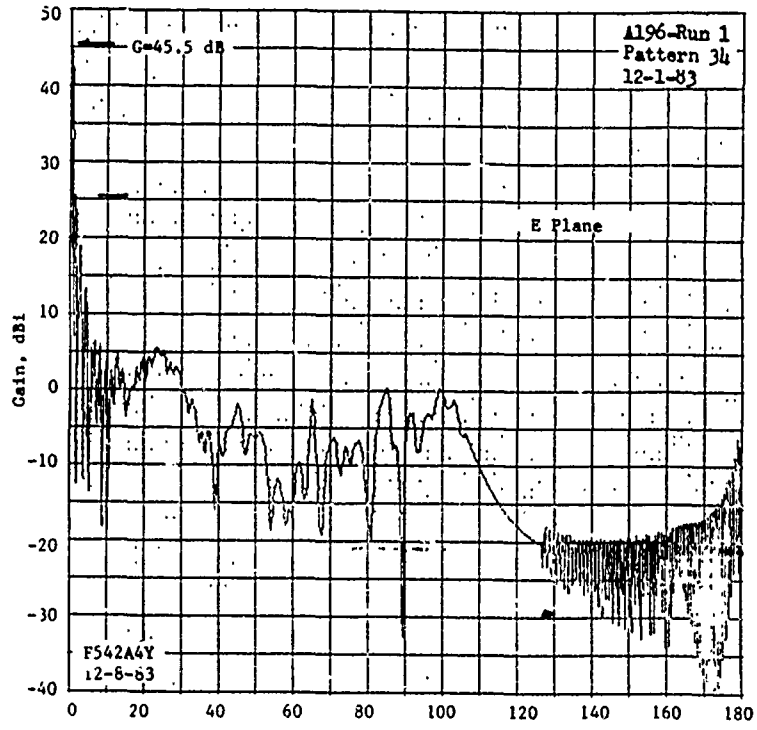

a) E Plane

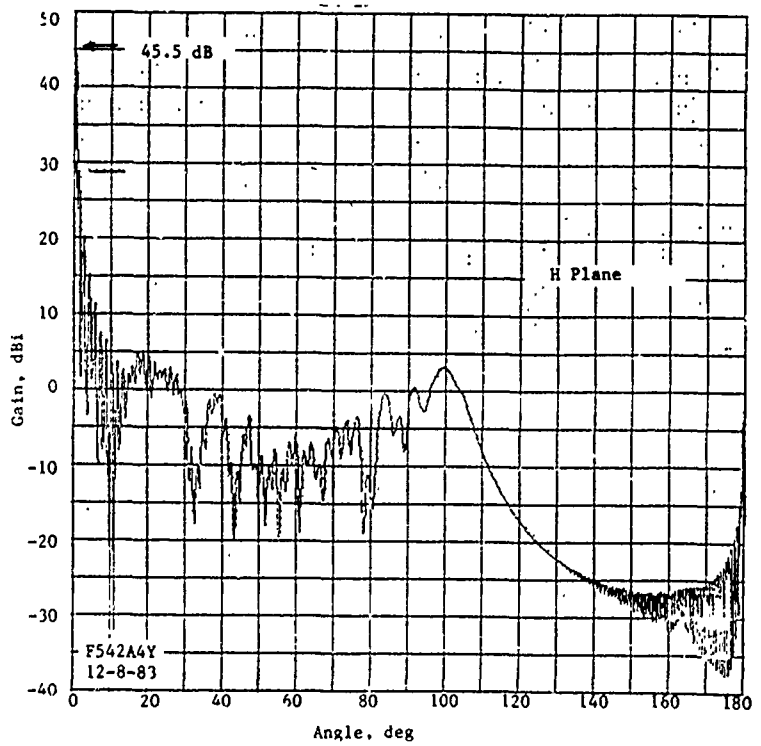

b) H Plane

Figure 55. 2-ft reflector computed patterns using the measured horn/oversized subreflector primary patterns

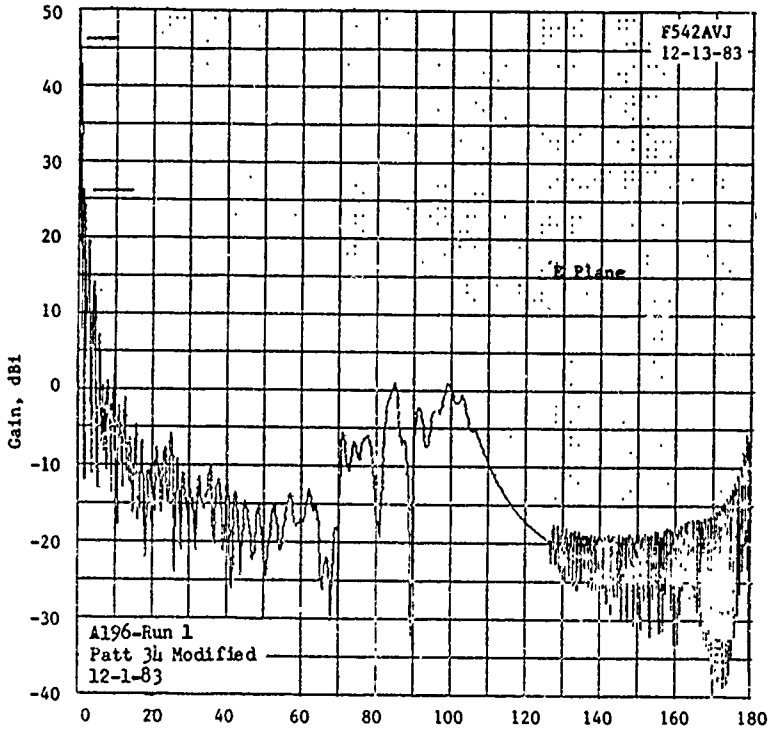

a) E Plane

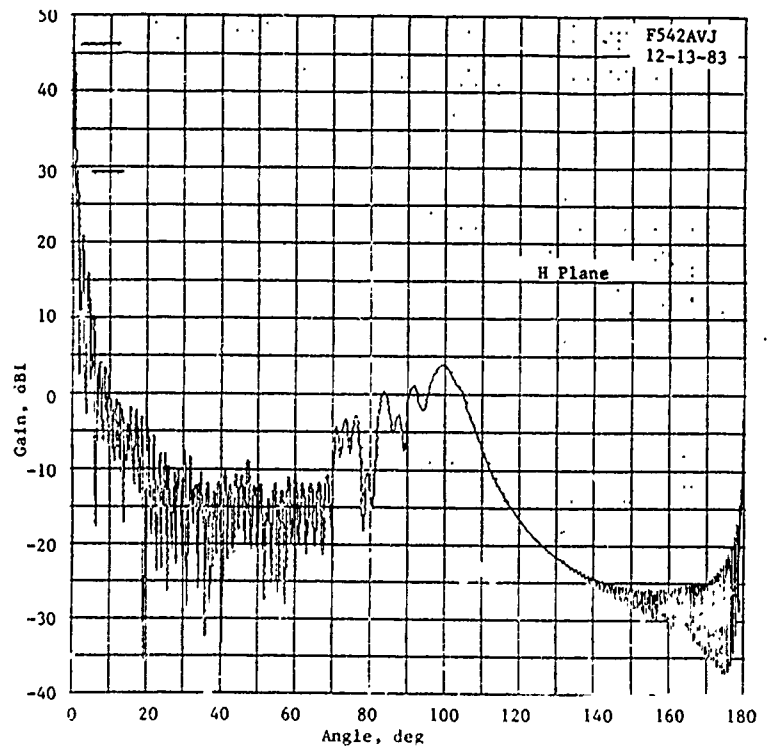

b) H Plane

Figure 56. 2-ft reflector computed patterns using horn/oversized subreflector spillover power of -20 dB

A comparison between the computed and the measured patterns can be observed in Fig. 57, where the locus of the measured patterns of Fig. 28 was transferred to the computed patterns. In the forward region there is good correlation between the measured and computed sidelobe levels. The sidelobe, caused by the spar scattering, at 84° is predominantly missing in the measured patterns. The reflector-edge diffracted backlobe region shows 5 to 10 dB discrepancies with the measured backlobe levels being lower. The discrepancy may be caused by the differences in the physical and mathematical models. The computations assume a knife-edge diffraction and without any physical objects in the rear of the dish. In the physical model, the reflector (Fig. 1) has a rolled edge ~0.4-in. radius and has an electronic box (Fig. 25) that has dimensions as large as the 2-ft reflector. A solid cylindrical spar was used in the mathematical model, rather than a truss structure.

2. Conventional Subreflector

Using the measured horn/conventional subreflector pattern (Fig. 20) as the primary pattern, the computed 2-ft reflector patterns are illustrated in Fig. 58. A comparison of the primary patterns between the oversized (Fig. 13) and the conventional subreflectors, show that the latter provides less uniform aperture distribution, lower edge illumination and less forward spillover power. Thus, the secondary patterns with the conventional subreflector show lower first sidelobes (tick marks indicated on each pattern), slightly less forward-region sidelobes, and a 10 dB reduction in the backlobe region ($\theta > 100°$). The computed directivity is 0.32 dB lower than for the oversized subreflector case.

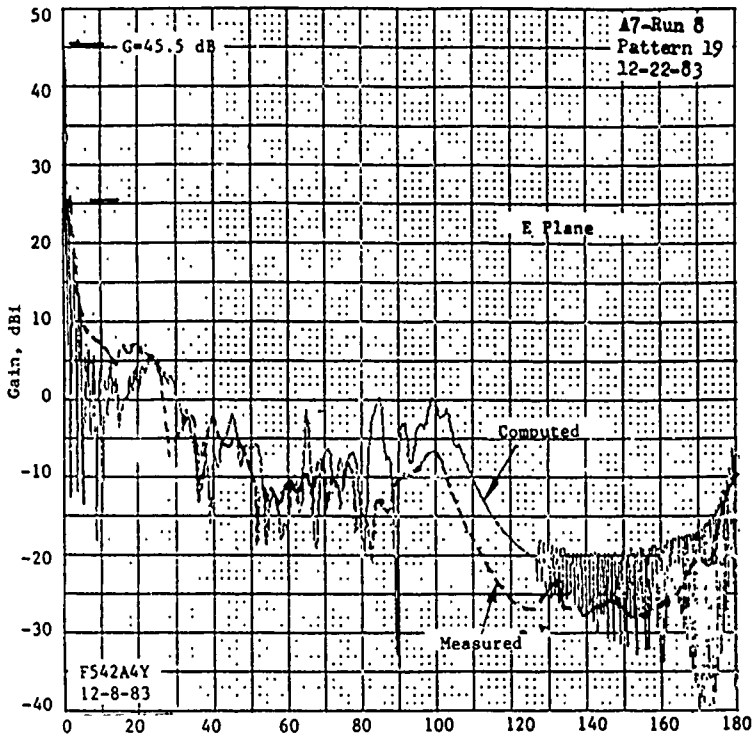

a) E Plane

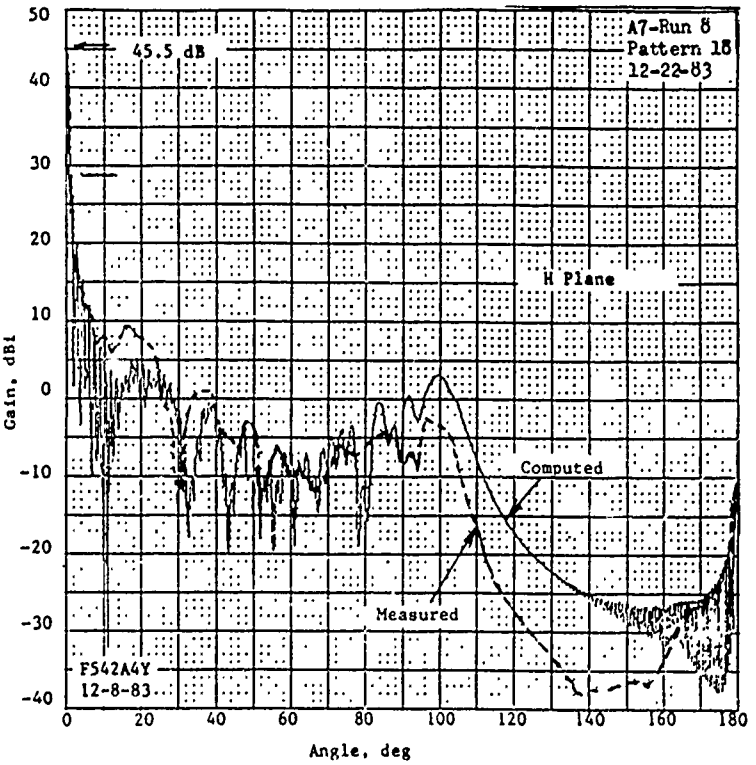

b) H Plane

Figure 57. Computed and measured 2-ft reflector patterns (oversized sub-reflector)

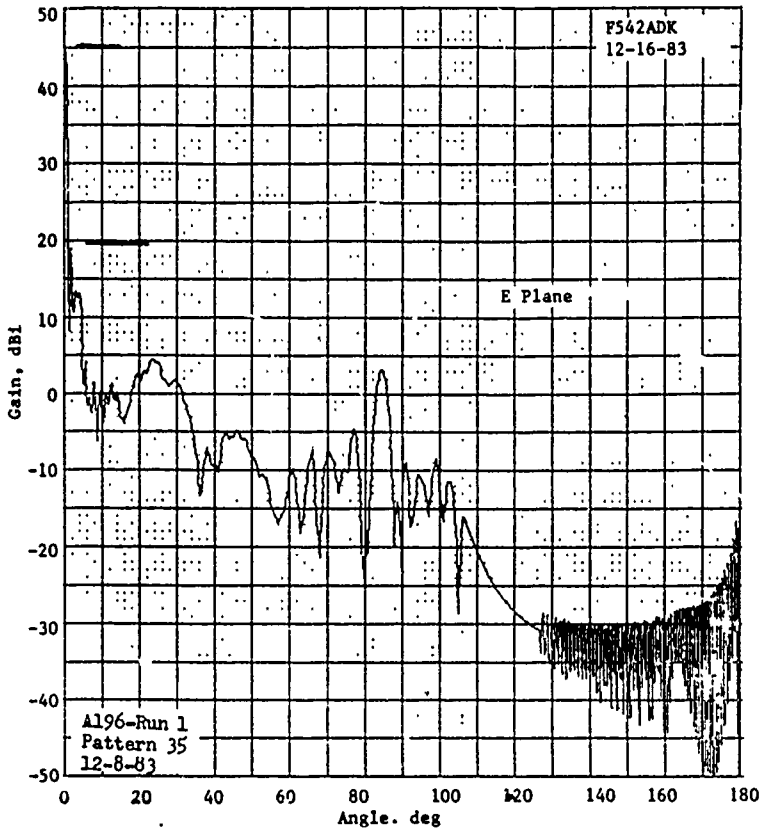

a) E Plane

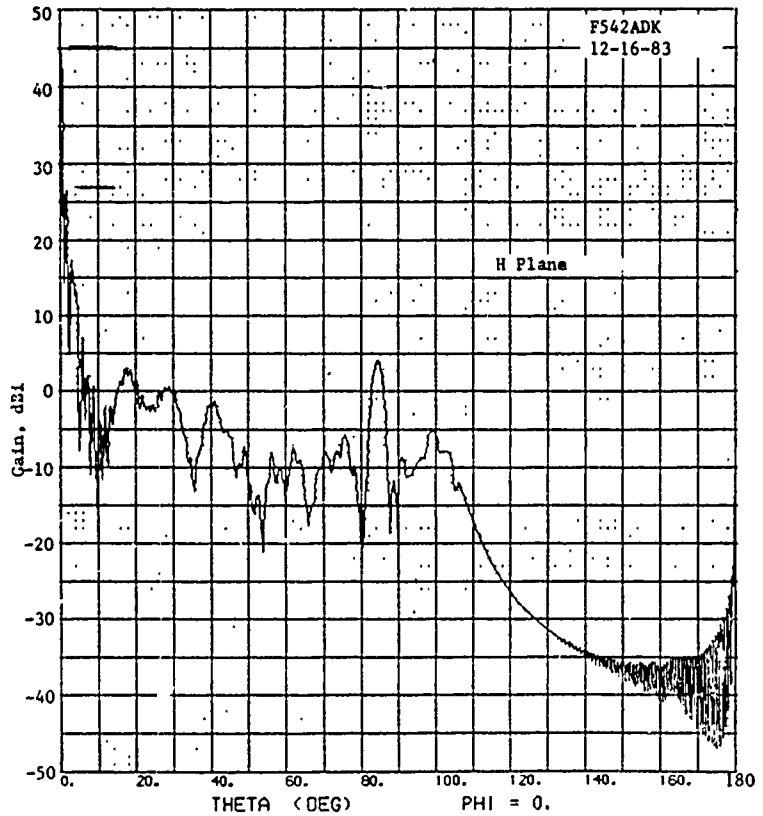

b) H Plane

Figure 58. 2-ft reflector computed patterns using the measured horn/conventional subreflector primary patterns

The measured 2-ft reflector pattern (conventional subreflector) locus of maximum points is replotted on the computed patterns; thus, a comparison between the measured and computed patterns can be seen on Fig. 59. Similar comments made on the comparison between computed and measured patterns for the oversized subreflector (Fig. 57) can be applied to the conventional subreflector secondary patterns. In general, the backlobe region measured pattern is 5 to 10 dB lower than the computed pattern.

A subreflector conical flange is one of the methods suggested to reduce the reflector sidelobes. The horn-subreflector patterns of Fig. 21 show some indications that the flange is possible because of the lower edge illumination and lower spillover power. To illustrate the potential of the conical flange, the secondary patterns were computed as shown in Fig. 60. As compared to the baseline conventional subreflector (Fig. 58), the conical flange attachment secondary patterns sporadically yield lower sidelobes in the forward region by several dB; while in the entire back region the levels are consistently lower by ~6 dB and 2 dB in the E and H planes, respectively.

The computed reflector patterns indicate that no one technique will provide a major breakthrough in sidelobe reduction. However, a combination with the reflector shroud or plates could provide adequate reduction to meet particular system-user requirements.

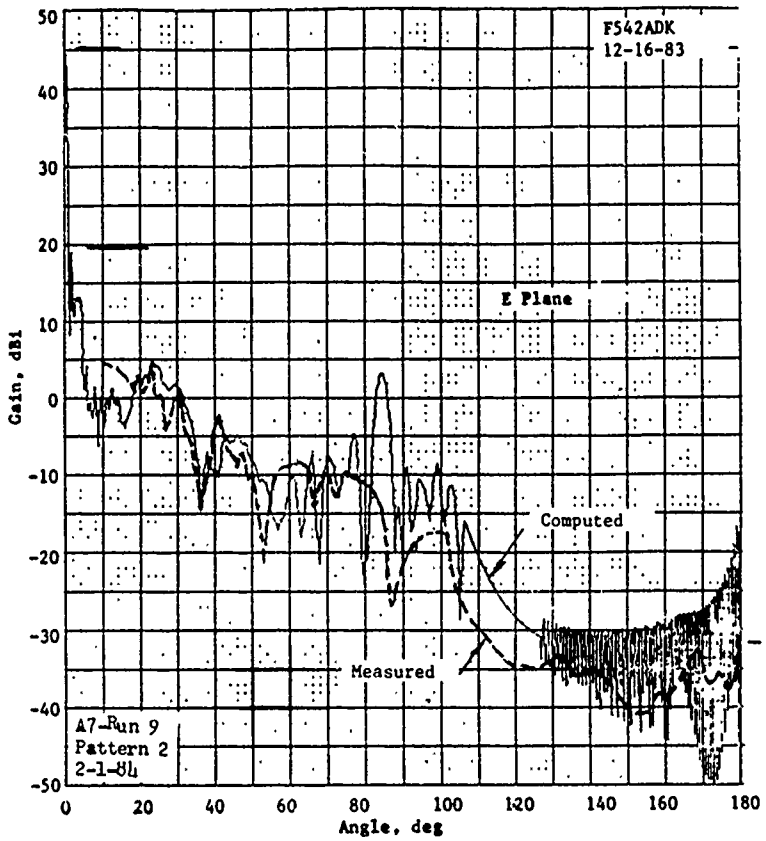

a) E Plane

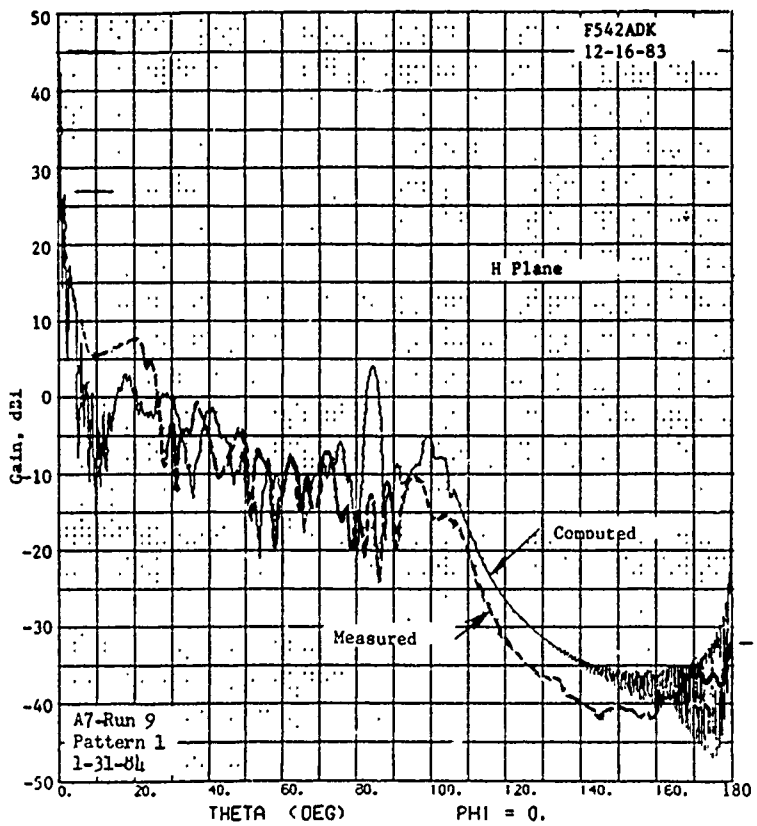

b) H Plane

Figure 59. Computed and measured 2-ft reflector patterns (conventional sub-reflector)

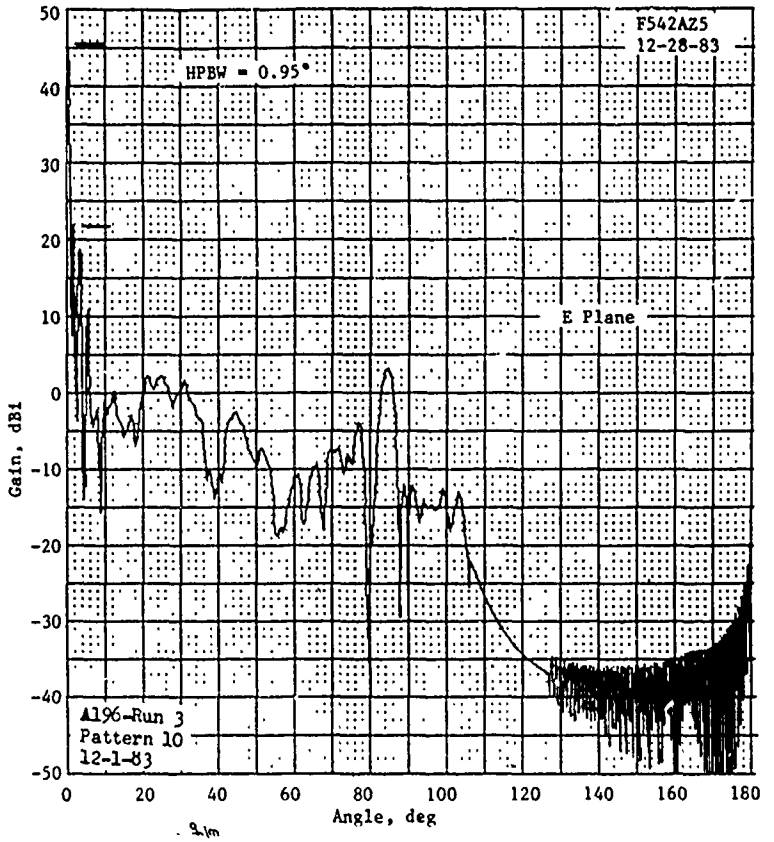

a) E Plane

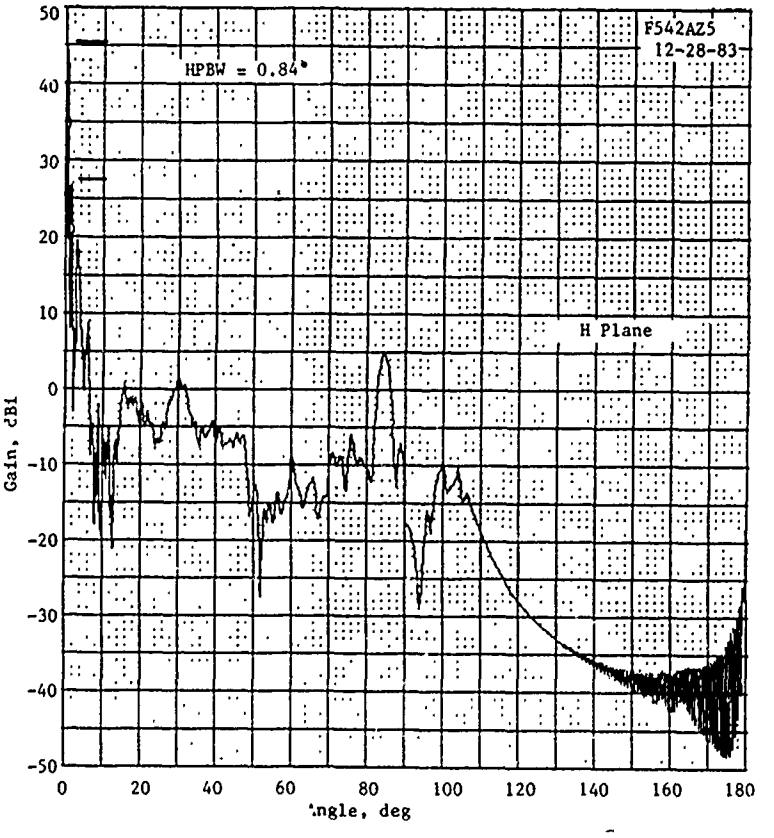

b) H Plane

Figure 60. 2-ft reflector computed patterns using the measured horn/conventional subreflector conical flange (1λ) primary patterns

B. OSU Analysis

Professor Rudduck and S. H. Lee[1] developed a useful computer code that can compute the far-field patterns of prime-focus paraboloidal reflector antennas that account for the feed pattern characteristics, feed blockage and the effects of the spars. Since then he has expanded the program to include near-field patterns, near-field coupling and the effects of obstacles in the vicinity of the reflector aperture[4]. However, Rudduck did not have the computer code developed for Cassegrain antennas. To enable him to derive shielding techniques to reduce sidelobes of Cassegrain antennas, it was necessary for him to develop a Cassegrain computer code. His approach was to compute the horn feed pattern for a specified horn, determine the horn-subreflector pattern, and then calculate the Cassegrain reflector secondary patterns. Section V.B. describes his results. The OSU accomplishment includes a parametric study on the optimum horn size to minimize the sidelobe levels. The effects of a space-frame radome on the reflector patterns were also computed.

1. Horn and Oversized Subreflector

The computed E and H plane amplitude patterns of the 1.2-in. diameter conical horn are shown in Fig. 61. The superimposed data points represent the measured data from Fig. 10. The correlation between measured and computed patterns is good. The phase patterns in the E and H planes are shown in Fig. 62.

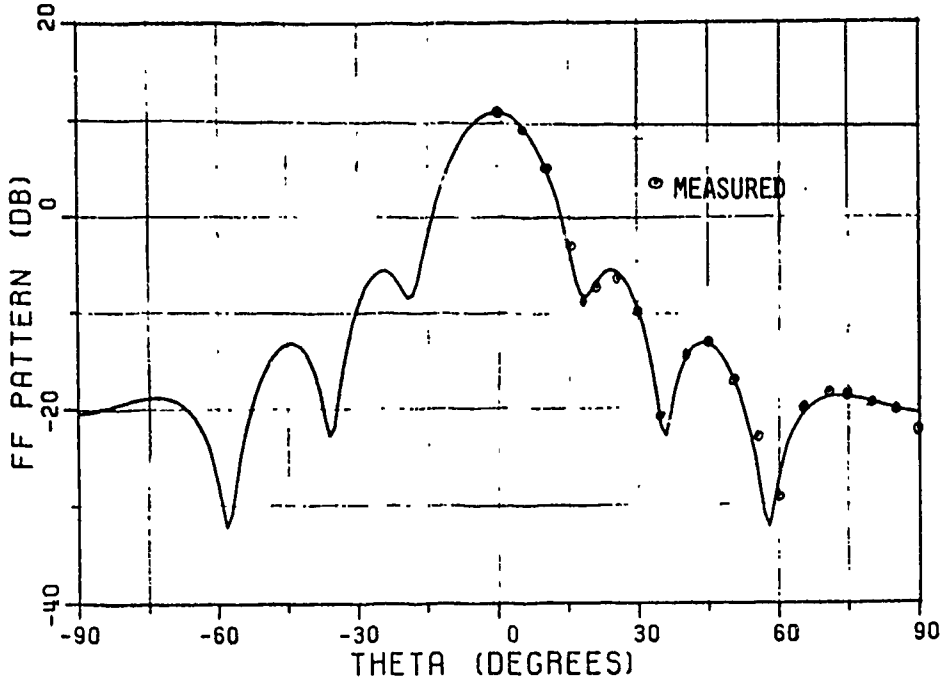

a) E Plane

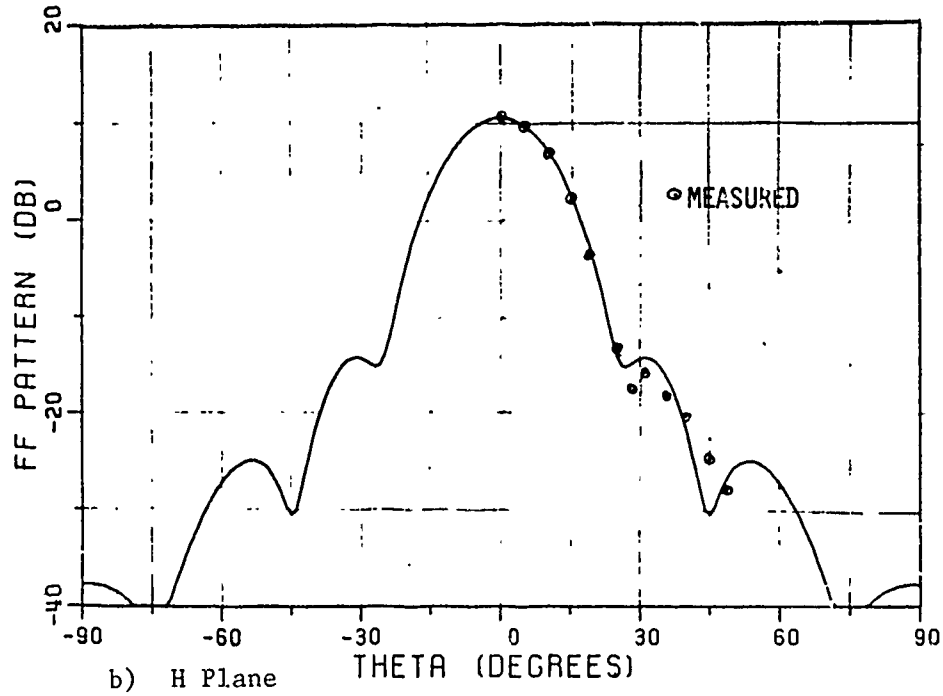

b) H Plane

Figure 61. Computed amplitude patterns of 1.2-in. diameter conical horn

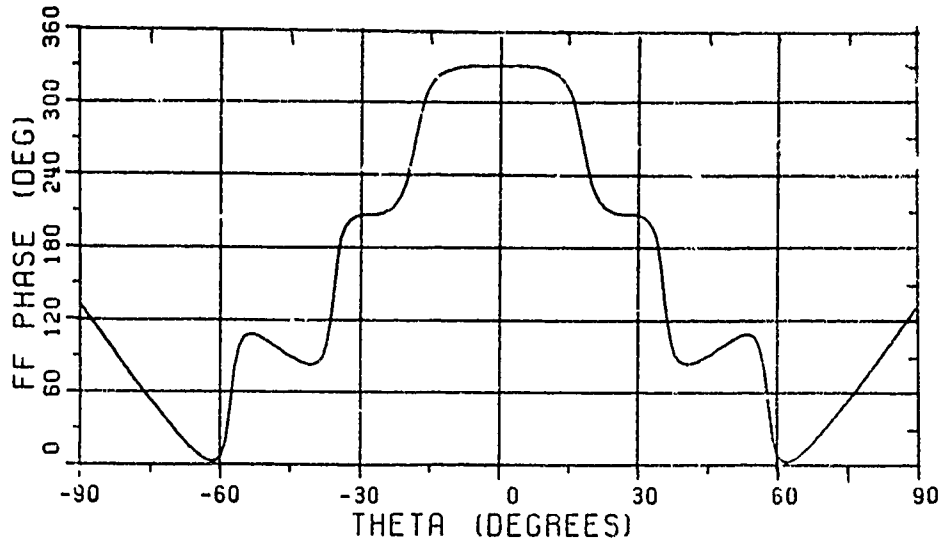

a) E Plane

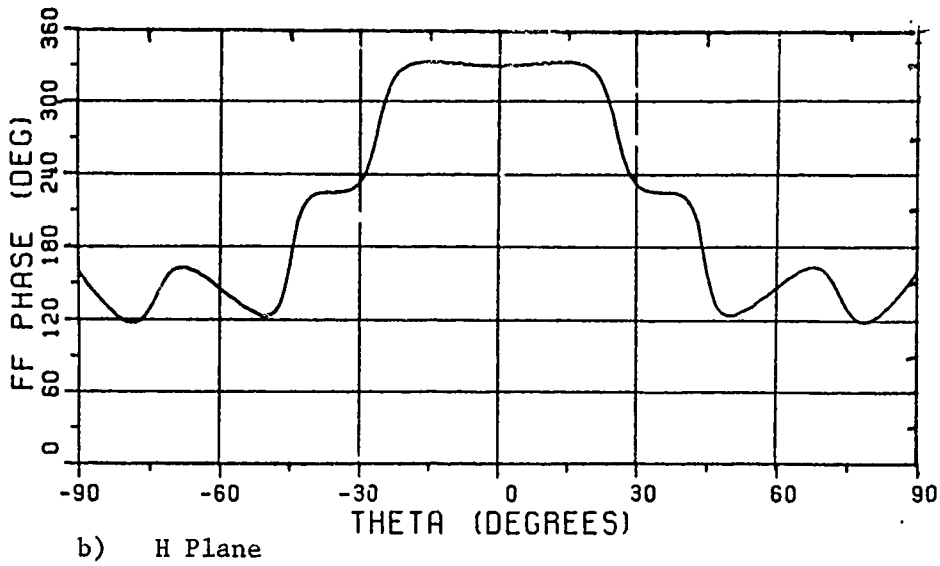

b) H Plane

Figure 62. Computed phase patterns of 1.2-in. diameter conical horn

The horn-subreflector (oversized) computed patterns are shown in Fig. 63 with the dB scale representing an absolute gain level. The computations accounting for the feed horn blockage and the circular subreflector correlate very well with the measured patterns of Fig. 13. The scales of the computed patterns have been selected to match those of the measured patterns to provide ease in making comparison of the computed and measured patterns.

Rudduck's 2-ft computed reflector patterns, shown in Fig. 64, do not account for the strut scattering which would show up in the region $75° < \theta < 90°$. (Subsequent reflector pattern computations, including the struts, show that the strut scatter tends to be buried in the horn-subreflector spillover.) These computed patterns correspond with our empirical plots of Fig. 55.

2. Conventional Subreflector

The horn-subreflector computed primary patterns are shown in Fig. 65, using the computed feed horn patterns of Fig. 61. In general, the computed patterns have a good comparison with the measured patterns of Fig. 20, except for a region near $\psi = 0°$.

The computed 2-ft reflector secondary patterns (without the struts), shown in Fig. 66, can be compared to our computed empirical patterns of Fig. 58 (including the struts). The two sets of computed dish patterns are very similar except for the prominent sidelobes at 84° which are attributable to the struts. With the conventional subreflector the 2-ft antenna has a computed directivity of 45.65 dB vs 46.36 dB for the oversized subreflector.

The ordinate and abscissa scales of the computed patterns of Fig. 66 were changed (as done in Fig. 67) to conform to the scales of the measured patterns to simplify the comparison of computed and measured data. Thus, the computed patterns of Fig. 67 can be overlaid onto the measured patterns of Fig. 41.

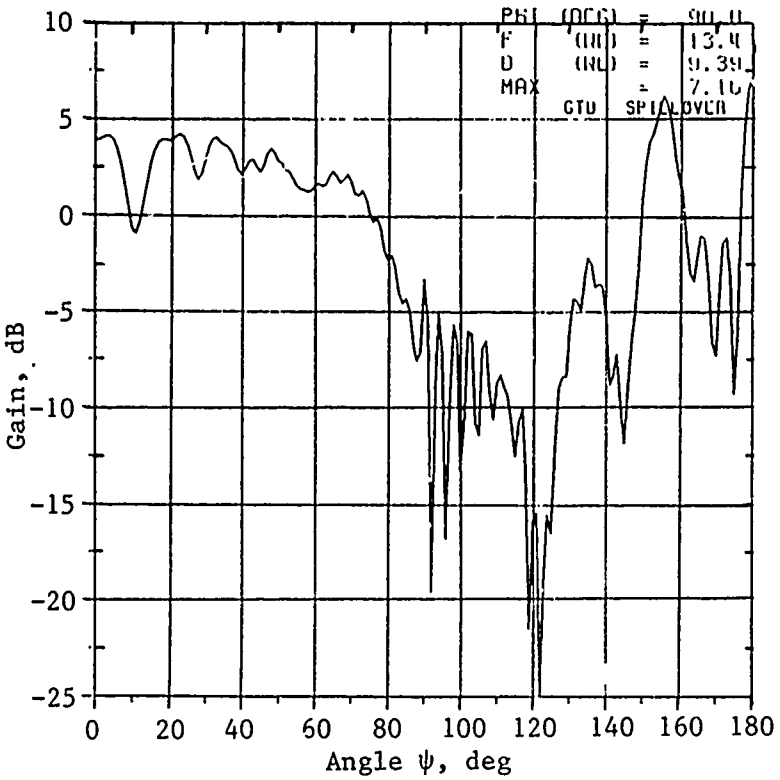

a) E Plane

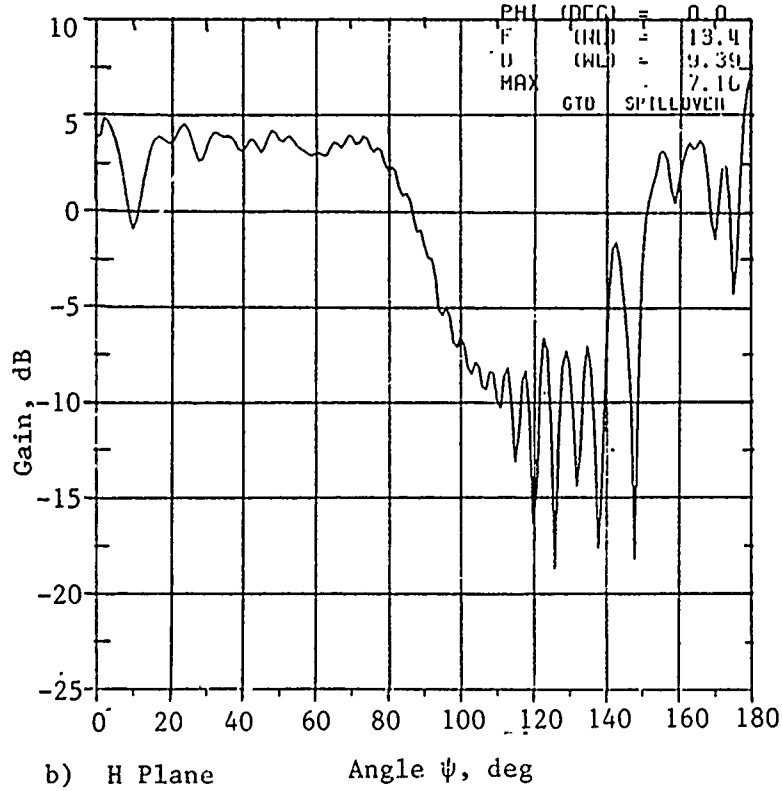

b) H Plane

Figure 63. Computed horn/oversized subreflector patterns

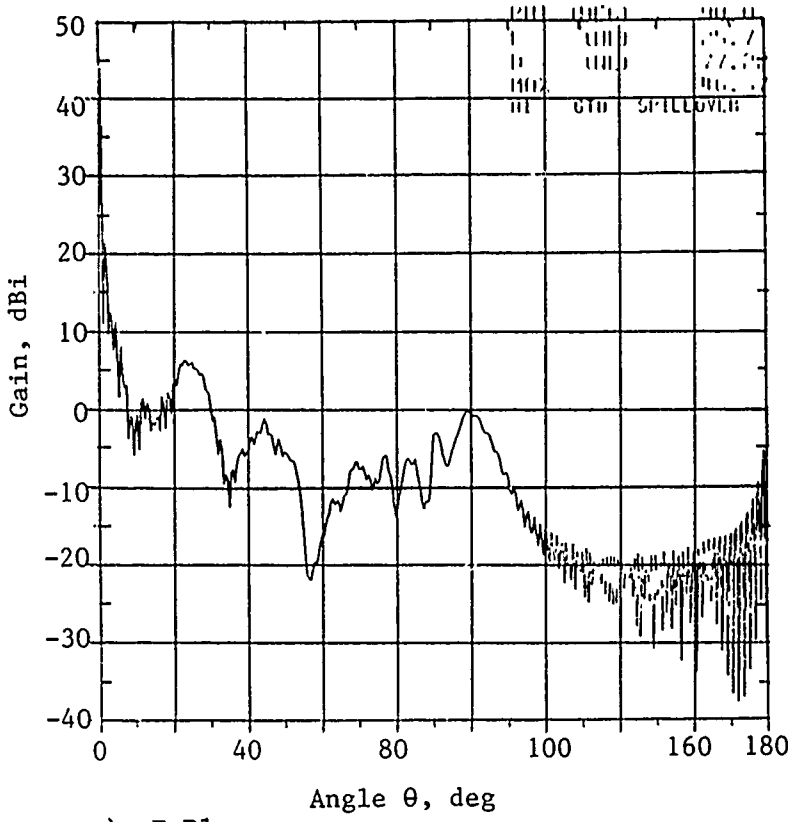

a) E Plane

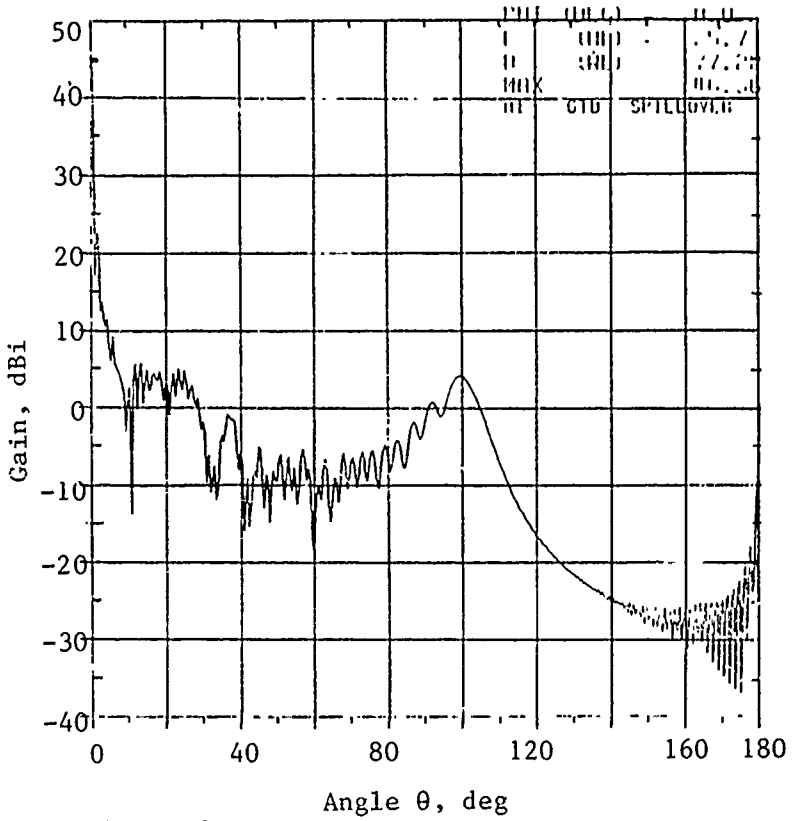

b) H Plane

Figure 64. Computed 2-ft reflector patterns (oversized subreflector)

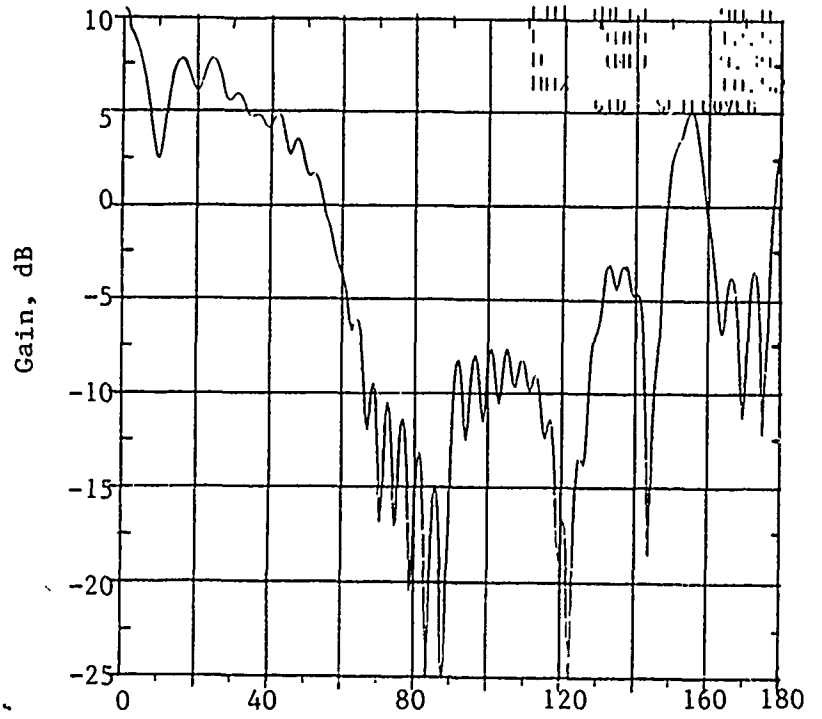

(a) E Plane

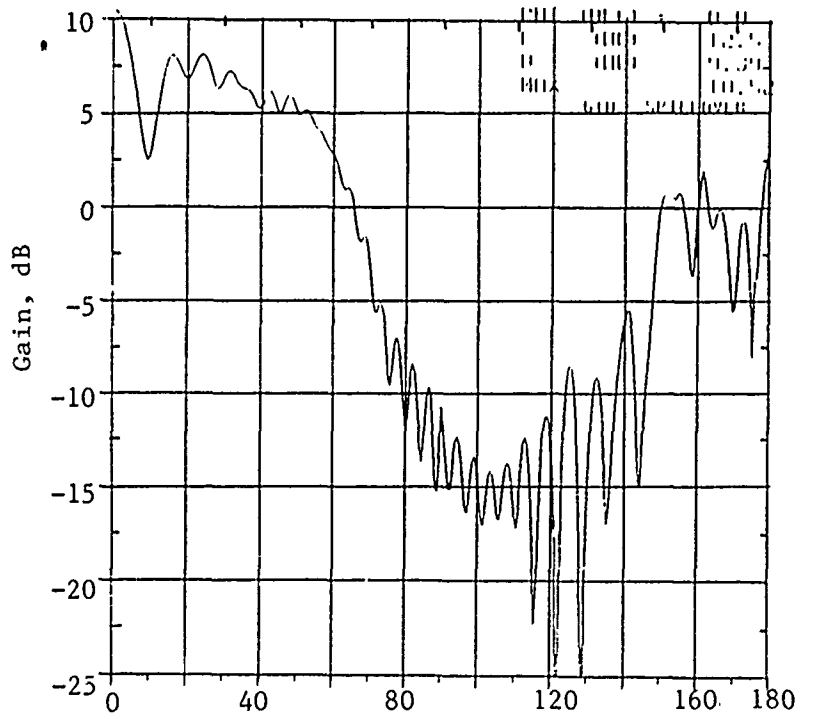

(b) H Plane

Figure 65. Computed horn/conventional subreflector patterns

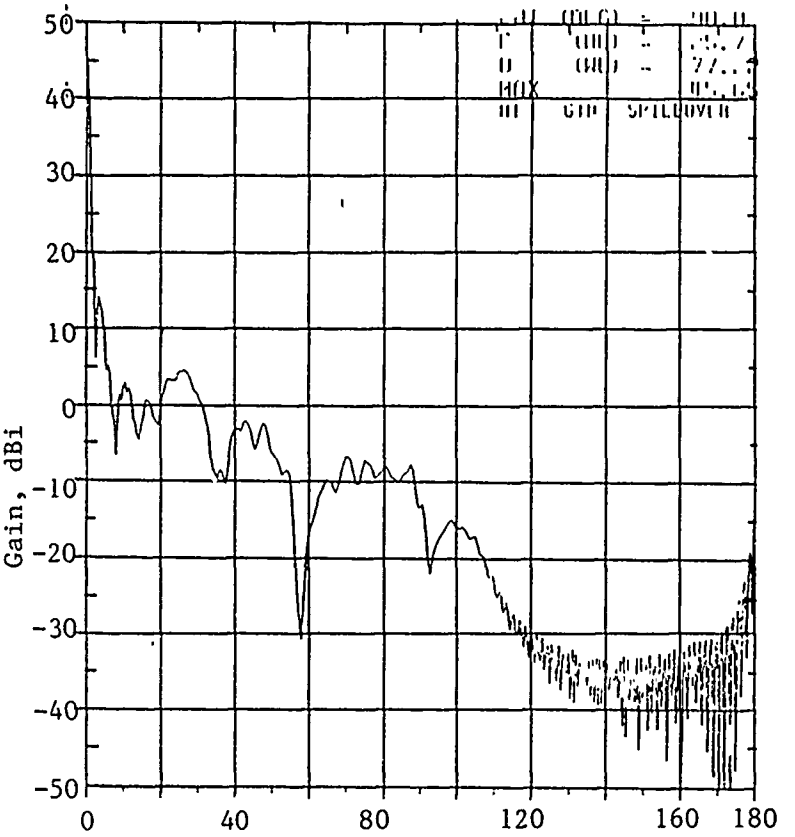

a) E Plane

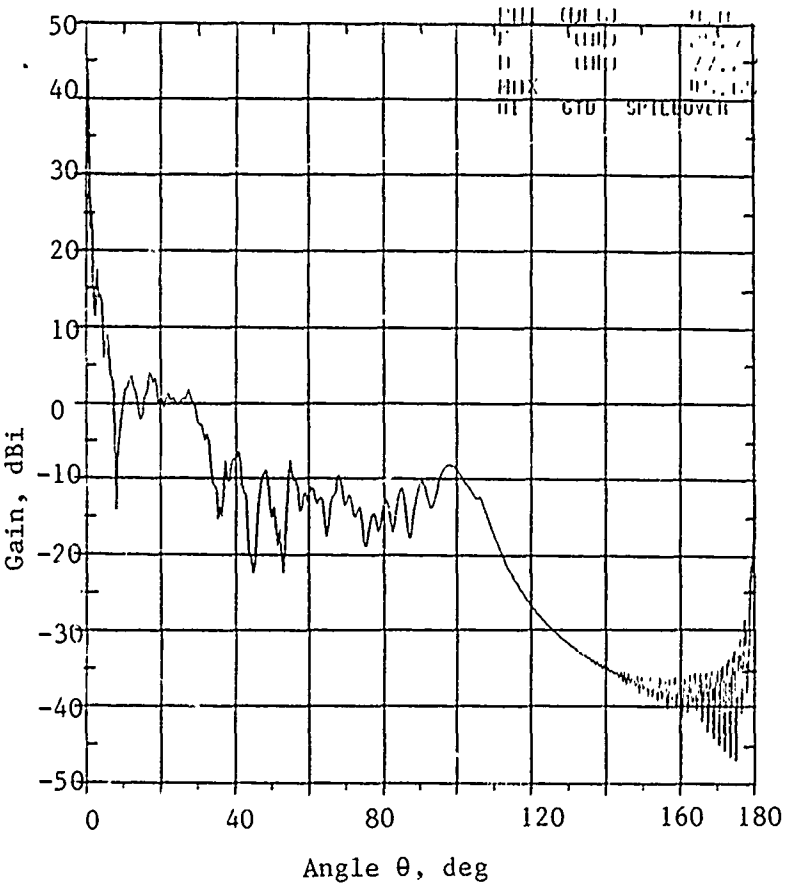

b) H Plane

Figure 66. OSU computed 2-ft reflector patterns (1.2-in. conical horn, conventional subreflector)

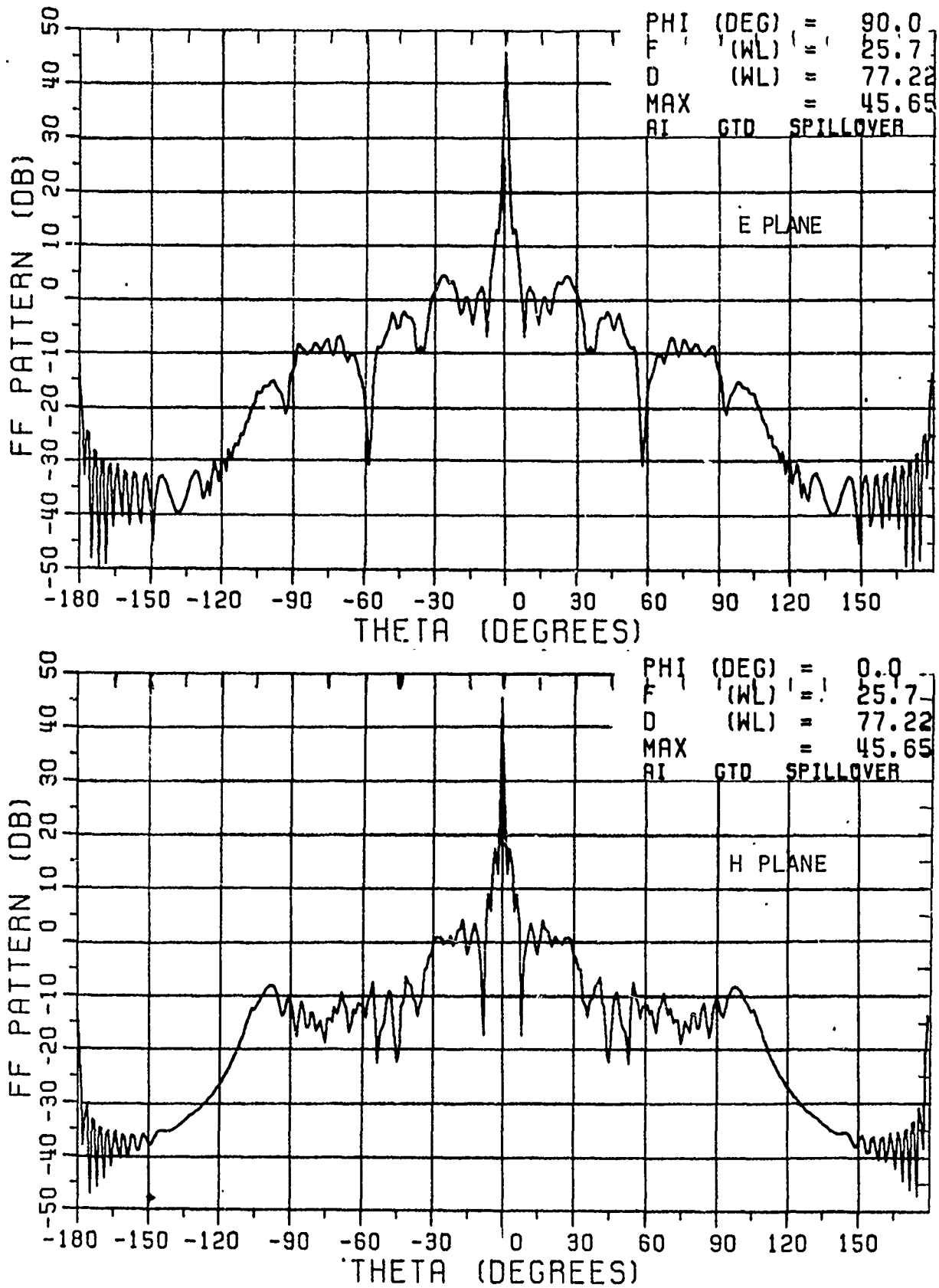

Figure 67. OSU computed 2-ft reflector patterns (1.2-in. conical horn, conventional subreflector) normalized to measured-pattern scales

OSU computed the pattern for the 3 x 6 in. plates mounted at the reflector edge as shown in Fig. 68. As compared to the measured patterns of Fig. 50, the computed forward region sidelobe levels are within a few dB. For the E-plane rear region, the measured levels are higher than those computed by ~10 dB and near the rear caustic region (θ near 180°), the measured backlobes are higher by 20 dB. However, in the H plane, the computed backlobe levels are ~10 dB higher than the measured patterns, except near the rear region where the measured levels are higher. The mathematical model does not incorporate both edge plates in the computation; thus, the region near 180° is not truly representative of the physical case.

OSU made a parametric study of the horn parameters to minimize the reflector sidelobe levels. A 1.4-in. diameter conical (10.83°) corrugated feed horn was found to be optimum with the reflector patterns shown in Fig. 69. As compared to the baseline 1.2-in. diameter smooth-wall conical horn patterns of Fig. 67, the 1.4-in. corrugated horn improved the patterns in the following manner: 1) the E plane improved in sidelobe levels by 5 to 10 dB in the forward region with no change in the rear region, and 2) the H plane patterns improved ~8 dB for the entire region $\theta > 75°$.

Figure 70 shows the computed wide-angle reflector patterns with the addition of the 3 x 6 in. plates to the reflector edge. As compared to the bare reflector pattern of Fig. 60, the backlobes can be improved by a minimum of ~15 dB.

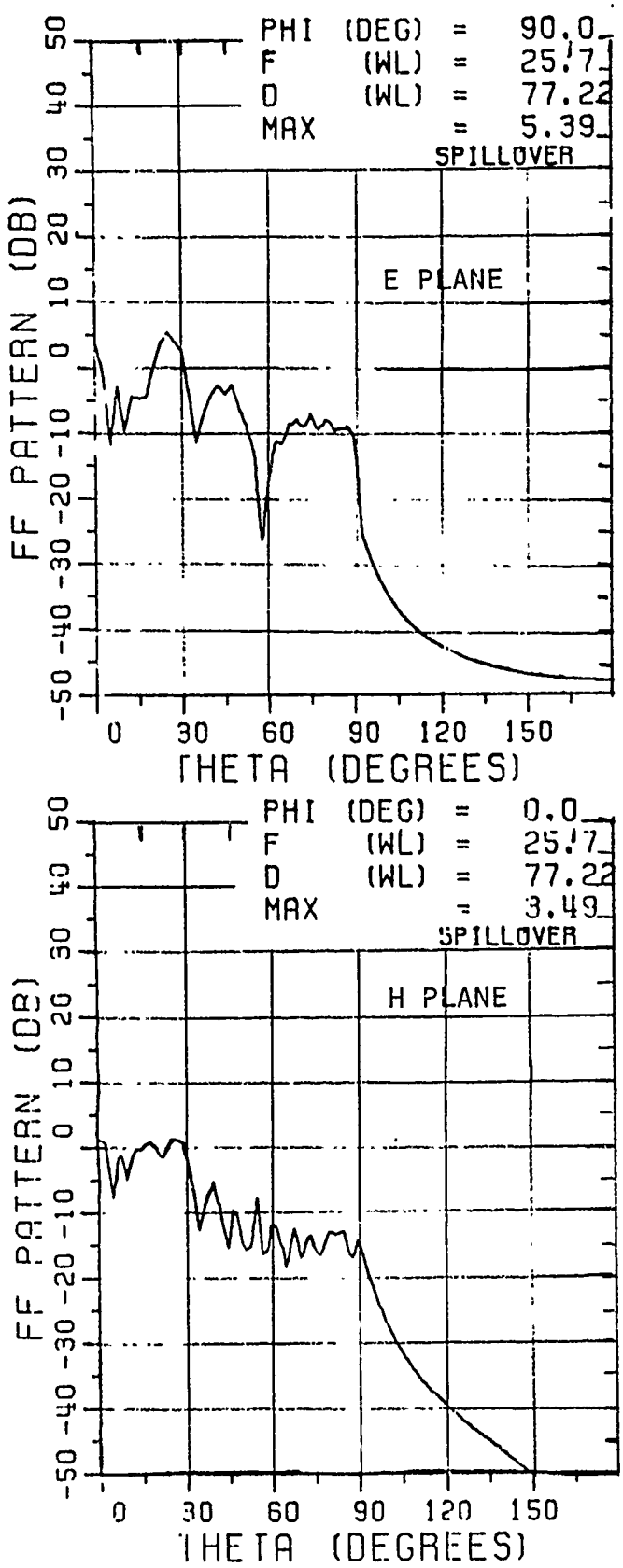

Figure 68. OSU computed 2-ft reflector wide-angle sidelobe patterns (1.2-in. conical horn, conventional subreflector) with 3 x 6-in. plates

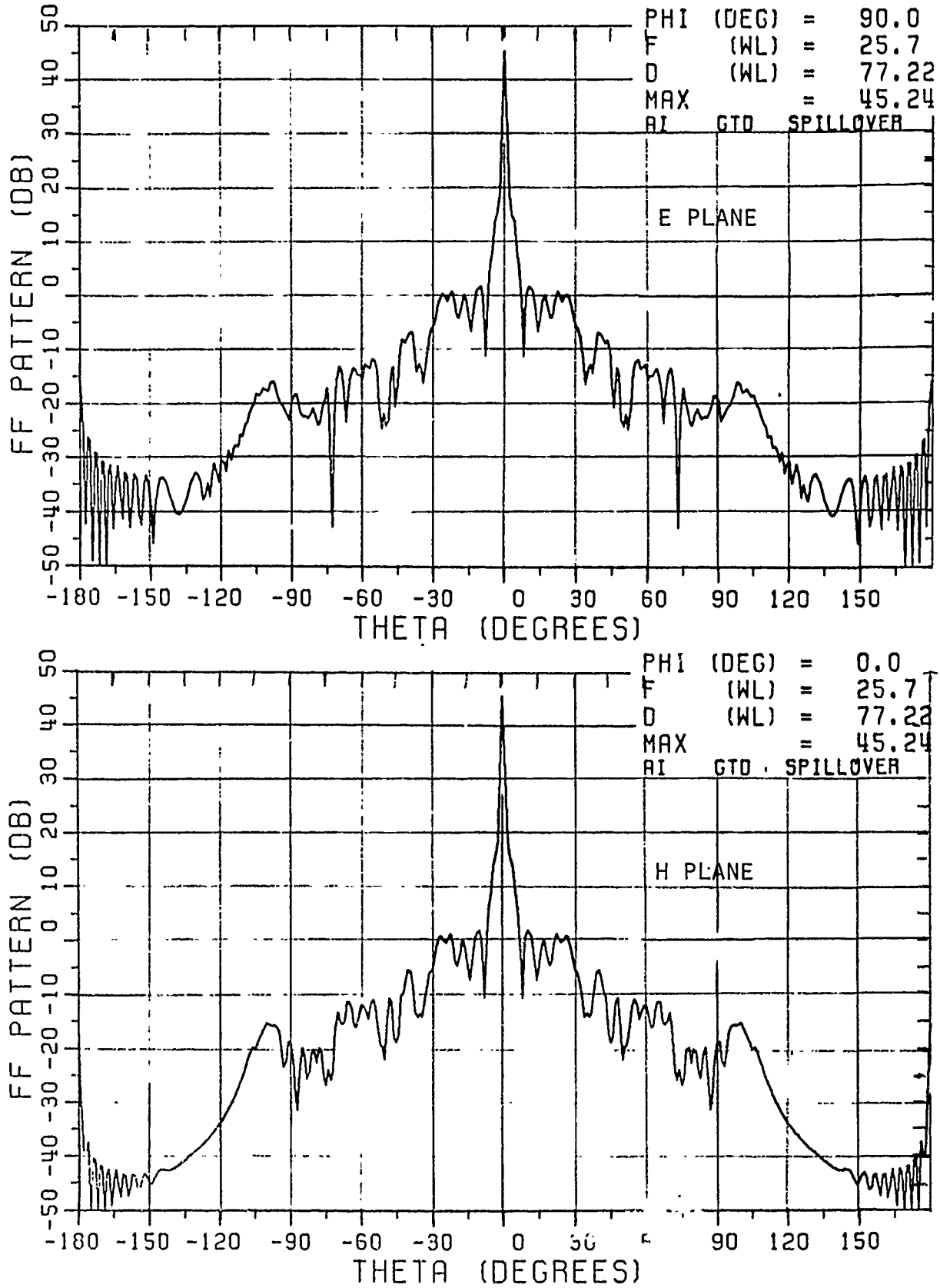

Figure 69. OSU computed 2-ft reflector patterns with 1.4-in. diameter corrugated feed horn and conventional subreflector

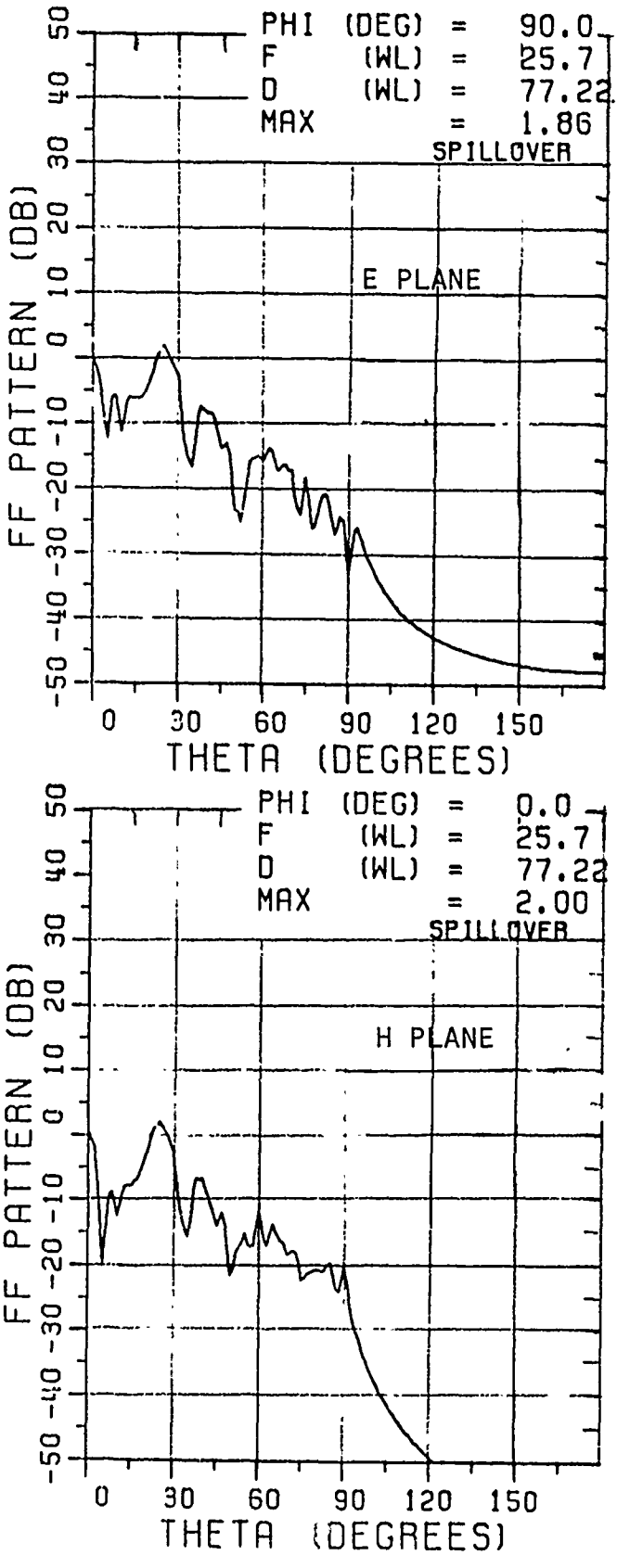

Figure 70. OSU computed 2-ft reflector wide-angle sidelobe with 3 x 6-in. edge plates (1.4-in. corrugated horn, conventional subreflector)

3. Space Frame Radome

The effects of a metal space frame radome on the sidelobe levels of a reflector antenna were determined by computations.* A 60-ft diameter reflector enclosed in a 93-ft diameter radome (ESSCO Type 7000) was selected for the analysis. The horn-subreflector pattern of Fig. 63 (oversized subreflector) illuminated the main reflector. The spherical metal space frame was simulated by a planar surface as illustrated in Fig. 71. The planar configuration was chosen because it presented a worst case for sidelobe deterioration as compared to the spherical model and also the planar model was simpler to analyze.

The metallic members were simulated as a rectangular bar 1.1 in. wide x 4-in. deep (should have been 4.6 in.). The ~6.3 in. diameter hubs (or flange) that connects the size space frame members together at a common point were not included in the analysis. The thin dielectric membranes were considered to have negligible effects on the sidelobe patterns so they were not included.

Figure 72 shows the H-plane patterns of a 60-ft dish (struts not included) with and without the radome. The sidelobe levels contributed by the radome itself are illustrated in Fig. 73. The co-polarized radome pattern level varies from +5 dBi to -10 dBi level which contributed to ~5 dB increase in the 60-ft dish sidelobe levels. The cross-polarized levels generated by the radome are several orders of magnitude lower (Fig. 73b) resulting in the 60-ft dish cross-polarized pattern of Fig. 74.

The expanded patterns ($\theta < 10°$) for the no-radome case and with radome are shown in Fig. 75. The radome-only scatter pattern is plotted in Fig. 76.

*To be described in a forthcoming OSU technical report

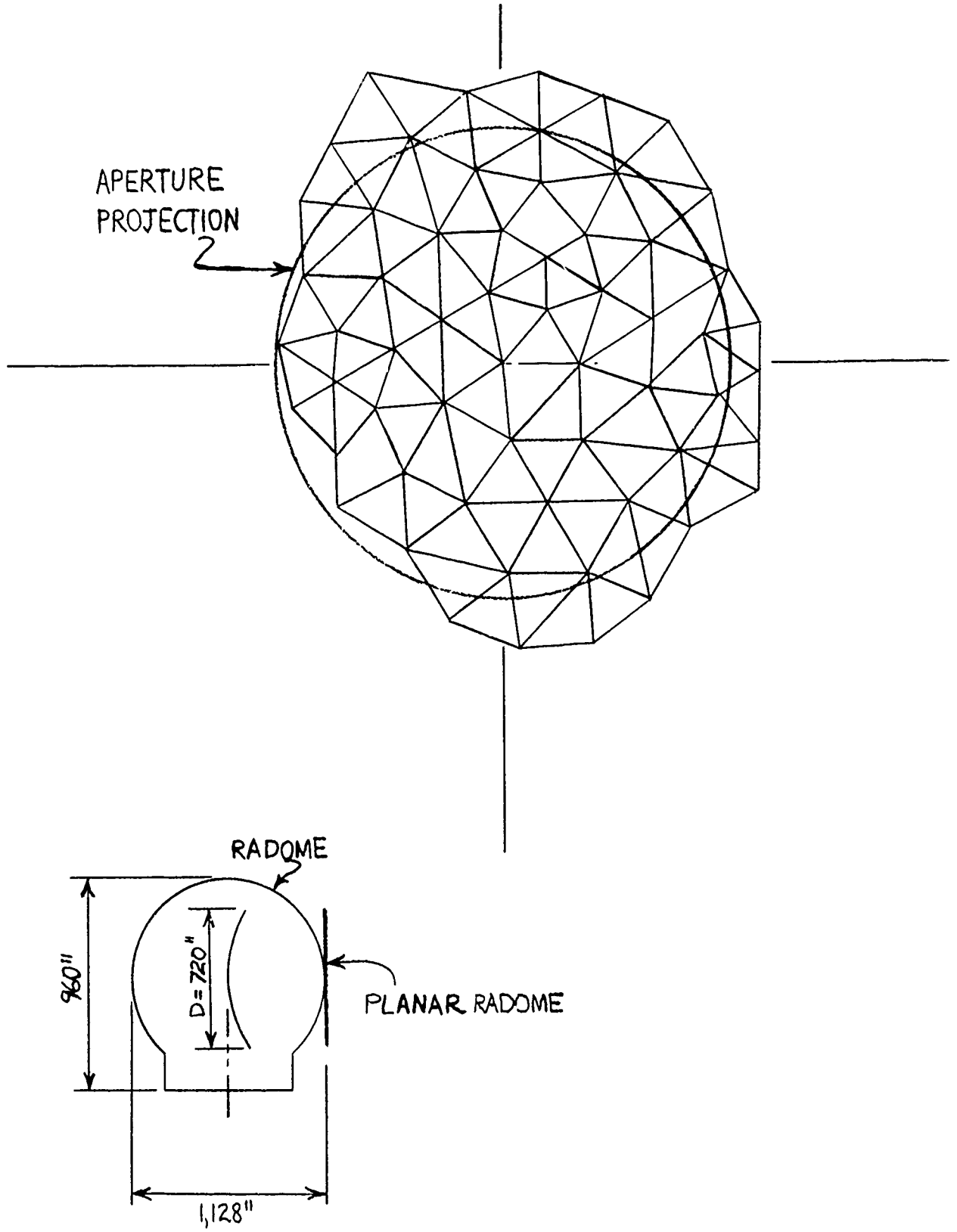

Figure 71. Metal space frame geometry

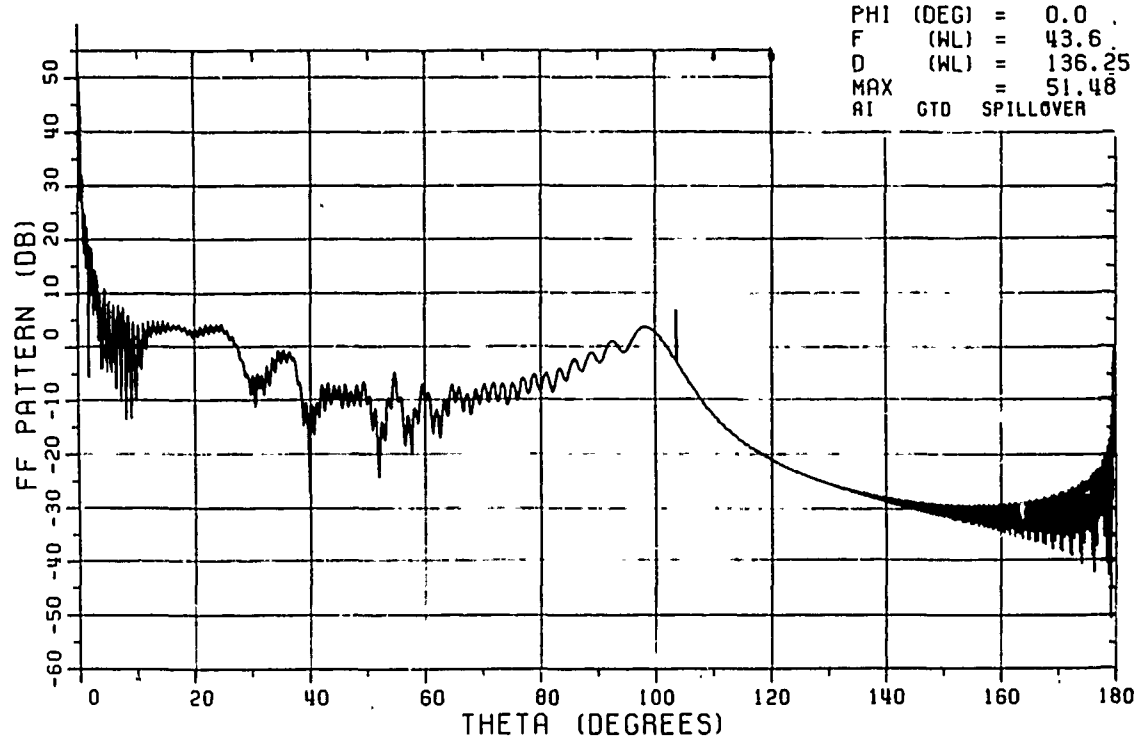

(a) Without radome

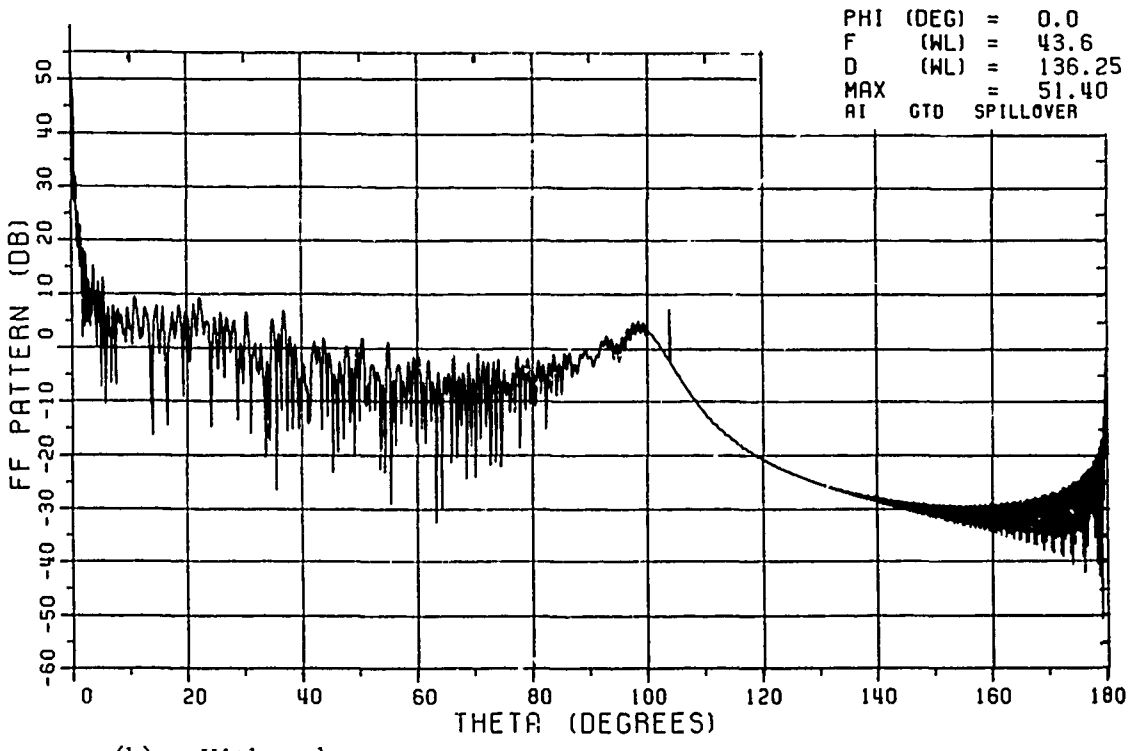

(b) With radome

Figure 72. 60-ft dish patterns with and without metal space frame radome

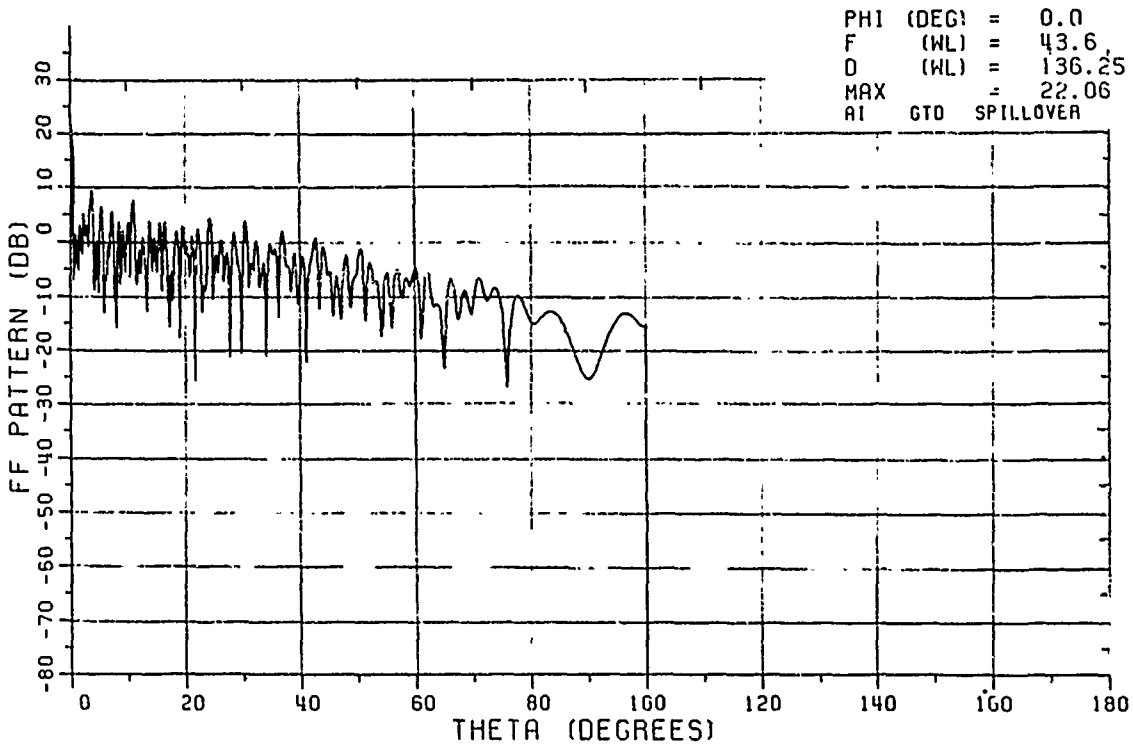

(a) Copolarization

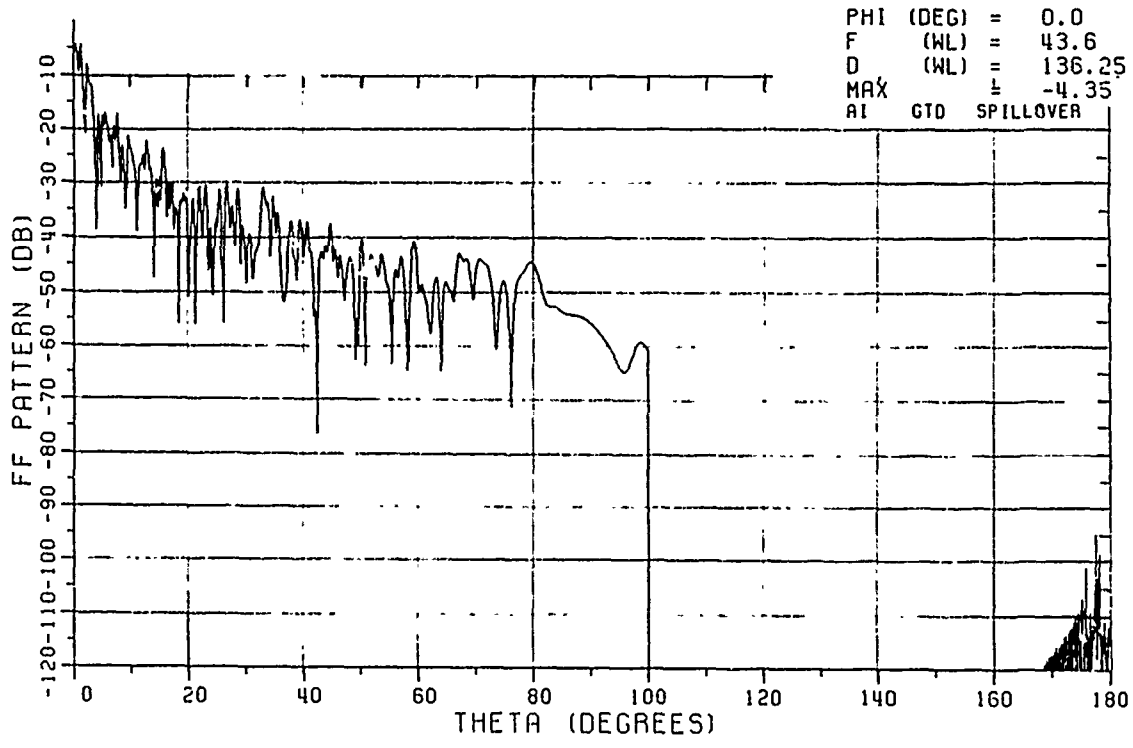

(b) Cross polarization

Figure 73. Scatter patterns of metal space frame radome structure

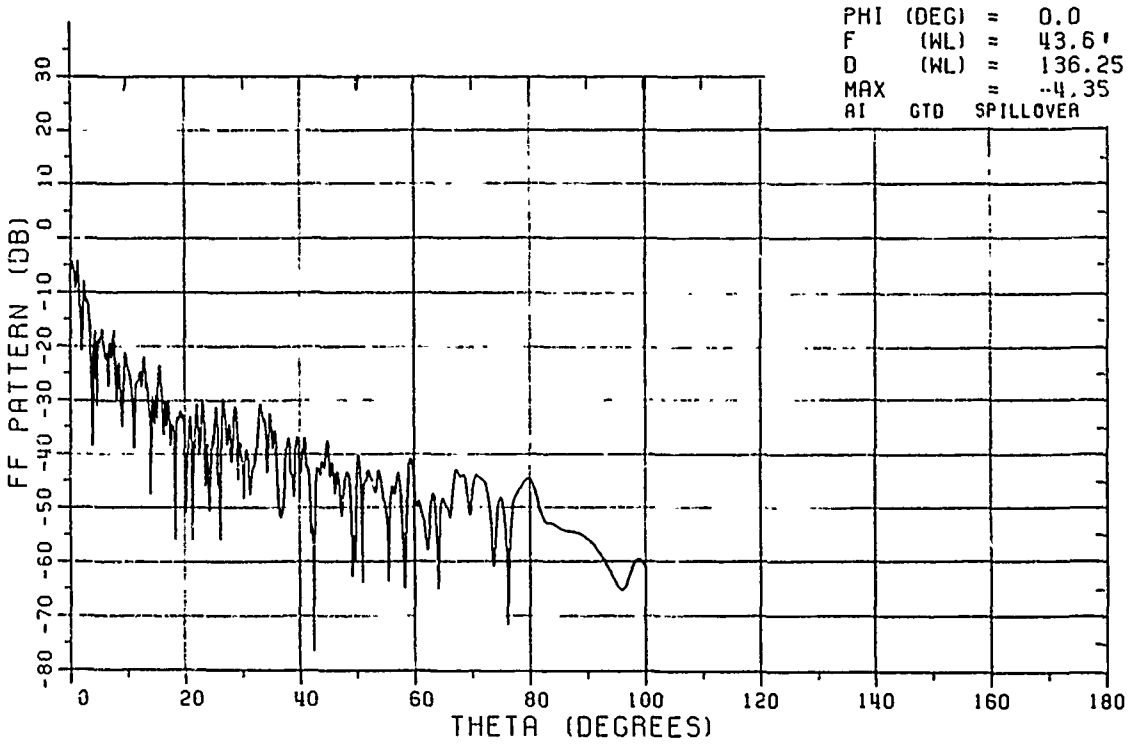

Figure 74. Cross-polarized 60-ft dish pattern with radome

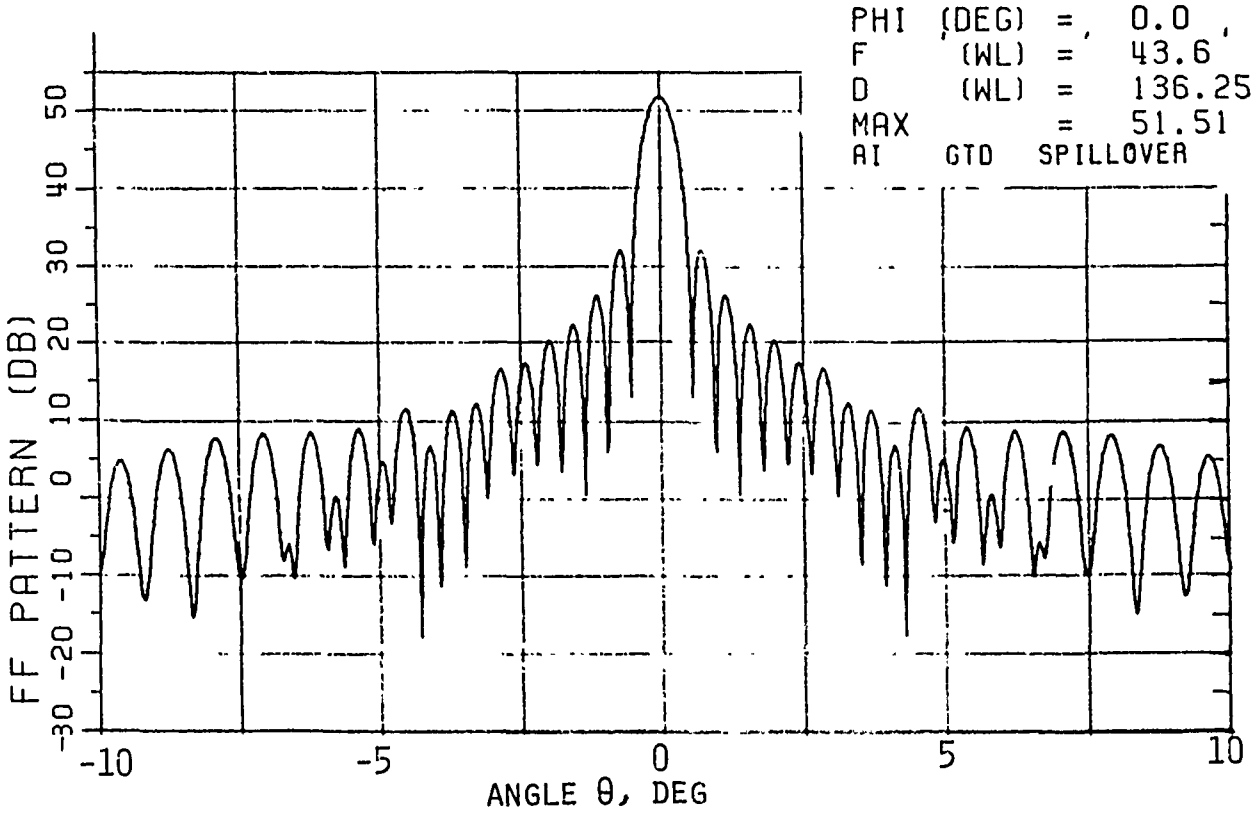

(a) Without radome

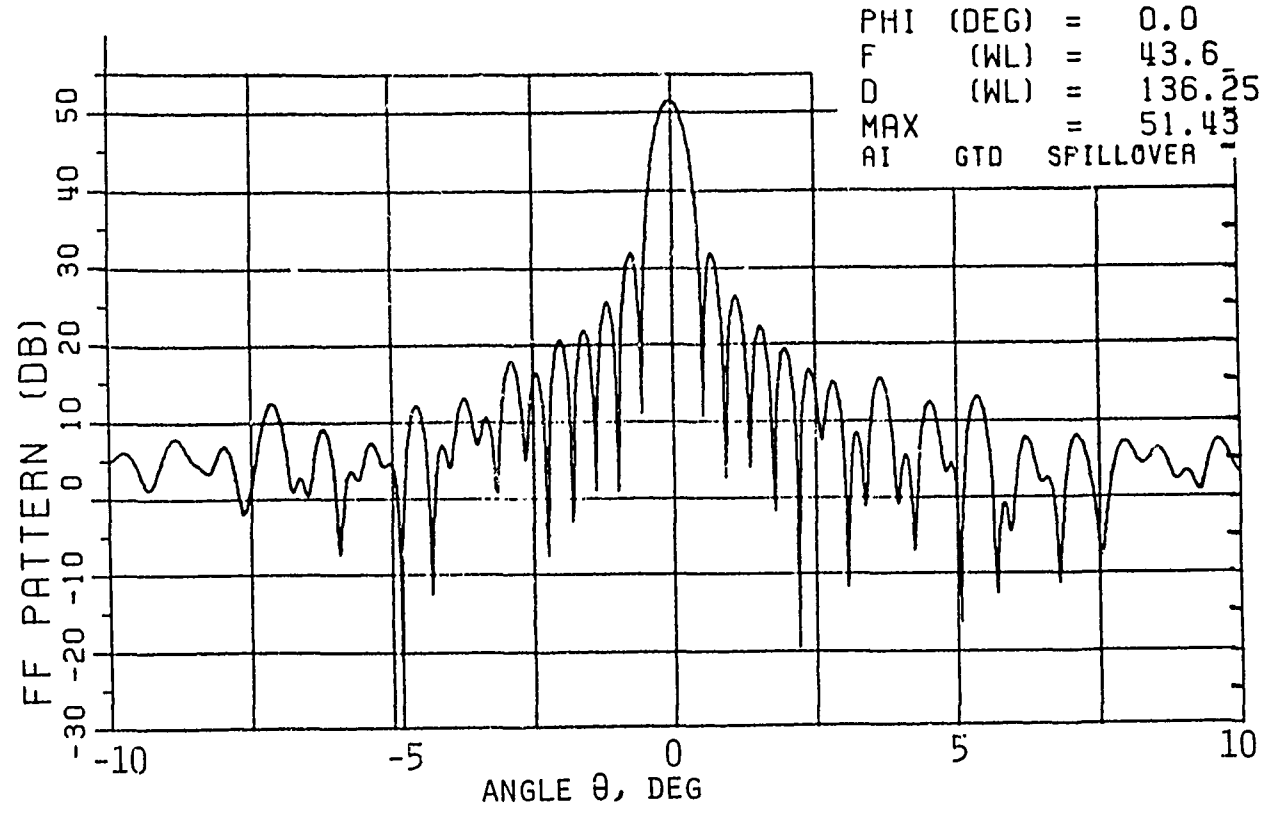

(b) With radome

Figure 75. Expanded patterns of 60-ft dish, with and without metal space frame radome

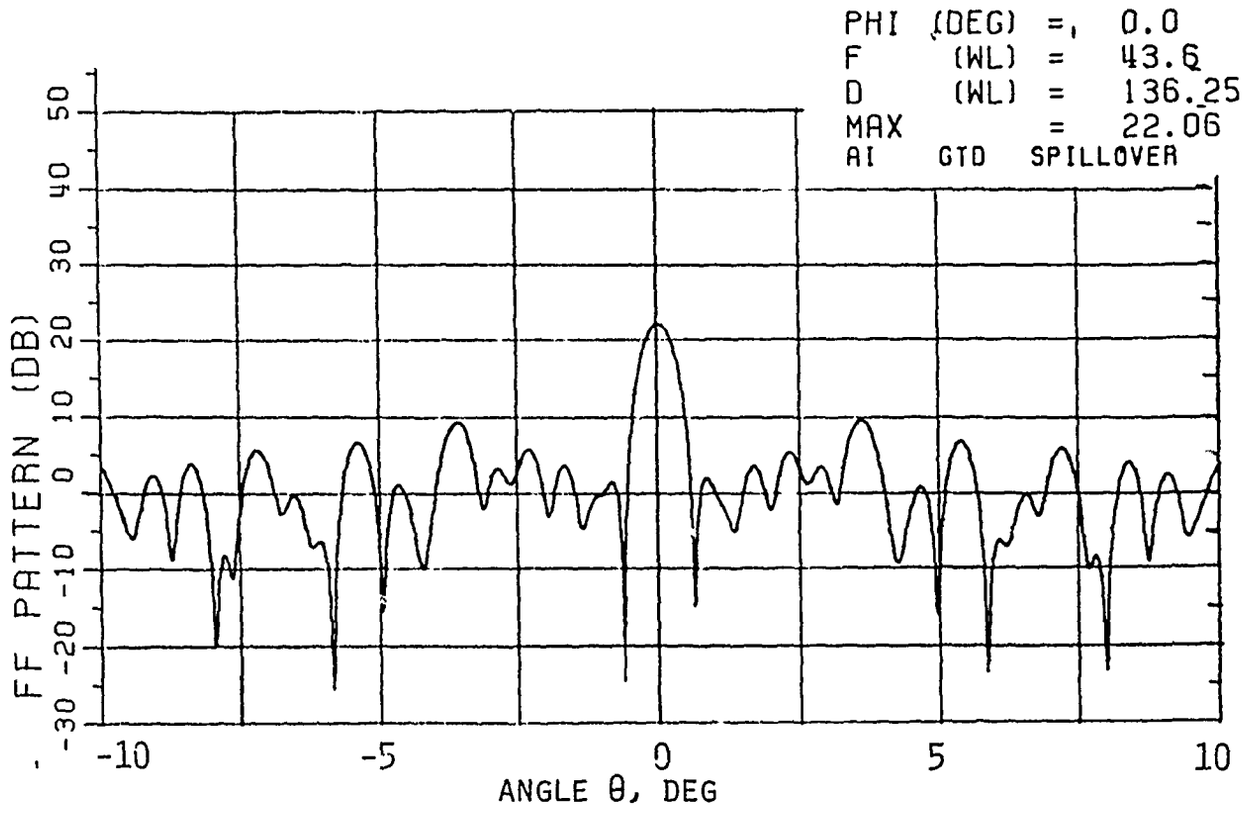

Figure 76. Expanded pattern of metal space frame radome structure

C. DISCUSSION

Since the measured and computed patterns for the Cassegrain reflector antenna compare reasonably well, it appears that OSU's computer codes should be used in subsequent studies to determine shielding techniques for sidelobe reduction. OSU has the capability of simulating the reflector shroud or plates so the optimum length can be established by computer design. OSU also has the theoretical capability to simulate the attachments, such as those illustrated in Figs. 6 and 7, but at the present time all these individual programs are not incorporated into the Cassegrain reflector code. Of course, like any computer design, experimental verification would eventually be required.

Our approach to use the measured horn-subreflector as primary patterns to calculate the reflector secondary patterns is an effective experimental/theoretical technique. The horn-subreflector data was digitized to enable it to be transferred to the central computer for computing the reflector patterns; thus, all the combinations were easily computed. Since there were no major breakthroughs in sidelobe reduction, only a few reflector patterns were included in this report. To note the change in sidelobe levels by reviewing the computed secondary patterns is probably a more effective means as compared to studying the measured patterns. Making high-gain reflector pattern measurements is difficult because of the low sidelobe levels to be measured and the complexity in the measurement equipment and environment, which often results in anomalous measurements.

VI. CONCLUSIONS

Experimental and analytical work are reported in an effort to reduce the far-out sidelobe levels of a 38 GHz, 2-ft diameter Cassegrain reflector antenna by 10 to 20 dB. The user had specified a monopulse feed, with a central conical feed horn diameter of 1.2 in. Also, two subreflector shapes were considered as the baseline configurations. One subreflector was defined "oversized" because the hyperboloidal shape yielded almost uniform aperture illumination and a conventional subreflector provided the normal 10 to 15 dB edge taper. With these physical constraints, the sidelobe level reduction approaches included the following; horn-aperture chokes and shrouds, shroud around the subreflector, conical flange mounted to the subreflector, absorber rings attached to the subreflector, corrugations (chokes) surrounding the subreflector, and circumferential (and partial) shroud around the main reflector edge.

The experimental procedure was to measure the patterns of various horn-subreflector assemblies to determine the potential for secondary pattern sidelobe reduction. Thus, only promising combinations were selected for the reflector secondary pattern measurements.

No one technique was found capable of reducing the sidelobe levels 10 to 20 dB over a wide angular region. The most effective reduction technique is the addition of a circumferential shroud (or a partial one) to the main reflector edge, which reduced the backlobes 10 to 20 dB but had negligible change in the forward-region lobes. The angular region for gain values <-20 dBi can be increased 30° to 50° in the rear region of the reflector by adding 3-in. wide circumferential shroud to the parabolic reflector. The measured reflector patterns also showed that two plates (partial shroud), 3 in. x 6 in. long, mounted on opposite edges of the reflector are as effective

as a full circumferential shroud for pattern cuts through the plates. Principal plane patterns show the major improvement. However, for great-circle pattern cuts 35° to 45° off the main beam the sidelobe reduction for the shroud is not as prominent over an extended angular region as compared to the principal-plane patterns.

For the conventional subreflector a conical flange, absorber ring or circumferential corrugations (chokes) provides some minor improvements. A combination of one of these attachments with the parabolic reflector shroud will yield the maximum sidelobe level reduction, with the physical constraints imposed by the user.

The oversized subreflector resulted in secondary patterns with the characteristic higher sidelobe levels in both the forward and rear region, as compared to the patterns with the conventional subreflector. The higher sidelobe levels were expected because of the almost uniform aperture illumination and high-level edge taper generated by the oversized subreflector. A shroud around the oversized subreflector creates higher-order modes resulting in a large amplitude variation (10 to 20 dB) across the reflector aperture. Corrugations, absorber rings and conical flanges were not satisfactory for sidelobe reduction.

The monopulse horn and the shroud placed over the monopulse horn had minimal effect on the 1.2-in. diameter horn pattern.

The theoretical pattern computations for the horn, horn-subreflector assemblies and the Cassegrain reflector systems compared very well with the measured reflector patterns. It was difficult to quantify the correlation; however, we can say the measured and computed patterns for the horn were within a few-tenths of a dB down to the 25 dB pattern level. The horn-subreflector patterns were within a few dB with the beam shape and sidelobe

locations in good agreement. The forward region of the reflector patterns were in agreement within a few dB, while the backlobes differ by 5 to 15 dB in the -65 to -75 dB pattern sidelobe levels. These large discrepancies were expected because of the differences in the mathematical and experimental reflector models.

The technique using the measured horn-subreflector pattern as the prime-focus primary feed pattern is a convenient means to compute the secondary pattern, since an in-house computer code for a Cassegrain reflector system was not available. This empirical approach provides a more quantitative and quicker comparison of sidelobe reduction techniques as compared to making a series of measurements on the main reflector.

Independent analytical computations by Prof. R. Rudduck, of Ohio State University, showed that the computed patterns for the horn, horn-subreflector, main reflector and reflector with shroud shows good correlation with the measured patterns. A 1.4-in. diameter corrugated horn (10.83° cone angle) with a conventional subreflector provides an improved design over the 1.2-in. conical horn by 5 to 10 dB over wide angular regions. A metal space frame radome increases the sidelobe levels ~5 dB in the forward region.

REFERENCES

1. S. H. Lee, R. C. Rudduck, C. A. Klein, R. G. Kouyoumjian, "A GTD Analysis of the Circular Reflector Antenna Including Feed and Strut Scatter," The Ohio State University, Electrical Engineering Department, TR 4381-1, May 25, 1977.

2. M. S. Narasimhan, P. Ramanujam, K. Raghaven, "GTD Analysis of a Hyperboloidal Subreflector with a Conical Flange Attachment," IEEE Trans Antennas and Propagation, AP-29, 865-871, November 1981.

3. R. B. Dybdal, T. T. Mori, H. E. King, "High Sensitivity Millimeter-Wave Instrumentation," IEEE Antennas and Propagation International Symposium Digest, 219-222, June 1981.

4. R. C. Rudduck and Y. C. Chang, "Numerical Electromagnetic Code -- Reflector Antenna Code, NEC-REF (Version 2)," Part I: User's Manual, The Ohio State University ElectroScience Laboratory, Technical Report 712242-16, December 1982.

☆U.S. GOVERNMENT PRINTING OFFICE: 1985—585—706/N·9205

LABORATORY OPERATIONS

The Laboratory Operations of The Aerospace Corporation is conducting experimental and theoretical investigations necessary for the evaluation and application of scientific advances to new military space systems. Versatility and flexibility have been developed to a high degree by the laboratory personnel in dealing with the many problems encountered in the nation's rapidly developing space systems. Expertise in the latest scientific developments is vital to the accomplishment of tasks related to these problems. The laboratories that contribute to this research are:

Aerophysics Laboratory: Launch vehicle and reentry fluid mechanics, heat transfer and flight dynamics; chemical and electric propulsion, propellant chemistry, environmental hazards, trace detection; spacecraft structural mechanics, contamination, thermal and structural control; high temperature thermomechanics, gas kinetics and radiation; cw and pulsed laser development including chemical kinetics, spectroscopy, optical resonators, beam control, atmospheric propagation, laser effects and countermeasures.

Chemistry and Physics Laboratory: Atmospheric chemical reactions, atmospheric optics, light scattering, state-specific chemical reactions and radiation transport in rocket plumes, applied laser spectroscopy, laser chemistry, laser optoelectronics, solar cell physics, battery electrochemistry, space vacuum and radiation effects on materials, lubrication and surface phenomena, thermionic emission, photosensitive materials and detectors, atomic frequency standards, and environmental chemistry.

Computer Science Laboratory: Program verification, program translation, performance-sensitive system design, distributed architectures for spaceborne computers, fault-tolerant computer systems, artificial intelligence and microelectronics applications.

Electronics Research Laboratory: Microelectronics, GaAs low noise and power devices, semiconductor lasers, electromagnetic and optical propagation phenomena, quantum electronics, laser communications, lidar, and electro-optics; communication sciences, applied electronics, semiconductor crystal and device physics, radiometric imaging; millimeter wave, microwave technology, and RF systems research.

Materials Sciences Laboratory: Development of new materials: metal matrix composites, polymers, and new forms of carbon; nondestructive evaluation, component failure analysis and reliability; fracture mechanics and stress corrosion; analysis and evaluation of materials at cryogenic and elevated temperatures as well as in space and enemy-induced environments.

Space Sciences Laboratory: Magnetospheric, auroral and cosmic ray physics, wave-particle interactions, magnetospheric plasma waves; atmospheric and ionospheric physics, density and composition of the upper atmosphere, remote sensing using atmospheric radiation; solar physics, infrared astronomy, infrared signature analysis; effects of solar activity, magnetic storms and nuclear explosions on the earth's atmosphere, ionosphere and magnetosphere; effects of electromagnetic and particulate radiations on space systems; space instrumentation.

. . .